Reaching for the Stars: Ecology and Skeletal Morphology of Pacific Northwest Sea Stars

Mo Turner

A dissertation

submitted in partial fulfillment of the

requirements for the degree of

Doctor of Philosophy

University of Washington

2022

Reading Committee:

Jennifer Ruesink, Chair

Megan Dethier

Adam Summers

Program Authorized to Offer Degree:

Biology

University of Washington

Abstract

Reaching for the Stars: Ecology and Skeletal Morphology of Pacific Northwest Sea Stars

Mo Turner

Chair of Supervisory Committee:
Jennifer L. Ruesink
Biology

Intertidal habitats exist at the interface of land and water, requiring the organisms that live there to inhabit two very different fluids, while also generating webs of interaction that span terrestrial and marine environments. This thesis addresses the functional groups and functional traits of intertidal organisms related primarily to trophic interactions, how these interactions change with habitat heterogeneity (e.g., seagrass on soft sediment, crevices on rocky shores), and skeletal morphology, in terms of three-dimensional ossicle organization, as a novel set of traits in sea stars (Asteroidea).

Tidal flats exposed at low tide frequently consist of a mosaic of habitat types. In Washington State, USA, tidal flats typically contain eelgrass (*Zostera marina*) patches intermixed with areas devoid of vegetation. Seagrasses represent a functionally important coastal habitat, serving as protection and nursery grounds for aquatic organisms, but less is known regarding avian use at low tide. Waterbirds in different functional feeding groups may interact differently with vegetation on tidal flats, and birds may make different choices when foraging or resting. In this study, community scientists collected observational data bimonthly during daytime low tides in

summer (April to August). Scan surveys and focal follows of waterbirds were carried out in paired patches of two lower intertidal habitats (eelgrass and unvegetated) across five sites. Ninety-nine percent of birds seen were gulls, crows, herons, and geese, and half of all birds observed were actively foraging. Total bird abundance within a patch did not differ between habitat types; among the four functional groups (corvids, gulls, herons, waterfowl), herons were more abundant in eelgrass than unvegetated patches. Waterbirds overall were more likely to be observed foraging in eelgrass than in unvegetated patches, and this difference also was seen in the activity budgets of herons. These tidal flats were occasionally visited by humans during low tide surveys. Human presence nearby did not appear to alter bird abundance overall or for any functional group. Overall, while low-tide eelgrass patches were valuable for foraging for some functional groups, a mosaic of habitats was used by waterbird communities. Global declines in eelgrass could lead to population decreases of herbivorous birds that directly consume eelgrass as well as wading birds, such as herons, that take advantage of prey living within seagrass beds.

Ochre sea stars (*Pisaster ochraceus*) are an apex, keystone predator on wave-exposed coastlines of the US Pacific Ocean, responsible for establishing the vertical zonation of mussel beds and therefore controlling benthic diversity. The studies that have formed the basis of understanding of this sea star's diet have primarily occurred at low tide and in areas with dominating mussel beds. However, given that intertidal organisms must live in both air and water, often with differing tasks or behaviors depending on where they find themselves, it is critical to study their behavior holistically. Additionally, *P. ochraceus* can be found in relatively high abundance in rocky intertidal habitats devoid of mussels, which may alter the functional role of this predator. This observational study addressed the diet and feeding behavior of *P. ochraceus* in the field through the tidal cycle at three sites around San Juan Island, Washington, USA, a region

that is not currently dominated by mussels. Study design accounted for their time in and out of water, the microhabitats they use, and their size. Sea stars were more likely to be found feeding at high than low water, when outside than in crevices, and as body size increased. When *P. ochraceus* were feeding, they consumed larger prey at low than high water, when inside than outside crevices, and as body size increased. Mussels were rare on these shores and represented <1% of feeding records. With no mussels to consume, *P. ochraceus* may not play the role of a keystone predator in this area. This effort to further understand the role of sea stars in intertidal communities is important because *P. ochraceus* is widespread in many wave exposure regimes but was reduced in density by the recent sea star wasting disease (SSWD) events that caused major population losses of this predator along the US Pacific Coast.

Armor in sea stars (Asteroidea) comes in the form of a highly articulated endoskeleton made up of individual pieces called ossicles. Many descriptive studies have been conducted on the basic patterning of sea star skeletons, with differences in shapes of ossicles forming the basis of early echinoderm phylogenies. However, the functional value of sea star ossicles is not necessarily in the characteristics of individual pieces, but rather in how those pieces are arranged and their relative contributions to the skeleton as a whole. In this study, micro-computed tomography was used to measure and compare morphological differences in the patterns of endoskeleton allocation of nine sea star species local to Washington, USA. Based on 14 quantitative morphological traits, analyses addressed: 1) correlations and tradeoffs among these traits and 2) correspondence of morphological similarity to two possible predictors, specifically ecology and phylogeny. Given the ecological and phylogenetic diversity of stars included in this study, expected patterns included 1) differences in the amount of armoring (relative volume of skeleton) and 2) those differences arise from varying allocation and shape of ossicles across different regions of the body. While all

sea stars share the same five basic types of ossicles, the amount of skeletal armoring across the body varied by at least an order of magnitude across species and differed in its distribution across ossicle types. Heavily armored stars invest in larger, boxy body wall ossicles, whereas a reduction in armor volume was often paired with more intricately shaped body wall ossicles and an increase in the number and complexity of spines. Skeletal patterning and allocation are more correlated with phylogenetic than ecological differences. More research is needed to understand which morphological traits are phylogenetically conserved, which could provide an opportunity to better use phylogeny to understand trait evolution.

TABLE OF CONTENTS

Chapter 1: Summer-season abundance and foraging of waterbirds across a habitat mosaic on intertidal flats

Abstract

Tidal flats exposed at low tide frequently consist of a mosaic of habitat types. In Washington State, USA, tidal flats typically contain eelgrass (*Zostera marina*) patches intermixed with areas devoid of vegetation. Seagrasses represent a functionally important coastal habitat, serving as protection and nursery grounds for aquatic organisms, but less is known regarding avian use at low tide. Waterbirds in different functional feeding groups may interact differently with vegetation on tidal flats, and birds may make different choices when foraging or resting. In our study, community scientists collected observational data bimonthly during daytime low tides in summer (April to August). They conducted scan surveys and focal follows of waterbirds in paired patches of two lower intertidal habitats (eelgrass and unvegetated) across five sites. Ninety-nine percent of birds seen were gulls, crows, herons, and geese, and half of all birds observed were actively foraging. Total bird abundance within a patch did not differ between habitat types; among the four functional groups (corvids, gulls, herons, waterfowl), herons were more abundant in eelgrass than unvegetated patches. Waterbirds overall were more likely to be observed foraging in eelgrass than in unvegetated patches, and this difference also was seen in the activity budgets of herons. These tidal flats were occasionally visited by humans during low tide surveys. Human presence nearby did not appear to alter bird abundance overall or for any functional group. Overall, while low-tide eelgrass patches were valuable for foraging for some functional groups, a mosaic of habitats was used by waterbird communities. Global declines in eelgrass could lead to

population decreases of herbivorous birds that directly consume eelgrass as well as wading birds, such as herons, that take advantage of prey living within seagrass beds.

Introduction

Marine shorelines provide a spatially diverse patchwork of habitat types spanning multiple ecological functions. This ecological mosaic allows mobile organisms, such as birds and other higher trophic level taxa, to access several habitat types and thus exploit multiple resources and habitat functions in close proximity. In Washington State, USA, tidal flats exposed at low tide frequently consist of a mosaic of habitat types, with fringing eelgrass patches intermixed with areas devoid of vegetation due to drying, sloughs, or water motion (Christiaen et al., 2017). These low-intertidal areas often harbor high densities of infauna that are consumed by shorebirds (Wilson, 1994), aquatic vegetation that is consumed by waterfowl (Baldwin & Lovvorn, 1994), and mobile fish and invertebrates that are hunted by wading birds in shallow water (Yeoh et al., 2017). Consequently, foraging is expected to be the primary driver of intertidal habitat use for many bird species (Beerens et al., 2015; Raposa et al., 2009). Ecological value of these habitats for higher trophic organisms has typically been inferred by using prey density as a proxy, however these habitats may be used for more than just feeding. In the present study, we directly observed tidal flat use by diverse bird species, examining what behaviors they exhibit in these habitats (foraging or other), and in what ways they use vegetated and unvegetated patches at low tide.

For some taxa, we might expect seagrass to be preferred over unvegetated areas. As a biogenic habitat, seagrasses provide protection and nursery grounds for lower-trophic organisms such as juvenile fish and invertebrate species (Heck et al., 2003; Lee et al., 2001; McDevitt-Irwin

et al., 2016). Epifaunal and infaunal densities are frequently elevated in seagrass relative to nearby unvegetated tidal flats (Ferraro & Cole, 2012; Posey, 1988). Small fishes also occur at higher density in eelgrass than in unvegetated areas (Gross et al., 2017). During periods of low tide, these habitats become extremely shallow or fully exposed, allowing non-diving birds to take advantage of potentially high prey availability. On the southern coast of British Columbia, the Great Blue Heron (*Ardea herodias*), a piscivorous wading bird, forages extensively in eelgrass beds and exerts strong top-down control on the fish and invertebrate assemblages contained within (Huang et al., 2015). For some herbivorous waterfowl, eelgrass habitats are the only places on tidal flats where they would be expected to forage. Some species, such as Black Brant (*Branta bernicla*), consume *Zostera marina* directly and are clearly tied to vegetative habitat for their foraging success (Kollars et al., 2017). However, many shorebirds are more likely to utilize unvegetated habitats, as they use resources (i.e. biofilms) associated with and/or require unimpeded access into the mudflat sediments (Mathot et al., 2018). Overall, the fraction of time spent foraging as well as the abundances of birds should serve as indicators for the value of different intertidal habitats for waterbirds.

While food diversity and density are drivers of intertidal habitat use, waterbirds may also react directly to physical structure. Structures placed by humans on tidal flats can either attract or repel birds, depending on taxa (Hilgerloh et al., 2001). Similarly, biogenic organisms such as marsh plants and reef-building shellfish can change habitat suitability for birds that use tidal flats, either by restricting access to the sediment or modifying prey densities (Patten & O'Casey, 2007; van der Zee et al., 2012). As these structures may be elevation-specific (e.g. marsh plants higher on shore, oyster reefs lower), studies of tidal flat use by birds must therefore control for tidal

elevation (e.g. Frazier et al., 2014). Observations at particular water levels can help account for densities that might shift as birds track water levels during foraging (Granadeiro et al., 2006).

Humans, like birds, access intertidal habitats at low tide for foraging opportunities (e.g. commercial or recreational shell-fishing), or they may visit tidal flats for recreational or esthetic amenities. Therefore, waterbird distribution may reflect not just underlying habitat and resources, but disturbance from humans. Disturbances within 100m of waterbirds have been shown to induce flight in many species, and shorelines with regular visitation by humans may have reduced numbers of some waterbirds (Burger et al., 2004; Burton et al., 2002). For example, human settlements reduced shorebird abundance but increased gull abundance in lagoons along the coast of Brazil (Tavares et al., 2015).

Different waterbird functional groups show habitat distributions that indicate distinct responses to landscape features (Wei et al., 2017). For example, in an Oregon estuary, waterfowl density was greater in seagrass habitats than in other tidal flat areas, whereas shorebird densities exhibited the opposite distribution (Frazier et al., 2014). In our study, we examined the low-tide associations between waterbirds and two habitats (eelgrass, unvegetated) in Washington State to address the following questions: 1) How are different bird functional groups distributed across tidal flat habitats? 2) How does foraging behavior differ between eelgrass and unvegetated habitats? and 3) Are results sensitive to whether humans are nearby? Including both behavior and abundance as response variables was a strategy to overcome limitations of density alone as an index of habitat quality (Horne, 1983). Given the abundance and diversity of prey available in eelgrass beds, we hypothesize that greater bird abundance and foraging activity occurs in eelgrass habitats. Additionally, functional groups are predicted to specialize in their use of habitats: eelgrass

grazers will be found more often in eelgrass, whereas more generalist or opportunistic birds, like gulls and crows, will be found more evenly spread between habitats.

Methods

Study sites

Birds were observed in paired patches of eelgrass (*Z. marina*) and unvegetated tidal flats in a nested design. The design included five sites (= bays in Washington State, USA) where two to four subsites were identified within each site. Each subsite consisted of a patch of eelgrass and unvegetated tidal flat, which were paired in the design due to their close proximity (usually adjacent), observation during the same low-tide event, and similar spatial area. We did not specifically map the borders of these patches to calculate their area, but found patches that stretched approximately 100-200 meters along shore, and confined our observations to similar shore lengths within each pair of patches. The borders of each patch were demarcated using fixed landmarks for repeated sampling. Subsites were selected where habitat patches were exposed when tidal height dropped below mean lower low water (MLLW), and where a publicly accessible shoreline was available less than 300 m from the habitat patches. Finally, at the largest sampling scale, the five sites in Washington State estuaries were Birch Bay, Nisqually Delta, Port Gamble, Skokomish shoreline and Willapa Bay (Fig 1). Typically, *Z. marina* occupies a tidal elevation at and below the MLLW level (Thom et al., 2003), making this habitat available to surface-foraging birds only on extreme low tides. In Washington State, such extreme low tides occur during the daytime in summer and during the nighttime in winter (https://tidesandcurrents.noaa.gov/tide_predictions.html?gid=1415). Sites were surveyed up to

twice per month from April to August 2016 during the spring-tide series, within a 1-hour window on either side of the predicted daytime low tide. Each subsite (paired eelgrass and unvegetated patch) was observed on average 9 times (range 6 to 13). Bird abundance was not converted to density, but rather maintained as number per patch; this approach introduces no bias because eelgrass and unvegetated patches were selected for similar size in each subsite.

Community Scientists

Community-scientist volunteers were selected from birdwatchers with self-identified waterbird identification experience. Volunteers were required to attend a half-day training session before the first daylight extreme low tide cycles of the season. During the training, we reviewed bird identification, survey methods and data notation, followed by a supervised practice survey in the field. Volunteers were assigned to a single site for the season. We (the authors) were present at the first survey of every site with community-science volunteers in order to verify both the patch boundaries and their understanding of the survey methods. In addition, we surveyed each site with the community scientists at least twice in the season to ensure consistent survey methods and accurate bird identification.

Scan surveys

For each survey event, observers stood at a fixed point 100-300m away from the paired habitat patches and performed a slow visual sweep from one side of each patch to the other, locating birds on the tidal flat. These surveys typically lasted between 5 and 15 minutes, depending on how many birds were present in the patch. Any birds flying over the patch or swimming in deeper waters were not counted. Each bird observed was identified to the lowest possible taxonomic level, counted, and assigned a behavior. Behaviors were categorized as resting, moving,

foraging, and preening. Bird species were designated into functional groups, which decreased data resolution (functional group rather than species) but increased accuracy and confidence in identifications. Functional groups included corvids (crows, ravens), gulls (gulls, terns), herons (herons, egrets), and waterfowl (geese, ducks). Human activity in the area was also recorded, including people, boats, or dogs within and up to 10m from each patch.

Focal follows

Activity budgets of individual birds using a habitat patch at low tide were determined using focal follows. The focal bird was selected haphazardly from among those in the patch, following the scan survey. Throughout the study, a total of 117 birds were observed, each for 5 minutes or until leaving the patch. Focal follows were conducted by a pair of observers, with one watching the bird and relaying changes in behavior and the other observer keeping time and translating information to the datasheet. Behaviors were binned into categories: resting, moving, foraging, preening, and exiting the plot.

Data analysis

Generalized linear mixed models were not suitable for analyzing bird abundance because neither negative binomial nor Poisson distributions could account for overdispersion of data. Zero-inflation was due to 48% of patch observations with zero birds present. Instead, a non-parametric alternative was implemented via univariate permutational analysis of variance (PERMANOVA) assuming Euclidian distances. Bird abundance per patch (total birds, and by functional group) was the response variable, and habitat type (eelgrass, unvegetated) the fixed effect. Subsite was a random effect (strata) to account for the spatial structure (paired patches) and temporal structure (multiple observations per patch through the summer). Accordingly,

permutations were carried out within these pairs (as strata in the adonis function of the vegan package, Oksanen et al., 2015; R v 3.3.2). The total number of patch observations was 276 (2 habitats x 2-4 subsites x 5 sites x 6-13 observations through the summer). We did not include date as a fixed effect because most birds that appeared in our observations are resident in Washington, and preliminary analyses showed no seasonal trends.

Analyses of bird behavior were carried out on both scan surveys and focal follows. For scan surveys, behavioral data were binned into two categories, foraging and not foraging, and converted to a proportion of birds foraging per patch per observation. The total number of patch observations with birds was 142 (85 in eelgrass, 57 unvegetated). Focal follow analyses of behavior were carried out considering individual birds, rather than patches, as replicates. Based on their activity budget, fraction of time foraging (of up to 5 minutes) was used as a response variable. Of 117 birds with data from focal follows, 71 were in eelgrass and 46 in unvegetated, with necessarily smaller sample sizes by functional group (gulls: 32, 28; crows: 8, 6; herons: 27, 9; waterfowl: 4, 3). In both cases, PERMANOVA was used to test for differences between birds in eelgrass and unvegetated patches with no random effects.

To examine the effect of human presence on bird abundance, human activity was transformed into presence/absence data in or around the habitats; only patches that experienced both conditions during the study were included for analysis (10 eelgrass, 7 unvegetated, but habitat was not included as a predictor in this analysis). Bird abundance at an individual patch was averaged across samples experiencing each condition (humans present, humans absent). PERMANOVA was used to test for differences between bird abundance when humans were present or absent, using patch as a random effect to account for pairing of the same patch with and without humans.

Results

Over the six-month study, 1134 total birds were counted in low intertidal habitat patches. Gulls/terns were most common (58.9%), followed by waterfowl (16.8%), herons (*A. herodias* and one *A. alba*, 14.9%), and corvids (*Corvus brachyrhynchos* and *Corvis caurinus*, 8.5%). The functional group including gulls and terns consisted primarily of gulls (92%). The waterfowl functional group comprised of 99% Canada geese (*Branta canadensis*) and 1% Common Goldeneye (*Bucephala clangula*). Although waterfowl were the second most abundant functional group, they were only observed on eight occasions across four subsites (1 to 61 individuals), restricting data analysis for variables other than abundance of this functional group. The remaining 0.9% of birds consisted of raptors, kingfishers, passerines, and shorebirds, and were not included in data analysis. See Table 1 for a full list of observed species.

The total number of birds within a patch was highly variable, ranging from 0 to 96 individuals, but did not differ overall between habitat types (Table 2, Fig 2). Within functional groups, herons were observed with a much higher abundance in eelgrass (1.072 ± 0.374 birds per patch) than in unvegetated tidal flat (0.203 ± 0.056), with ranges of 0-47 and 0-4 birds respectively. Gulls, crows, and waterfowl did not differ in abundance by habitat type (Table 2).

Types of behavior observed in eelgrass vs. unvegetated patches varied for some groups but not others. Overall, waterbirds were 1.6 times more likely to be observed foraging when in eelgrass than in unvegetated patches ($p = 0.033$), however this pattern was not significant when analyzed within individual functional groups in the scan surveys (Table 2, Fig 3). Gulls and crows were regularly observed both foraging and not foraging, and there were no significant differences in

behavior between habitats in focal follows (Table 2). Herons exhibited a higher proportion of foraging in eelgrass in the focal follows but not in the scan surveys (p = 0.017 and p = 0.522 respectively, Fig 3). Although foraging behavior did not differ between habitats in most analyses, scan samples and focal follows provided similar estimates of proportion foraging for gulls (25% in scans, 32% activity budgets), herons (56% in scans, 54% activity budgets), and crows (42% in scans, 33% activity budgets) (Fig 3).

Total bird abundance within habitat patches did not differ in the presence or absence of humans (Table 3, Fig 4). Within functional groups, no differences were detected, but this result of "no effect" may also reflect that some taxa had few patches experiencing both human and no-human conditions (Table 3, Fig 4).

Discussion

On low intertidal tidal flats of Washington State in summer, eelgrass habitat provides a trophic link to birds, while unvegetated areas may serve as a place of rest or refuge from land-based predators. During summer low tides, birds were equally likely to be seen in eelgrass and unvegetated habitats (Fig. 2). However, waterbirds as a group were more likely to be observed foraging in eelgrass habitats (Fig 3).

Among functional groups, herons were the only common waterbird that showed a significant eelgrass response, increasing both their abundance and foraging in eelgrass relative to unvegetated patches. Habitat preference by herons may arise because extreme low tides give them access to eelgrass beds in shallow depressions of water, in which schooling fish can reach high densities (Gross et al., 2017). We have also observed that pelagic fish such as anchovies can get

caught in eelgrass at low tide (JLR, author pers. obs.) and become accessible to opportunists such as gulls and crows. However, this infrequent event was not observed during our surveys. At a larger scale, the area of foraging habitat is positively correlated with the number of nests in heron breeding grounds (Butler et al., 2002; Dowty, 2005; Gibbs & Kinkel, 1997). The Nisqually Delta, one of the sites in the study (Fig. 1), is a known heron breeding ground and also had the highest counts of herons (112 herons, as compared to 28 where they were next most abundant). This functional group exhibits a slow and methodical hunting behavior (Kelly et al., 2003) that could explain the differences in feeding behavior between the two survey methods. A heron holding still in preparation for a strike may be noted as "resting" when quickly identified in a scan, whereas longer observation of an individual during a focal follow might place that same immobile behavior in the context of foraging. Thus, based on activity budgets, herons spent a significantly greater proportion of time foraging in eelgrass patches than when they were in an unvegetated patch.

Herbivorous waterfowl (geese and certain duck species) were expected to be more abundant and foraging more often in eelgrass due to their ability to consume eelgrass directly (Bakker et al., 2016; Frazier et al., 2014), however our quantitative surveys did not support this habitat difference. During several observations, bird numbers ranging from just a few individuals to large flocks of over 50 waterfowl swam near a habitat patch without entering it (community scientist reported). Canada geese (*Branta canadensis*) were observed to pass through an unvegetated patch to forage directly on *Z. marina*. They displayed previously reported behavior of digging their bills into the sediment and pulling the eelgrass up by its roots (Kollars et al., 2017; Thayer et al., 1984). In addition, three-quarters of waterfowl individuals were seen in July and August, which aligns with their autumn migration along the Pacific Flyway and with several waterfowl foraging studies (Baldwin & Lovvorn, 1994; Kollars et al., 2017).

Shorebirds were infrequently observed in this study, precluding an assessment of their response to eelgrass on tidal flats. Other works regionally have shown that shorebirds more frequently use sand and mudflats when foraging than eelgrass beds or other vegetated regions (Lamberson et al., 2011; Patten & O'Casey, 2007). The lack of data on shorebirds in our study may be due to missing portions of the spring and autumn migratory period, and/or because small patch size may prevent bird occupation during the observation periods. Shorebirds foraging on tidal flats are often found close to the water's edge, so they shift their intertidal distribution through tidal cycles. This behavior may apply in particular to shorebirds foraging for infauna, due to sediment characteristics and behavior of infauna when the sediments are water-saturated (Miller & de Rivera, 2014; Nebel et al., 2005). Although many shorebird species are considered 'tide-followers', much of the habitat use is still in the upper intertidal zone (Butler et al., 2002; Granadeiro et al., 2006; Jiménez et al., 2015).

Although they were relatively small (ca. 100 m length), most habitat patches experienced nearby human activity at some point during the study. The same selection criteria for sites used in this study, namely being accessible to community scientists and close to shore, were also favorable for human recreational activities. Activities such as boating, fishing, wildlife viewing, and hiking have been shown to disturb waterbirds in both physiological (Fowler, 1999; Müllner et al., 2004) and behavioral responses (McLeod et al., 2013; Navedo & Herrera, 2012), ultimately reducing bird use in some habitats (Burger et al., 2010; Burton et al., 2002). Our binary criterion for human presence was necessarily simplistic, integrating across a variety of activities and distances. Despite absence of any statistical evidence of human presence disturbing birds, we noted some cases in which dog-walkers disrupted all birds present (community scientist reported; Lafferty, 2001). Additionally, sites that were close to shore in city parks were not included in the study design

because no birds were present in preliminary surveys. At the rural sites remaining in the survey, small recreational clamming practices could attract generalists scavenging for scraps.

Use of intertidal habitats by waterbirds differs with the tidal cycle (Granadeiro et al., 2006) as well as seasonally due to migratory patterns by certain functional groups of birds (Frazier et al., 2014). Because we specifically focused on comparing eelgrass-vegetated and unvegetated habitat patches, set up in a paired design, our observations were restricted to the time of year when extreme low tides occurred during daylight hours. Exploratory analyses did not reveal temporal patterns in bird use due to patchy distributions, so we focused our attention on habitat differences and, when appropriate, bird responses to nearby humans. We found that the use of low intertidal habitats differs by functional groups of waterbirds. Great blue herons may be considered a form of eelgrass specialist, in addition to herbivorous birds that consume eelgrass directly. However, a mosaic of low-intertidal habitat types appears valuable for common waterbirds in Washington State. Global declines in eelgrass could lead to population loss of not only herbivorous birds that directly consume eelgrass but also wading birds, similar to the Great Blue Heron, that take advantage of the high prey densities living within seagrass beds (Waycott et al., 2009).

Acknowledgements

This work would not have been completed without my collaborators, Dr. Thomas P. Good and Dr. Jennifer Ruesink, who would both be considered co-authors when developing the manuscript for publication. The following individuals were instrumental in data collection: Abigail Ames, Joy Polston Barnes, Betsy Cooper, Bobbee Davidson, Katie Dobkowski, Donna LaCasse, Cindi Nevins, Victoria Poage, Mardi Prescott, Niki Quester, Kathy Ruesink, Esther Schmall, Sharon Smuin, Bob Thurston, Randi Thurston, Alan Trimble, Don Willott and Judy Willott.

Tables

Table 1. Waterbird species observed in low intertidal eelgrass (*Zostera marina*) and unvegetated habitats of Washington State, USA during summer 2016 across all sites. Uncommon functional groups (kingfisher, passerines, shorebirds, and raptors) were identified and counted but excluded from data analyses due to low abundance and observation frequency.

Functional Group		Habitat		
Common	Common Name, Species	*Z. marina*	Unvegetated	Total
Corvid	American Crow, *Corvus brachyrhynchos*	40	32	72
	unidentified corvid spp., *Corvus spp.*	7	16	23
Gulls/Terns	Caspian Tern, *Hydroprogne caspia*	26	29	55
	Glaucous-winged gull, *Larus glaucescens*	107	21	128
	Mew gull, *Larus canus*	6	1	7
	Western gull, *Larus occidentalis*	5	4	9
	unidentified gull spp., *Larus spp.*	230	233	463
Heron	Great Blue Heron, *Ardea herodias*	148	27	175
	Great Egret, *Ardea alba*	0	1	1
Waterfowl	Canada Goose, *Branta canadensis*	91	97	188
	Common Goldeneye, *Bucephala clangula*	3	0	3
Uncommon	-	-	-	-
Kingfisher	Belted Kingfisher, *Megaceryle alcyon*	0	1	1
Passerine	European Starling, *Sturnus vulgaris*	1	0	1
Shorebird	Greater Yellowlegs, *Tringa melanoleuca*	4	0	4
	Killdeer, *Charadrius vociferus*	0	1	1
Raptor	Bald Eagle, *Haliaeetus leucocephalus*	2	0	2
	Osprey, *Pandion haliaetus*	0	1	1
Grand Total	-	670	464	1134

Table 2. Results of one-way PERMANOVAs testing for differences between eelgrass and unvegetated habitats in abundance and foraging behavior of waterbirds. Subsite was a random factor to account for the paired design of adjacent eelgrass and unvegetated patches, each of which was surveyed multiple times. Results are presented for four dominant functional groups and for all waterbirds combined (total), based on a scan of all birds present and activity budgets developed for individual birds. Df = degrees of freedom (numerator, denominator).

Scan surveys			
Abundance	DF	Pseudo-F	P-value
Total	1, 275	1.335	0.183
Corvids	1, 275	0.003	1.000
Gulls	1, 275	0.751	0.301
Herons	1, 275	5.276	**2e-04***
Waterfowl	1, 275	0.001	0.975
Behavior	DF	Pseudo-F	P-value
Total	1, 141	4.637	**0.033***
Corvids	1, 36	2.547	0.212
Gulls	1, 110	0.305	0.582
Herons	1, 56	0.721	0.522
Waterfowl	NA	NA	NA

Focal follow surveys			
Behavior	DF	Pseudo-F	P-value
Total	1, 116	3.566	**0.060**
Corvids	1, 13	0.705	0.411
Gulls	1, 59	1.204	0.274
Herons	1, 35	6.414	**0.017***
Waterfowl	NA	NA	NA

Table 3. Results of a one-way PERMANOVA testing for differences in bird abundance in the presence or absence of humans. Patch was a random factor to account for pairing of the same patch with and without humans. Results are presented for the three dominant functional groups and for all waterbirds combined (total).

Scan surveys			
Human presence	DF	Pseudo-F	P-value
Total	1, 33	0.386	0.263
Corvids	1, 5	8.763	0.286
Gulls	1, 29	0.126	0.577
Herons	1, 13	0.272	0.233

Figures

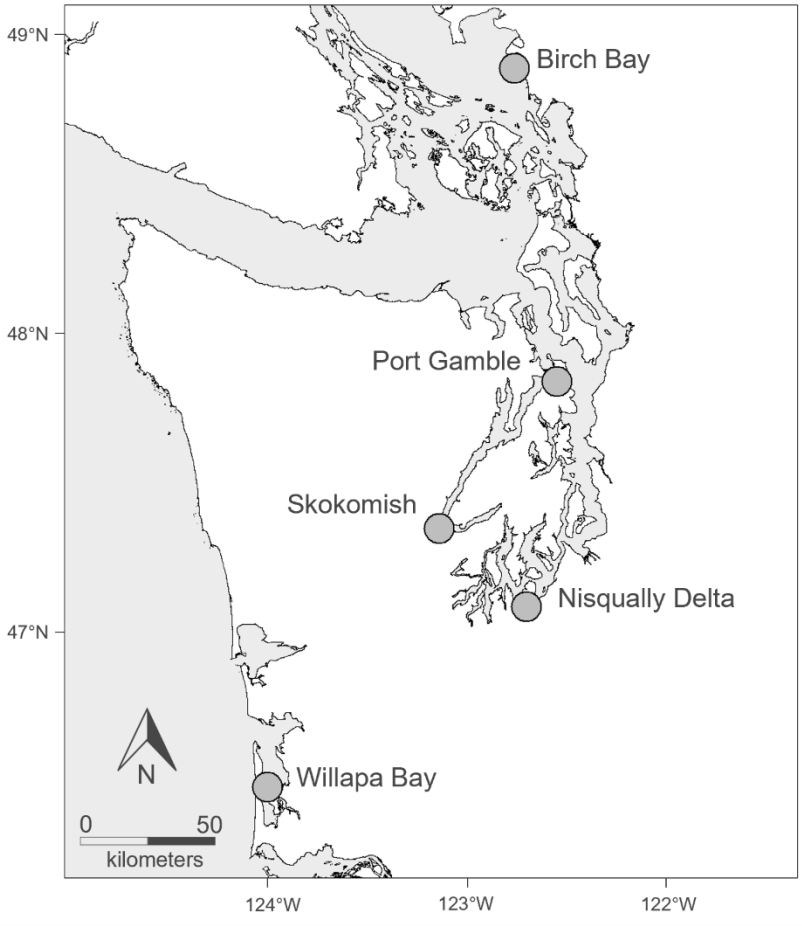

Figure 1. Map of Washington State showing the five study sites, which included Birch Bay (North Puget Sound; N48.89, W122.78), Port Gamble (North Hood Canal; N47.85, W122.57), Skokomish (South Hood Canal; N47.36, W123.15), Nisqually Delta (South Puget Sound; N47.10, W122.72), and Willapa Bay (Coastal estuary; N46.5, W124.0).

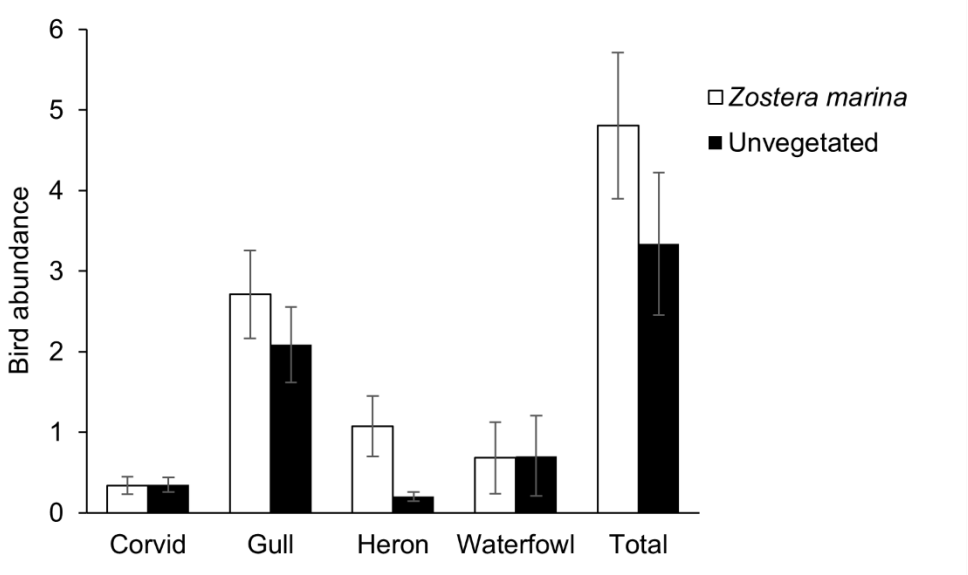

Figure 2. Waterbird abundance during scans of low intertidal habitat patches (eelgrass [*Zostera marina*] and unvegetated) during summer 2016 in Washington State. Data are presented for four dominant functional groups as well as for all waterbirds combined (total). For display of data, means and standard errors were calculated using each observation as a sample, but statistical significance (*) is derived from randomization tests (PERMANOVA) with subsite as a random effect (5 sites in Washington State, 2-4 subsites per site, each observed multiple times).

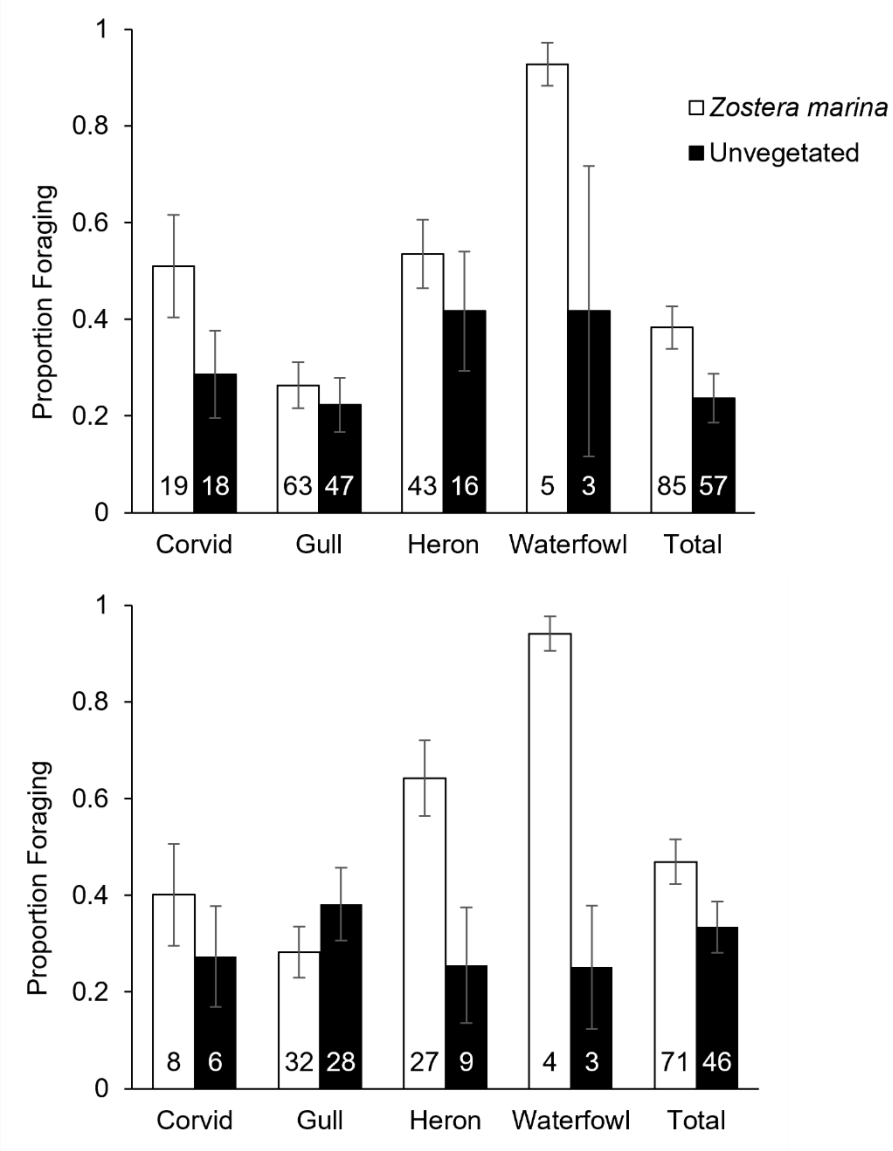

Figure 3. Waterbird behavior in low intertidal eelgrass (*Zostera marina*) and unvegetated habitat patches in Washington State in summer 2016 as quantified in A) scan surveys and B) focal follows. Numbers on bars indicate sample size in terms of A) number of patches where birds were present, and B) number of activity budgets with each bird as a replicate. Statistical significance (*) is derived from randomization tests (PERMANOVA). Waterfowl data is displayed, however the sample size was too low for statistical analysis.

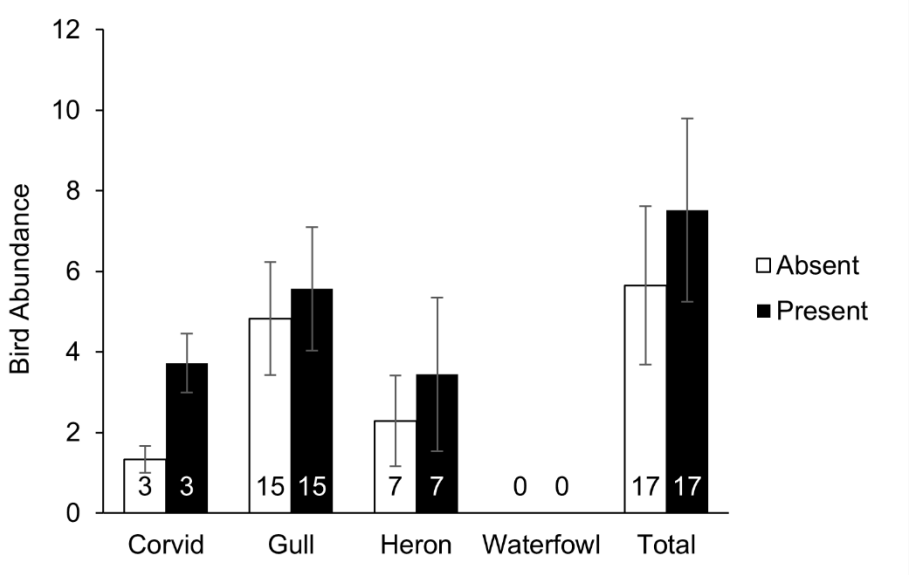

Figure 4. Waterbird abundance in low intertidal habitats as a function of human presence and absence, within and adjacent to a survey patch. Means and standard deviations based on bird abundance per patch averaged across surveys experiencing each condition (humans absent, humans present).

Literature Cited

Bakker, E. S., Wood, K. A., Pagès, J. F., Veen, G. F. (Ciska), Christianen, M. J. A., Santamaría, L., Nolet, B. A., & Hilt, S. (2016). Herbivory on freshwater and marine macrophytes: A review and perspective. *Aquatic Botany*, *135*, 18–36. https://doi.org/10.1016/j.aquabot.2016.04.008

Baldwin, J. R., & Lovvorn, J. R. (1994). Habitats and tidal accessibility of the marine foods of dabbling ducks and brant in Boundary Bay, British Columbia. *Marine Biology*, *120*(4), 627–638. https://doi.org/10.1007/BF00350084

Beerens, J. M., Noonburg, E. G., & Gawlik, D. E. (2015). Linking dynamic habitat selection with wading bird foraging distributions across resource gradients. *PLOS ONE*, *10*(6), e0128182. https://doi.org/10.1371/journal.pone.0128182

Burger, J., Gochfeld, M., Jenkins, C. D., & Lesser, F. (2010). Effect of approaching boats on nesting Black Skimmers: Using response distances to establish protective buffer zones. *Journal of Wildlife Management*, *74*(1), 102–108. https://doi.org/10.2193/2008-576

Burger, J., Jeitner, C., Clark, K., & Niles, L. J. (2004). The effect of human activities on migrant shorebirds: Successful adaptive management. *Environmental Conservation*, *31*(4), 283–288. https://doi.org/10.1017/S0376892904001626

Burton, N. H. K., Armitage, M. J. S., Musgrove, A. J., & Rehfisch, M. M. (2002). Impacts of man-made landscape features on numbers of estuarine waterbirds at low tide. *Environmental Management*, *30*(6), 857–864. https://doi.org/10.1007/s00267-002-2732-5

Butler, R. W., Shepherd, P. C., & Lemon, M. J. (2002). Site fidelity and local movements of migrating Western Sandpipers on the Fraser River estuary. *The Wilson Bulletin*, *114*(4), 485–490.

Christiaen, B., Ferrier, L., Dowty, P., Gaeckle, J., & Berry, H. (2017). *Puget Sound seagrass monitoring report: Monitoring year 2015* (Nearshore Habitat Program). Washington State Department of Natural Resources.

Dowty, P. (2005). *A study of sampling and analysis methods: Submerged vegetation monitoring project at year 4* (Nearshore Habitat Program, p. 139). Washington State Department of Natural Resources.

Ferraro, S. P., & Cole, F. A. (2012). Ecological periodic tables for benthic macrofaunal usage of estuarine habitats: Insights from a case study in Tillamook Bay, Oregon, USA. *Estuarine, Coastal and Shelf Science*, *102–103*, 70–83. https://doi.org/10.1016/j.ecss.2012.03.009

Fowler, G. S. (1999). Behavioral and hormonal responses of Magellanic penguins (*Spheniscus magellanicus*) to tourism and nest site visitation. *Biological Conservation*, *90*(2), 143–149.

Frazier, M. R., Lamberson, J. O., & Nelson, W. G. (2014). Intertidal habitat utilization patterns of birds in a Northeast Pacific estuary. *Wetlands Ecology and Management*, *22*(4), 451–466. https://doi.org/10.1007/s11273-014-9346-6

Gibbs, J. P., & Kinkel, L. K. (1997). Determinants of the size and location of Great Blue Heron colonies. *Colonial Waterbirds*, *20*(1), 1. https://doi.org/10.2307/1521757

Granadeiro, J. P., Dias, M. P., Martins, R. C., & Palmeirim, J. M. (2006). Variation in numbers and behaviour of waders during the tidal cycle: Implications for the use of estuarine sediment flats. *Acta Oecologica*, *29*(3), 293–300. https://doi.org/10.1016/j.actao.2005.11.008

Gross, C., Donoghue, C., Pruitt, C., Trimble, A. C., & Ruesink, J. L. (2017). Taxonomic and functional assessment of mesopredator diversity across an estuarine habitat mosaic. *Ecosphere*, *8*(4). https://doi.org/10.1002/ecs2.1792

Heck, K., Hays, G., & Orth, R. (2003). Critical evaluation of the nursery role hypothesis for seagrass meadows. *Marine Ecology Progress Series*, *253*, 123–136. https://doi.org/10.3354/meps253123

Hilgerloh, G., Halloran, J. O., Kelly, T. C., & Burnell, G. M. (2001). A preliminary study on the effects of oyster culturing structures on birds in a sheltered Irish estuary. *Coastal Shellfish — A Sustainable Resource*, 175–180. https://doi.org/10.1007/978-94-010-0434-3_17

Horne, B. V. (1983). Density as a misleading indicator of habitat quality. *The Journal of Wildlife Management*, *47*(4), 893. https://doi.org/10.2307/3808148

Huang, A. C., Essak, M., & O'Connor, M. I. (2015). Top-down control by Great Blue Herons *Ardea herodias* regulates seagrass-associated epifauna. *Oikos*, *124*(11), 1492–1501. https://doi.org/10.1111/oik.01988

Jiménez, A., Elner, R. W., Favaro, C., Rickards, K., & Ydenberg, R. C. (2015). Intertidal biofilm distribution underpins differential tide-following behavior of two sandpiper species (*Calidris mauri* and *Calidris alpina*) during northward migration. *Estuarine, Coastal and Shelf Science*, *155*, 8–16. https://doi.org/10.1016/j.ecss.2014.12.038

Kelly, J. F., Gawlik, D. E., & Kieckbusch, D. K. (2003). An updated account of wading bird foraging behavior. *The Wilson Bulletin*, *115*(1), 105–107. https://doi.org/10.1676/02-053

Kollars, N. M., Henry, A. K., Whalen, M. A., Boyer, K. E., Cusson, M., Eklöf, J. S., Hereu, C. M., Jorgensen, P., Kiriakopolos, S. L., Reynolds, P. L., Tomas, F., Turner, M. S., & Ruesink, J. L. (2017). Meta-analysis of reciprocal linkages between temperate seagrasses and waterfowl with implications for conservation. *Frontiers in Plant Science*, *8*. https://doi.org/10.3389/fpls.2017.02119

Lafferty, K. D. (2001). Disturbance to wintering western snowy plovers. *Biological Conservation*, *101*(3), 315–325. https://doi.org/10.1016/S0006-3207(01)00075-1

Lamberson, J. O., Frazier, M. R., Nelson, W. G., & Clinton, P. (2011). *Utilization patterns of intertidal habitats by birds in Yaquina estuary, Oregon* (EPA/600/R-11/118). U.S. Environmental Protection Agency, Office of Research and Development, National Health and Environmental Effects Research Laboratory, Western Ecology Division.

Lee, S. Y., Fong, C. W., & Wu, R. S. S. (2001). The effects of seagrass (*Zostera japonica*) canopy structure on associated fauna: A study using artificial seagrass units and sampling of natural beds. *Journal of Experimental Marine Biology and Ecology*, *259*, 23–50. https://doi.org/10.1016/S0022-0981(01)00221-0

Mathot, K. J., Piersma, T., & Elner, R. W. (2018). Shorebirds as integrators and indicators of mudflat ecology. In P. G. Beninger (Ed.), *Mudflat Ecology* (pp. 309–338). Springer International Publishing. https://doi.org/10.1007/978-3-319-99194-8_12

McDevitt-Irwin, J., Iacarella, J., & Baum, J. (2016). Reassessing the nursery role of seagrass habitats from temperate to tropical regions: A meta-analysis. *Marine Ecology Progress Series*, *557*, 133–143. https://doi.org/10.3354/meps11848

McLeod, E. M., Guay, P.-J., Taysom, A. J., Robinson, R. W., & Weston, M. A. (2013). Buses, cars, bicycles and walkers: The influence of the type of human transport on the flight responses of waterbirds. *PLoS ONE*, *8*(12), e82008. https://doi.org/10.1371/journal.pone.0082008

Miller, A. K., & de Rivera, C. E. (2014). Small tidal channels improve foraging opportunities for *Calidris* shorebirds. *The Condor*, *116*(1), 113–121. https://doi.org/10.1650/CONDOR-13-003-R1.1

Müllner, A., Eduard Linsenmair, K., & Wikelski, M. (2004). Exposure to ecotourism reduces survival and affects stress response in hoatzin chicks (*Opisthocomus hoazin*). *Biological Conservation*, *118*(4), 549–558. https://doi.org/10.1016/j.biocon.2003.10.003

Navedo, J. G., & Herrera, A. G. (2012). Effects of recreational disturbance on tidal wetlands: Supporting the importance of undisturbed roosting sites for waterbird conservation. *Journal of Coastal Conservation*, *16*(3), 373–381.

Nebel, S., Jackson, D. L., & Elner, R. W. (2005). Functional association of bill morphology and foraging behaviour in calidrid sandpipers. *Animal Biology*, *55*(3), 235–243.

Oksanen, J., Blanchet, F. G., Friendly, M., Kindt, R., Legendre, P., McGlinn, D., Minchin, P. R., O'Hara, R. B., Simpson, G. L., Solymos, P., Stevens, M. H. H., Szoecs, E., & Wagner, H. (2015). *Vegan: Community ecology package* (2.2-1) [Computer software]. https://cran.r-project.org/web/packages/vegan/index.html

Patten, K., & O'Casey, C. (2007). Use of Willapa Bay, Washington, by shorebirds and waterfowl after *Spartina* control efforts. *Journal of Field Ornithology*, *78*(4), 395–400. https://doi.org/10.1111/j.1557-9263.2007.00128.x

Posey, M. H. (1988). Community changes associated with the spread of an introduced seagrass, *Zostera japonica*. *Ecology*, *69*(4), 974–983. https://doi.org/10.2307/1941252

Raposa, K. B., McKinney, R. A., & Beaudette, A. (2009). Effects of tide stage on the use of salt marshes by wading birds in Rhode Island. *Northeastern Naturalist*, *16*(2), 209–224. https://doi.org/10.1656/045.016.0204

Tavares, D. C., Guadagnin, D. L., de Moura, J. F., Siciliano, S., & Merico, A. (2015). Environmental and anthropogenic factors structuring waterbird habitats of tropical coastal

lagoons: Implications for management. *Biological Conservation*, *186*, 12–21. https://doi.org/10.1016/j.biocon.2015.02.027

Thayer, G. W., Bjorndal, K. A., Ogden, J. C., Williams, S. L., & Zieman, J. C. (1984). Role of larger herbivores in seagrass communities. *Estuaries*, *7*(4), 351. https://doi.org/10.2307/1351619

Thom, R. M., Borde, A. B., Rumrill, S., Woodruff, D. L., Williams, G. D., Southard, J. A., & Sargeant, S. L. (2003). Factors influencing spatial and annual variability in eelgrass (*Zostera marina* L.) meadows in Willapa Bay, Washington, and Coos Bay, Oregon, estuaries. *Estuaries*, *26*(4), 1117–1129. https://doi.org/10.1007/BF02803368

van der Zee, E. M., van der Heide, T., Donadi, S., Eklöf, J. S., Eriksson, B. K., Olff, H., van der Veer, H. W., & Piersma, T. (2012). Spatially extended habitat modification by intertidal reef-building bivalves has implications for consumer-resource interactions. *Ecosystems*, *15*(4), 664–673. https://doi.org/10.1007/s10021-012-9538-y

Waycott, M., Duarte, C. M., Carruthers, T. J. B., Orth, R. J., Dennison, W. C., Olyarnik, S., Calladine, A., Fourqurean, J. W., Heck, K. L., Hughes, A. R., Kendrick, G. A., Kenworthy, W. J., Short, F. T., & Williams, S. L. (2009). Accelerating loss of seagrasses across the globe threatens coastal ecosystems. *Proceedings of the National Academy of Sciences*, *106*(30), 12377–12381. https://doi.org/10.1073/pnas.0905620106

Wei, P., Zan, Q., Tam, N. F. Y., Shin, P. K. S., Cheung, S. G., & Li, M. (2017). Impact of habitat management on waterbirds in a degraded coastal wetland. *Marine Pollution Bulletin*, *124*(2), 645–652. https://doi.org/10.1016/j.marpolbul.2017.02.068

Wilson, W. H. (1994). The effects of episodic predation by migratory shorebirds in Grays Harbor, Washington. *Journal of Experimental Marine Biology and Ecology*, *177*(1), 15–25.

Yeoh, D. E., Valesini, F. J., Hallett, C. S., Abdo, D. A., & Williams, J. (2017). Diel shifts in the structure and function of nearshore estuarine fish communities. *Journal of Fish Biology*, *90*(4), 1214–1243. https://doi.org/10.1111/jfb.13222

Chapter 2: Tidal influence on feeding behavior of *Pisaster ochraceus* in a rocky intertidal habitat without mussel beds.

Abstract

Ochre sea stars (*Pisaster ochraceus*) are an apex, keystone predator on wave-exposed coastlines of the US Pacific Ocean, responsible for establishing the vertical zonation of mussel beds and therefore controlling benthic diversity. The studies that have formed the basis of our understanding of this sea star's diet have primarily occurred at low tide and in areas with dominating mussel beds. However, given that intertidal organisms must live in both air and water, often with differing tasks or behaviors depending on where they find themselves, it is critical to study their behavior holistically. Additionally, *P. ochraceus* can be found in relatively high abundance in rocky intertidal habitats devoid of mussels, which may alter the functional role of this predator. Here I present an observational study to understand the diet and feeding behavior of *P. ochraceus* in the field through the tidal cycle at three sites around San Juan Island, Washington, USA, a region that is not currently dominated by mussels. I specifically took into account their time in and out of water, the microhabitats they use, and their size. Sea stars were more likely to be found feeding at high than low water, when outside than in crevices, and as body size increased. When *P. ochraceus* were feeding, they consumed larger prey at low than high water, when inside than outside crevices, and as body size increased. Mussels were rare on these shores and represented <1% of feeding records. With no mussels to consume, *P. ochraceus* may not play the role of a keystone predator in this area. This effort to further understand the role of sea stars in intertidal communities is important because *P. ochraceus* is widespread in many wave exposure regimes but was reduced in density by the recent sea star wasting disease (SSWD) events that caused major population losses of this predator along the US Pacific Coast.

Introduction

Ochre sea stars (*Pisaster ochraceus*) are known for their role as an apex, keystone predator on wave-exposed coastlines of the US Pacific Ocean, responsible for establishing the vertical zonation of mussel beds and therefore controlling benthic diversity (Menge et al., 1994; Paine, 1966, 1969). These wave-exposed rocky shorelines typically have a zone of large mussels (*Mytilus californianus*), which are limited by abiotic conditions at their upper boundary, while predation sets their lower limits. Under laboratory conditions, mussels are a strongly preferred food source, but *P. ochraceus* is also a generalist and consumes many different intertidal invertebrates (Mauzey et al., 1968). In addition to these wave-exposed, mussel-dominated habitats, *P. ochraceus* regularly occupies more wave-protected intertidal habitats that are not characterized by extensive mussel beds. In this study, I observe *P. ochraceus* feeding in one of these areas that lack mussel beds to better understand their diet and feeding behavior.

Intertidal organisms may be considered marine organisms that have to endure being exposed to air for a period of time before returning to their activities. An alternative framework is that they live in both air and water, often with differing needs or behaviors depending on where they find themselves at any given moment. It is critical to study behavior of intertidal organisms holistically, rather than picking and choosing moments and developing an incomplete idea of their interactions. The literature that has formed the basis of our understanding of sea star diet (Feder, 1959; Mauzey, 1966; Paine, 1966) has primarily been based on observations at low tide and in areas with dominating mussel beds.

Water level should strongly influence the performance of sea stars (Fly et al., 2012), which may contribute to their migrating vertically with tides. Water and air temperatures are often distinct, with air temperatures being more variable and more likely to be stressful. Additionally, feeding can be particularly risky in the intertidal zone, as coming out of the water exposes the sea star to stressful abiotic conditions (Burnaford & Vasquez, 2008; Monaco et al., 2015) and terrestrial predators such as birds (Rogers & Elliott, 2013; Suraci & Dill, 2013). Staying lower in the intertidal means avoiding emergence into the air, however there is more competition with other benthic predators. In lab experiments, increased aerial temperatures significantly decreased feeding in *P. ochraceus* (Pincebourde et al., 2008). In the San Juan Islands, extreme low tides occur at night in the winter, but during the summer they coincide with the midday heat and sun exposure. Sea stars frequently find crevices in which to stay cool and moist, avoiding UV exposure and radiative heat gain, particularly during daytime low tides (Monaco et al., 2015). Moving up to reduce competition and find prey can simultaneously increase risk of desiccation and heat stress in the summer if a sea star is caught in the upper intertidal zone as the tide goes out.

Feeding rates and preferences, scaled up by density, directly determine the functional role of sea stars in intertidal systems. Temperature provides a strong control on feeding rate of *P. ochraceus*, as shown by comparison along coasts with different levels of cold-water upwelling (Sanford, 1999), as well as seasonal feeding patterns (higher feeding rates in the summer than winter; (Mauzey, 1966). Both temperature and desiccation can change for sea stars over a tidal cycle, but daily feeding patterns in relation to the tidal cycle have not previously been reported for *P. ochraceus*, likely due to the challenges of observations at shallow depths with high water motion.

In addition to the cyclical change in abiotic conditions in the intertidal zone, body size of can also influence feeding rates and prey composition. Diets of many predators change ontogenetically or depending on size (Nakazawa, 2015). Generally larger predators are expected to be able to consume larger prey, which is one aspect of optimal foraging (Costa et al., 2008; MacArthur & Pianka, 1966). *P. ochraceus* can reach sizes of 2.5 kg wet mass, with maximum size apparently constrained by local prey availability (Paine, 1976).

Here I present an observational study to understand the diet and feeding behavior of *P. ochraceus* in the field through the tidal cycle, taking into account their time in and out of water. Specifically, I test whether feeding rates and diet composition are dependent on 1) vertical location of the sea stars on the rocks, 2) water level (high and low tide, influencing whether sea stars were immersed vs emerged), and 3) the size of the sea star individual. The goal is to establish a better understanding of the diet of *P. ochraceus* living in an area lacking mussel beds, where they cannot act as keystone predators. The specific expectations are: 1) feeding probabilities and diet composition of *P. ochraceus* will reflect access to higher tidal elevations when water levels are higher, and therefore smaller but abundant invertebrate prey are included in diets and 2) feeding probabilities and diet composition change with sea star size. Larger sea stars might feed more frequently, as their size gives them access to a wider spatial area for foraging, and perhaps they can withstand the abiotic conditions of the intertidal better than small stars, yet larger stars might also subsist on their own energy stores, therefore requiring less frequent feeding than in juveniles.

Methods

Study Sites

I observed *P. ochraceus* at three rocky intertidal sites on San Juan Island, WA, USA during the summers of 2017 to 2020 [Point Caution (48.56212, -123.01743), Reuben Tarte (48.61283, -123.09799), Pile Point (48.48238, -123.08750)]. These sites were chosen due to their high sea star abundance relative to other shorelines on the island, with each site having an assigned fixed plot within which every *P. ochraceus* individual was measured throughout the study (Point Caution, $50m^2$; Reuben Tarte, $80m^2$; Pile Point, $100m^2$). None of these sites contains a zone of mussels. Barnacles occupy zones above 0 MLLW on open rock surfaces (outside of crevices).

Data collection

For each individual found, I noted the microhabitat (in or out of crevice), feeding status (feeding or not feeding), and longest arm length to the nearest cm. The longest arm length was measured as the distance from the center of the central disc to the tip of the longest arm. Growth in sea stars is indeterminate, as they grow and shrink with accessibility to prey, and they are highly mutable (can stretch and compress), therefore any size measurements should be taken as approximations. To identify feeding status, I pried each individual off the substrate and observed the oral surface for signs of feeding in or around the mouth. If the individual was feeding, I recorded the identity of their prey to species where possible. Each individual was returned to the substrate as close to where they were picked up as possible. I did not re-survey the same site for a minimum of 48 hours to allow individuals to readjust to their environment after being handled. If the individual was out of reach or too firmly attached to substrate to remove without causing excessive damage, the longest arm length was measured or estimated, and its feeding status was marked as unknown. Out of reach individuals were recorded to gain the most accurate sense of the population size of *P. ochraceus* at the study sites.

The San Juan Islands experience mixed semidiurnal tides, resulting in daytime extreme low tides in the summers and nighttime extreme low tides in the winters. The tidal amplitude is large (mean diurnal tidal range = 2.34 m; https://tidesandcurrents.noaa.gov/stationhome.html?id=9449880). These extreme low tide events resulted in a tidal exchange with a maximum range of 3.46 meters during the time of the study. I classified tidal height into three categories based on Mean Lower Low Water (MLLW) retrieved from the WWW Tide and Current Predictor (Pentcheff, 2019): low tides (below 0m MLLW), medium tides (0 to 1.5m MLLW), and high tides (1.5m and greater MLLW). On days with extreme low tides, I walked along the intertidal zone to collect data, and on days with medium tides, I snorkeled within that same fixed plot. The survey sites did not extend deeper than -1m MLLW due to the thick kelp zone preventing accurate counts within the limited tide survey windows. However, it is possible that stars moved into the kelp zone, where they were not observed/counted. This movement could account for discrepancies in sea star counts at the same site on different days. Water levels higher than +1.5m MLLW limited the surveyor's capability to dive down to retrieve all sea stars within the plot while snorkeling, increasing observation bias, and therefore was set as the upper survey limit.

Analysis

Sea stars were combined for analysis across all sites and dates, and these factors were included as random effects in the statistical model. For all sea stars, I tested whether feeding was related to main effects of water level (below or above mean lower low water, e.g., low or higher tide), location in or out of crevice, and body size. This analysis required a generalized linear mixed model approach, with binomial error structure. Size of diet items was evaluated indirectly for the subset of sea stars that were observed feeding. Barnacles were the smallest prey items. I tested whether feeding on barnacles was related to main effects of water level, location in or out of crevice

and body size. As with feeding/ not feeding, this analysis required a generalized linear mixed model with binomial error. Calculations were carried out in R (R Core Team, 2020) using the lme4 package (Bates et al., 2015).

Results

P. ochraceus was observed 1,078 times in the field in this study around San Juan Island and was observed feeding in 18% of cases where it was possible to reach the sea star. Average density in the study plots across observations was 0.54 sea stars/m2 at Point Caution, 0.49 sea stars/m2 at Reuben Tarte, and 0.18 sea stars/m2 at Pile Point, and variability in number of sea stars observed had coefficient of variation of 58.8 (Fig. 1). Diet items included 13 different taxa of molluscs and crustaceans (Table 1). Probability of feeding was significantly related to all three predictors (Table 2). Sea stars were more likely to be found feeding at high than low water, when outside than in crevices, and as body size increased (Fig. 2 A-C).

Barnacles were the most common item on which *P. ochraceus* fed (Table 1) and were also substantially smaller than all other diet items. The fraction of barnacles (*Balanus glandula* and *Semibalanus cariosus*) in the diet was significantly related to all three predictors (Table 2). Sea stars consumed larger prey at low than high water, when inside than outside crevices, and as body size increased (Fig. 2 A-C). Mussels occurred once out of 170 feeding observations (0.6%).

Discussion

Documenting sea star diet is essential to understanding the effect sea stars have on their prey communities and predict community shifts if sea stars were removed from the system. While such a scenario may have previously seemed unlikely, the abundance of *Pisaster ochraceus* and other asteroids declined precipitously with sea star wasting disease (SSWD) in 2014 and 2015 along the Pacific coast of the US, with significant losses occurring in the San Juan Islands (Eisenlord et al., 2016). In this study, I expand on our understanding of the role of *P. ochraceus* as a benthic predator of the intertidal zone, with a particular focus on a region of their natural range that does not have extensive mussel beds.

Crevices are ideal hiding spots when the tide is low (reduces UV exposure and heat, avoids desiccation), however in the low intertidal zones in the San Juans Islands, these crevices are mostly devoid of their prey, and particularly do not have high representation of barnacles. This prey availability is a likely explanation for the patterns of both feeding frequency and diet composition in relation to habitat. I suggest a food/stress tradeoff in which sea stars are moving out of crevices to find food. This behavior would additionally explain why feeding frequency increased and the fraction of barnacles in the diet increased out of crevices vs. inside. This use of crevices to avoid stress occurs in addition to a more widely reported upward migration of sea stars coincident with higher water levels (Burnaford & Vasquez, 2008; Monaco et al., 2015).

Other studies of the diet of *P. ochraceus* have documented a wide range of prey (Feder, 1959; Mauzey, 1966; Paine, 1966, Fig. 3). Several field studies on feeding of *P. ochraceus* were carried out in the 1950-60s along the US Pacific coast where the dominant intertidal bivalve is *Mytilus californianus*. Barnacles were the most common prey item observed, followed by bivalves and gastropods, though the latter two have a substantially greater caloric value than barnacles

(Menge, 1972; Paine, 1966). In a study of sea star feeding in the San Juan Islands in the 1970s, a variety of prey items occurred (Mauzey, 1966), but apparently mussels (*Mytilus trossulus*) were more abundant at the time, given their representation in sea star diets. However, I did not resurvey the same site due to current low star population. Natural intertidal zonation contributes to *P. ochraceus* consuming different organisms depending on the zone in which they are foraging, since species found at higher elevations would be different from those found lower in the intertidal (C. D. G. Harley & Helmuth, 2003). In contrast to other diet studies, *P. ochraceus* rarely consumed mussels around San Juan Island, which reflects a diet when sea stars don't have mussel beds to feed on. Chitons are actually the most energy-dense prey in terms of calories (Paine, 1966), but they are not found along these intertidal areas in dense numbers. I observed relatively large numbers of katy chitons (*Katharina tunicata*) all along Pile Point, but never observed *Pisaster* feeding on them, only the less common *Mopalia* spp.

Body size in invertebrates is considered a central functional trait (Costello et al., 2015) as it influences the types and rates of interactions. In keeping with this perspective, *P. ochraceus* at larger body sizes were more likely to be feeding on larger-bodied prey, that is, the larger the star, the larger the prey item being eaten. On a mass-specific basis, some food choices are better than others. Optimal foraging incorporates not just energetic value of potential prey items, but also the cost of both searching and handling time (Werner & Mittelbach, 1981). For sea stars, this search time can be a complex function of abundance of prey at different tidal zones. Time is required for sea stars to move up in the intertidal zone at high tide, at which point one could expect that the prey being eaten would be reflective of the prey available at that intertidal height. At high tide, sea stars are exposed to both heat and UV radiation from the sun. To protect themselves, they move

lower in the intertidal into dark, moist crevices to avoid sun damage and desiccation. However, these crevices contain sparse densities of prey items, so the sea stars cannot stay there for feeding.

Since California mussels are the space-dominating species that creates the strong interaction making Pisaster a 'keystone' predator along the outer coast, a lack of those mussel beds in the San Juan Islands suggests the sea stars may not be playing the same 'keystone' role in this area. An alternative idea is that the sum of all top-down consumers completely exclude mussels. There are still mussels settling in the area, but they are rapidly eaten by predators (C. Harley, 2011). As a further example, exclusion cages that I placed at Reuben Tarte in 2019 were removed in 2021, at which point five of 54 cages contained *M. trossulus*. Therefore, if sea stars are preventing mussels from inhabiting lower intertidal zones (and therefore all zones in the San Juan Islands), I might still consider them to be keystone predators. Rather than keeping the mussels from spreading, predation keeps them from establishing. On the other hand, neither my cages nor prior work (C. Harley, 2011) distinguished which predators were being kept out by cages, so mussels might also be consumed by almost any mobile predator (sea stars, crabs, birds and large dog whelks).

This effort to record sea star feeding through the tidal cycle is important because *P. ochraceus* is still heavily studied, both for SSWD and in looking at its impact as a predator in the intertidal. My data suggest that continuing to survey sea stars at low tide (when convenient to most researchers) potentially misses a significant portion of the organism's life in which the behaviors are drastically different than when exposed to air.

Acknowledgements

Thank you to the many individuals who assisted me in the field surveying sea stars. I would particularly like to acknowledge Hilary Hayford for her insights on intertidal patterns of mobile benthic species and Chris Jendrey for his assistance in the field and supplemental work on *Pisaster ochraceus* movement using videography.

Tables

Table 1. Frequency of prey being fed on by *Pisaster ochraceus*, observed during the summers of 2018 to 2020 and summed across all three study sites on San Juan Island, WA.

Species	Group	Frequency
Balanus glandula	barnacle	115
Semibalanus cariosus	barnacle	23
Mopalia sp.	gastropod	14
Nucella lamellosa	gastropod	6
Tegula sp.	gastropod	2
Lottia sp.	gastropod	2
Calliostoma ligatum	gastropod	2
Pollicipes polymerus	barnacle	1
Crassostrea gigas	bivalve	1
Katharina tunicata	chiton	1
Hemigrapsus oregonensis	crab	1
Pagurus sp.	crab	1
Mytilus trossulus	bivalve	1
	Total	**170**

Table 2. Generalized linear regression model statistics using a binomial distribution. Both models used a feeding proportion as the response variable (model 1: proportion of stars feeding, model 2: proportion of feeding stars that were eating small prey), with tide height and star location as fixed effects, star radius as a covariate, and site and date as random effects.

Model 1	Estimate	SE	z-value	*p*-value
(Intercept)	-1.088	0.456	-2.387	0.017*
Tide height	-0.561	0.399	-1.403	0.161
Location (crevice)	-1.867	0.230	-8.100	< 0.001*
Star radius (size)	0.006	0.003	2.171	0.029*
Model 2	Estimate	SE	z-value	*p*-value
(Intercept)	4.7814	1.224	3.906	< 0.001*
Tide height	-1.410	0.478	-2.951	0.003*
Location (crevice)	-1.491	0.483	-3.086	0.002*
Star radius (size)	-0.026	0.008	-3.303	<0.001*

Figures

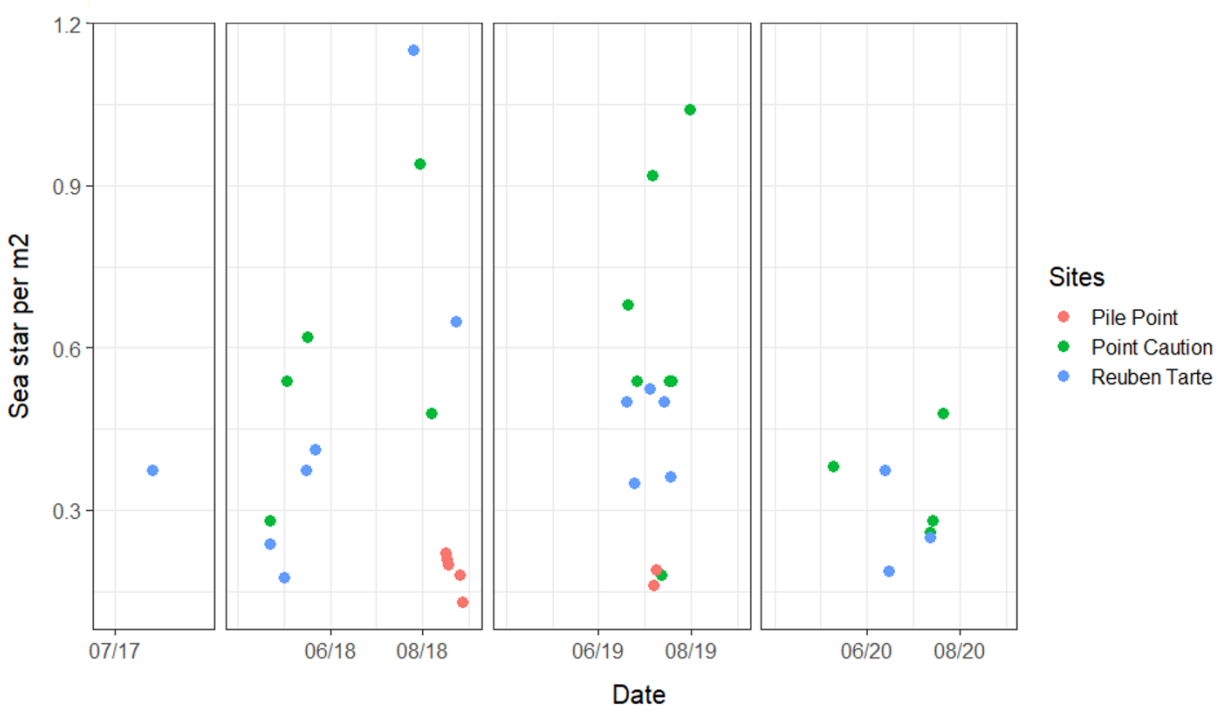

Figure 1. Density (number of individuals per m^2) of *Pisaster ochraceus* observed during the spring and summers of 2017 to 2020 across three sites (Pile Point, Point Caution, Reuben Tarte) in the San Juan Islands, Washington, USA.

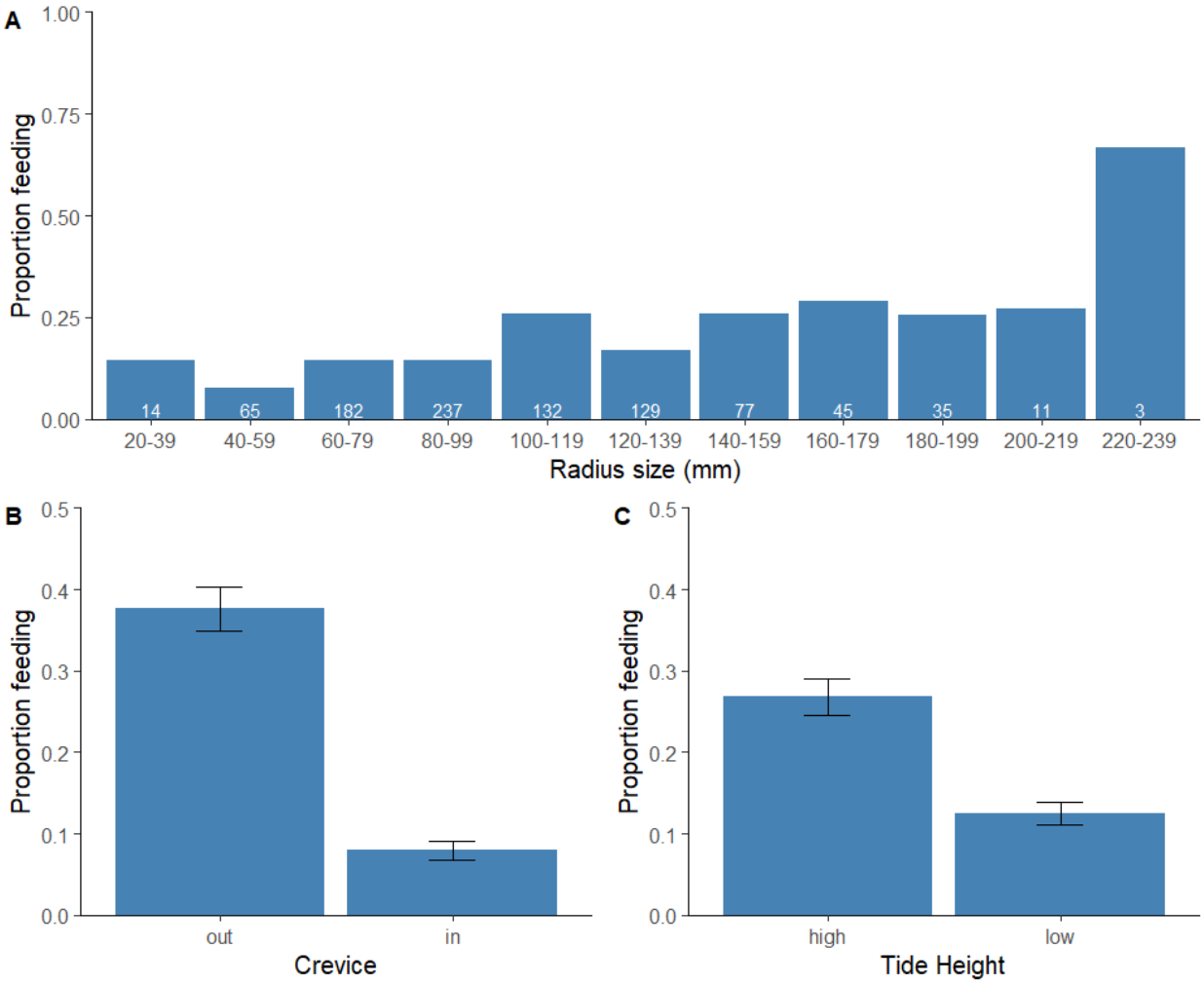

Figure 2. Top: A) Proportion of *Pisaster ochraceus* observed feeding relative to their radius (central disc to longest arm, 10mm bins) during the summers of 2017 to 2020 in the San Juan Islands, WA, USA. Numbers at the base of each bar indicates the sum of sea stars observed feeding for each size bin. Bottom: Proportion (mean ± SE) of sea stars observed feeding when B) water levels were high or low with the change of the tides and C) in and out of crevices.

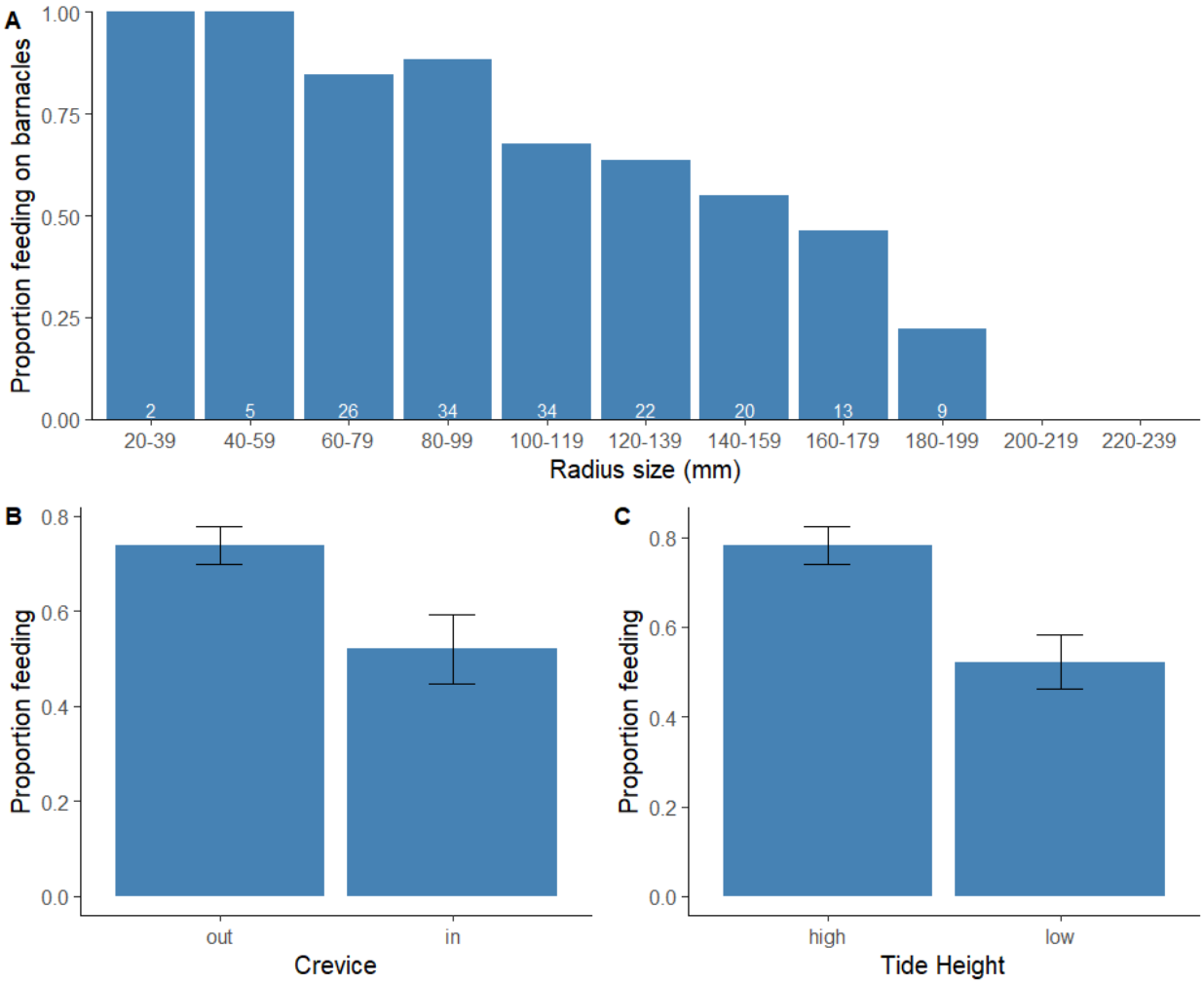

Figure 2. Top: A) Proportion of feeding *Pisaster ochraceus* observed eating small prey (= *Balanus glandula* and *Semibalanus cariosus*) relative to their radius (central disc to longest arm, 10mm bins) during the summers of 2017 to 2020 in the San Juan Islands, WA, USA. Numbers at the base of each bar indicates the sum of sea stars observed feeding for each size bin. Bottom: Proportion (mean ± SE) of sea stars observed feeding on small prey when B) water levels were high or low with the change of the tides and C) in and out of crevices.

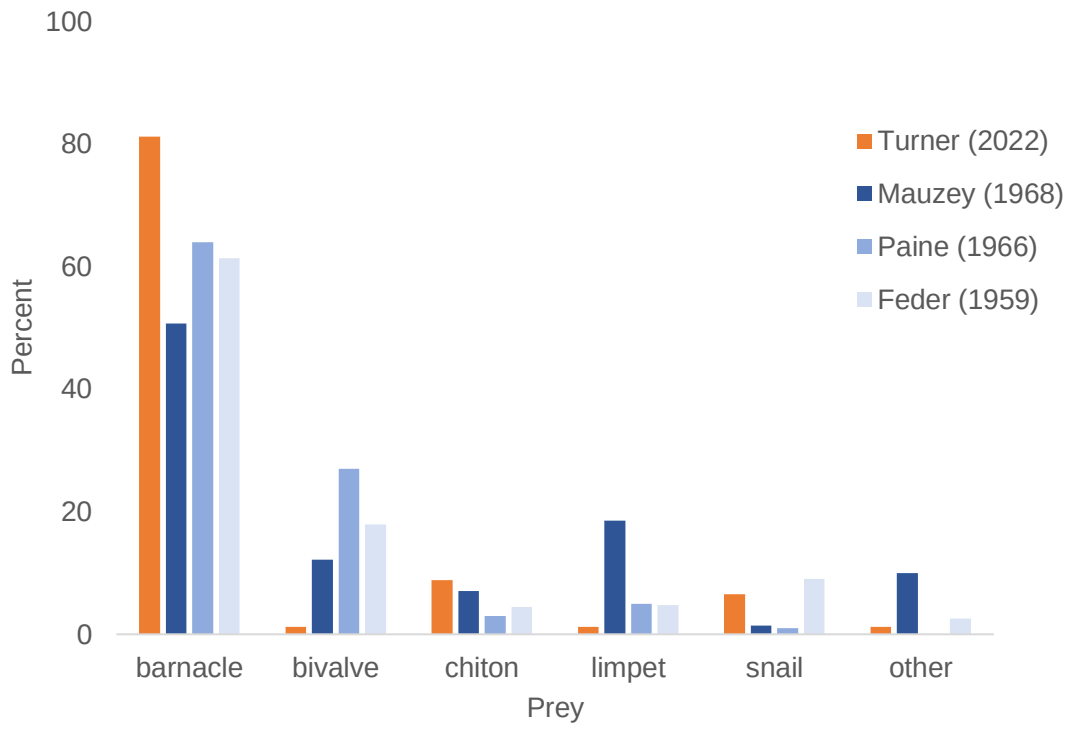

Figure 3. Comparison of diets of *Pisaster ochraceus* observed in the field from this study and three others from the literature: Mauzey et al. 1968, Paine 1966, Feder 1959. Both the Paine and Feder studies occurred along the outer Pacific Coast of the US, characterized by the presence of the dominant bivalve *Mytilus californianus*. The Mauzey and Turner studies occurred along the inner waters of Washington State, where there is little to no *M. californianus*.

Literature Cited

Bates, D., Maechler, M., Bolker, B., & Walker, S. (2015). Fitting Linear Mixed-Effects Models Using lme4. *Journal of Statistical Software*, *67*(1), 1–48. https://doi.org/10.18637/jss.v067.i01

Burnaford, J., & Vasquez, M. (2008). Solar radiation plays a role in habitat selection by the sea star Pisaster ochraceus. *Marine Ecology Progress Series*, *368*, 177–187. https://doi.org/10.3354/meps07598

Costa, G. C., Vitt, L. J., Pianka, E. R., Mesquita, D. O., & Colli, G. R. (2008). Optimal foraging constrains macroecological patterns: Body size and dietary niche breadth in lizards. *Global Ecology and Biogeography*, *17*(5), 670–677. https://doi.org/10.1111/j.1466-8238.2008.00405.x

Costello, M. J., Claus, S., Dekeyzer, S., Vandepitte, L., Tuama, É. Ó., Lear, D., & Tyler-Walters, H. (2015). Biological and ecological traits of marine species. *PeerJ*, *3*, e1201. https://doi.org/10.7717/peerj.1201

Eisenlord, M. E., Groner, M. L., Yoshioka, R. M., Elliott, J., Maynard, J., Fradkin, S., Turner, M., Pyne, K., Rivlin, N., van Hooidonk, R., & Harvell, C. D. (2016). Ochre star mortality during the 2014 wasting disease epizootic: Role of population size structure and temperature. *Philosophical Transactions of the Royal Society B: Biological Sciences*, *371*(1689), 20150212. https://doi.org/10.1098/rstb.2015.0212

Feder, H. M. (1959). The Food of the Starfish, Pisaster Ochraceus Along the California Coast. *Ecology*, *40*(4), 721–724. https://doi.org/10.2307/1929828

Fly, E. K., Monaco, C. J., Pincebourde, S., & Tullis, A. (2012). The influence of intertidal location and temperature on the metabolic cost of emersion in Pisaster ochraceus. *Journal of*

Experimental Marine Biology and Ecology, *422–423*, 20–28. https://doi.org/10.1016/j.jembe.2012.04.007

Harley, C. (2011). Climate Change, Keystone Predation, and Biodiversity Loss. *Science*, *334*(6059), 1124–1127. https://doi.org/10.1126/science.1210199

Harley, C. D. G., & Helmuth, B. S. T. (2003). Local- and regional-scale effects of wave exposure, thermal stress, and absolute versus effective shore level on patterns of intertidal zonation. *Limnology and Oceanography*, *48*(4), 1498–1508. https://doi.org/10.4319/lo.2003.48.4.1498

MacArthur, R. H., & Pianka, E. R. (1966). On Optimal Use of a Patchy Environment. *The American Naturalist*, *100*(916), 603–609. https://doi.org/10.1086/282454

Mauzey, K. P. (1966). Feeding behavior and reproductive cycles in Pisaster ochraceus. *The Biological Bulletin*, *131*(1), 127–144. https://doi.org/10.2307/1539653

Mauzey, K. P., Birkeland, C., & Dayton, P. K. (1968). Feeding Behavior of Asteroids and Escape Responses of their Prey in the Puget Sound Region. *Ecology*, *49*(4), 603–619. https://doi.org/10.2307/1935526

Menge, B. A. (1972). Foraging Strategy of a Starfish in Relation to Actual Prey Availability and Environmental Predictability. *Ecological Monographs*, *42*(1), 25–50. https://doi.org/10.2307/1942229

Menge, B. A., Berlow, E. L., Blanchette, C. A., Navarrete, S. A., & Yamada, S. B. (1994). The Keystone Species Concept: Variation in Interaction Strength in a Rocky Intertidal Habitat. *Ecological Monographs*, *64*(3), 249–286. https://doi.org/10.2307/2937163

Monaco, C., Wethey, D., Gulledge, S., & Helmuth, B. (2015). Shore-level size gradients and thermal refuge use in the predatory sea star Pisaster ochraceus: The role of environmental

stressors. *Marine Ecology Progress Series*, *539*, 191–205. https://doi.org/10.3354/meps11475

Nakazawa, T. (2015). Ontogenetic niche shifts matter in community ecology: A review and future perspectives. *Population Ecology*, *57*(2), 347–354. https://doi.org/10.1007/s10144-014-0448-z

Paine, R. T. (1966). Food web complexity and species diversity. *The American Naturalist*, *100*(910), 65–75.

Paine, R. T. (1969). A note on trophic complexity and community stability. *The American Naturalist*, *103*(929), 91–93.

Paine, R. T. (1976). Size-Limited Predation: An Observational and Experimental Approach with the Mytilus-Pisaster Interaction. *Ecology*, *57*(5), 858–873. https://doi.org/10.2307/1941053

Pentcheff, D. (2019). *WWW Tide and Current Predictor*. http://tbone.biol.sc.edu/tide/index.html

Pincebourde, S., Sanford, E., & Helmuth, B. (2008). Body temperature during low tide alters the feeding performance of a top intertidal predator. *Limnology and Oceanography*, *53*(4), 1562–1573. https://doi.org/10.4319/lo.2008.53.4.1562

R Core Team. (2020). *R: A language and environment for statistical computing*. R Foundation for Statistical Computing. https://www.R-project.org/

Rogers, T. L., & Elliott, J. K. (2013). Differences in relative abundance and size structure of the sea stars Pisaster ochraceus and Evasterias troschelii among habitat types in Puget Sound, Washington, USA. *Marine Biology*, *160*(4), 853–865. https://doi.org/10.1007/s00227-012-2139-7

Sanford, E. (1999). Regulation of Keystone Predation by Small Changes in Ocean Temperature. *Science*, *283*(5410), 2095–2097. https://doi.org/10.1126/science.283.5410.2095

Suraci, J. P., & Dill, L. M. (2013). Short timescale rate maximization by gulls and implications for predation on size-structured prey. *Behavioral Ecology*, *24*(1), 280–292. https://doi.org/10.1093/beheco/ars165

Werner, E. E., & Mittelbach, G. G. (1981). Optimal Foraging: Field Tests of Diet Choice and Habitat Switching. *American Zoologist*, *21*(4), 813–829. https://doi.org/10.1093/icb/21.4.813

Chapter 3: Comparative skeletal morphology of Pacific Northwest sea stars

Abstract

Armor in sea stars comes in the form of a highly articulated endoskeleton made up of individual pieces called ossicles. Many descriptive studies have been conducted on the basic patterning of sea star skeletons, with differences in shapes of ossicles forming the basis of early echinoderm phylogenies. However, the functional value of sea star ossicles is not necessarily in the characteristics of individual pieces, but rather in how those pieces are arranged and their relative contributions to the skeleton as a whole. In this study, we use micro-computed tomography to measure and compare morphological differences in the patterns of endoskeleton allocation of nine sea star species local to Washington, USA. For a set of 14 quantitative morphological traits, we tested for: 1) correlations and tradeoffs among these traits and 2) correspondence of morphological similarity to two possible predictors, specifically ecology and phylogeny. Given the ecological and phylogenetic diversity of stars included in this study, we expected to see 1) differences in the amount of armoring (relative volume of skeleton) and that 2) those differences arise from varying allocation and shape of ossicles across different regions of the body.

While all sea stars share the same five basic types of ossicles, the amount of skeletal armoring across the body varied by at least an order of magnitude across species and differed in its distribution across ossicle types. Heavily armored stars invest in larger, boxy body wall ossicles, whereas a reduction in armor volume was often paired with more intricately shaped body wall ossicles and an increase in the number and complexity of spines. Skeletal patterning and allocation are more correlated with phylogenetic than ecological differences. More research is needed to understand which morphological traits are phylogenetically conserved, which could provide an opportunity to better use phylogeny to understand trait evolution.

Introduction

Armoring appears frequently in animal evolution due to its value as protection, offense, camouflage, and structural support (Edmunds, 1974). Examples of armoring can be found across phyla and often manifest as shell, scales, thickened skin, spines, horns, and endo- or exoskeletons, each of which is accompanied by its own suite of tradeoffs (Lakowitz et al., 2008; Laver et al., 2020; Taylor & Patek, 2010; Yang et al., 2012). For invertebrates, the most common material used for armoring is calcium carbonate ($CaCO_3$; Vermeij, 1989). Varying the defensive capability of calcium carbonate is typically achieved through modifying the mass or shape of the armor or reinforcing it with a different material. Increasing the mass of armor (increasing extent or thickness) requires greater energy allocation and is heavier (Kruppert et al., 2020; Lakowitz et al., 2008), so that increased protection may come at the expense of speed. For example, limpets and snails are slow with heavy armor while shrimp are fast with light armor. Similarly, maneuverability and flexibility can be greatly affected by the amount of armoring (Hazerli & Richter, 2020). Invertebrates rarely have armor that can bend. Instead, flexibility is achieved at the junctions of armor, making it possible for a change in armor shape to increase mobility while still conferring protection.

In sea stars, armor comes in the form of a highly articulated endoskeleton made up of small calcium carbonate pieces called ossicles. These are heavily armored organisms, often perceived as slow or almost sedentary, however most are active predators, with the fastest species, *Pycnopodia helianthoides*, reaching speeds of up to 1.5m per minute (Mauzey et al., 1968). The skeleton creates a scaffolding just below the dermis that supports and protects the internal organs and can help maintain the shape of the organism when removed from the water. Sea stars are exclusively benthic

as adults and can be found from mid intertidal zones to the deepest ocean trenches. They exhibit a similarly wide range in diet, from scavengers and suspension feeders to active predators, cannibals, and specialist consumers of other sea star species (Lawrence, 2013). In many of their ecosystems, sea stars are the apex predator and, in some cases, a keystone species (Paine, 1966, 1969), so understanding the role their armor plays in keeping them protected and mobile is a worthy pursuit.

There are five major types of ossicles in the ray of a sea star: ambulacral, adambulacral, carinal, reticular, and marginal (Blowes et al., 2017; Eylers, 1976; Fig. 1). The adambulacral and ambulacral ossicles together form the ambulacral groove, creating a concave space on the oral side of the body that houses the soft tissue tube feet. The carinal, reticular, and marginal ossicles together make up the aboral body wall of the endoskeleton. The carinal ossicles are a central row of ossicles that run along the top of the aboral side of the body wall from ray tip to the center of the star like a spine of the ray. Marginal ossicles are a collection of ossicles that connect the body wall to the ambulacral groove. The remaining meshwork of the body wall consists of reticular ossicles. In addition to these five major types of ossicles, sea star species can also have spines, the presence, size, shape, and distribution of which is species specific. For species within the Superorder Forcipulatacea, the aboral surface of the body wall can be covered in pedicellariae, which are small pinching claws supported by a flexible, soft tissue stalk (Blake, 1987). The claws but not the stalks of the pedicellariae are made of calcium carbonate and therefore are visible as floating ossicles in an x-ray of a sea star skeleton. Many descriptive studies have been carried out on the basic patterning of sea star skeletons and the shapes of individual ossicles (e.g. Blowes et al., 2017; Fau & Villier, 2020; Gale, 2018). These descriptions of ossicles highlight that their shapes differ substantially and can be diagnostic of particular taxa (Fau & Villier, 2020). However, the functional value of sea star ossicles is not necessarily in the characteristics of individual pieces,

but rather in how those pieces are arranged and their relative contributions to the skeleton as a whole. Computed tomography (CT) has advanced as a method that enables three-dimensional resolution of skeletons of intact sea stars, a method that we apply here in the development of skeletal trait metrics.

In this study, we use micro-computed tomography to measure and compare morphological differences in the endoskeleton of nine sea star species local to Washington, USA. We qualitatively describe general patterns of shapes and arrangements of the ossicles and spines. The general sea star body plan in post-settlement stages has radial symmetry with four or more rays (Lawrence, 2013). In contrast, because of the known variety of ossicle shapes, size, and number, the endoskeleton in sea stars has the potential to span a much greater range of morphologies than the external body plan would indicate. In particular, we focus on traits that are newly amenable to quantification through the application of CT, particularly attributes of robustness (amount of endoskeletal material) and the distribution of that material in large "boxy" pieces or more structurally complex arrangements. We provide detailed views within the rays, as these reflect movement and protection capabilities, and the mouth, related to feeding capability. For a set of 14 quantitative morphological traits, we tested for: 1) correlations and tradeoffs among these traits, once size corrected, and 2) correspondence of morphological similarity to two possible predictors, specifically ecology and phylogeny. Given the wide ecological and phylogenetic diversity of stars included in this study, we expected to see 1) differences in the amount of armoring (relative volume of skeleton) and that 2) those differences arise not only in size but in varying allocation and shape of ossicles across different regions of the body.

Methods

Specimen collection and micro-computed tomography

Sea stars were collected in the San Juan archipelago (San Juan County, WA, USA) from tidepools by hand and the subtidal environment by SCUBA diving and trawling. Stars were relaxed in Magnesium chloride, then put in 10% formaldehyde for 24 hours, after which they were rinsed in water and put in 70% ethanol for storage. Stars were CT scanned wrapped in cheesecloth wetted with ethanol. All specimens were CT scanned with a Bruker SkyScan 1173, using the high-resolution detector, a 1mm aluminum filter, and energies ranging from 80-133kV and 40-80μA. Groups of specimens were wrapped in damp cheesecloth and placed together into a 3D printed plastic cylinder. The entire cylinder was wrapped in plastic film to ensure it was airtight, then mounted on a rotating stage in the scanner. Once the specimen scans were completed, approximately 10mm of a ray tip from each individual was removed using a scalpel and scanned again at a higher resolution (30-35μm/pixel for whole specimens, 8μm/pixel for arms). Images were reconstructed with nRecon (Bruker Systems) and visualized with 3D Slicer (Fedorov et al., 2012).

Segmentation and measurements

In CT-scan analysis, segmentation is the process of digitally isolating a portion of the 3D data that can then be manipulated or measured. Skeletal morphology and body tissue were segmented using grayscale intensity thresholding, grow seeds and manual slice-by-slice editing. In addition to creating segments of the different regions (body wall and ambulacral groove) and types of ossicles, we also isolated a cross-sectional unit of the ray representing one set of repeated ossicles (here referred to as a "ray band"). Volume (mm^3) of each segment was measured using

the Statistical Quantification Module in 3D Slicer. The total specimen volume included tissue, skeleton, and the internal body cavity. Since the specimens differed in absolute size, it was necessary to quantify traits that would enable comparison among species without a confounding effect of size, e.g. more total ossicle volume in larger specimens. Size correction was carried out in most cases by calculating ratios among body parts, which then emphasized shape rather than size characteristics (Table 1). Geometric morphometrics is another method for comparing shapes independent of size but is not suitable for flexible taxa since the landmarks must stay in the same relative positions (Zelditch et al., 2012). Ray length for each specimen was measured from the tip of the longest ray to the center of the central disc. The central disc radius was measured from the armpit to the center of the star.

Skeletal traits

We examined the CT-scan of each species and qualitatively described differences in endoskeletal arrangement of ossicles in terms of body wall organization, body wall ossicle shape, and spines. In addition, we extracted numerical trait values that corresponded to the number and robustness of different parts of the skeleton at different scales (from ossicle to whole-organism scale; Table 1). We specifically examined how much of the volume of each species consisted of skeleton (that is, armoring investment), and then used this gradient in armoring to explore 1) armoring specifically in ray tips, 2) relative amount of armoring around the ambulacral groove, 3) surface area relative to volume of ossicles within a ray band, an index of how convoluted the skeletal surface is, and 4) external shape in terms of ray length relative to central disc size. For mouth traits, we examined size of oral spines (here currently called teeth, standardized to body size) in relation to number; number of teeth was not size-standardized since it appears fixed within

species rather than changing ontogenetically. The full suite of 14 quantity and robustness traits were incorporated into principal components analysis (PCA; ggbiplot package in R, Vu, 2011) and hierarchical clustering to visualize correlations among traits and which species had particular suites of traits. PCA was carried out on scaled variables.

Comparison of morphological, ecological, and phylogenetic distance matrices

We calculated three distance matrices across the nine species based on morphological traits, ecological traits, and phylogenetic relationships. Ecological traits (diet, habitat, and predators) were collected from multiple literature sources (Flowers & Foltz, 2001; Kozloff et al., 1996; Mauzey et al., 1968; Rodenhouse & Guberlet, 1946), and converted into binary categories. For the ecological (Table 2) and morphological (Table 1) traits, dissimilarities were calculated using Gowers distances (FD package in R, Laliberté et al., 2014) for each pairwise species comparison. Phylogenetic distances were based on a consensus tree of base-pair substitutions in nuclear sequence data (18S rDNA, 28S rDNA, and histone H3) and mitochondrial sequence data (S12 rDNA, S16 rDNA, tRNA cluster, and cytochrome *c* oxidase 1) (Janies et al., 2011). Because one of our species (*Mediaster aequalis*) was not included in this published phylogenetic tree, we used a second published tree (C. Mah & Foltz, 2011) that contained that species and three others from this study to estimate relative distance. Correlations were tested statistically between the morphological distance matrix and the ecological and phylogenetic distance matrices.

Results

Overall comparative morphology

We surveyed nine species of sea stars: *Crossaster papposus* (Fig. 4-5), *Dermasterias imbricata* (Fig. 6-7), *Evasterias troschelii* (Fig. 8-9), *Henricia sp.* (Fig. 10-11), *Leptasterias sp.* (Fig. 12-13), *Mediaster aequalis* (Fig. 14-15), *Pisaster ochraceus* (Fig. 16-17), *Pteraster tesselatus* (Fig. 18-19) and *Solaster stimpsoni* (Fig. 20-21). In observing ossicle arrangement in the body wall, we characterized three general patterns: 1) ossicles aligned in one or more distinct rows running from ray tip to central disc, 2) an even, grid-like distribution of ossicles, and 3) a meshwork of connected ossicles in the form of polygons (pentagons or hexagons, depending on the species). The shape and size of the ossicles that make up the body wall were either relatively uniform across the body or a meshwork of larger ossicles connected by a series of smaller, elongated ossicles. Spines along the body wall were observed in eight of the nine species, with *D. imbricata* only having spines present along the ambulacral groove. When spines were present along the body wall, they were either found uniformly on every ossicle or only on select, larger ossicles. See Table 3 for the breakdown of species across these patterns. Using the 14 numerical traits on quantity and robustness of ossicles, a hierarchical cluster analysis of morphological dissimilarities (Fig. 22) suggests that the observed species fall into three clusters of skeletal organization. Heavily armored species appear in the upper right-hand section of the PCA biplot (Fig. 23). The loadings of traits show that the ossicles of less-armored species tend to be convoluted and highly represented by spines (lower left portion of graph). The three species with pedicellariae, which clustered in the lower right-hand section of the PCA biplot, also tended to have fewer teeth and ambulacral spines. PCA indicated a positive relationship between whole-body and ray-tip armoring (confirmed in Fig. 25), negative relationship between whole-body and ambulacral armoring (or, in other words, increased armoring disproportionately occurring not around the

ambulacral groove, Fig. 26), and tradeoffs between armoring and ossicle structural complexity (confirmed in Fig. 27).

Armor volume ratios

Total body armoring (volume of skeleton relative to total body volume) ranged from 3 to 39%, with *P. tesselatus* having the least amount of armor and *M. aequalis* and *Leptasterias sp.* having the most (37 and 39% respectively, Fig. 24). For all nine species, the ray tips were more heavily armored than the body as a whole (range 27-69%, Fig. 25). As total body armoring increased, armoring in the ray tips increased but at a slower rate and was not distributed evenly across the different ossicle types. In the least armored star, the ambulacral groove made up 62% of the ray tip skeleton but fell as low as 23% in more heavily armored stars (Fig. 26), suggesting that the increase in armoring in stars comes from adding more or larger reticular, marginal, and carinal ossicles and/or spines. This increase in body wall ossicles is also paired with a decrease in surface area to volume ratio, calculated from the cross-sectional ray band (Fig. 27). As armoring increases across the body, the overall shape becomes less convoluted. Along that same axis, overall body shape shifts from short to long arms relative to the length of the central disc (Fig. 28). Tooth length (relative to radius of the central disc) is not correlated with number of teeth per oral ossicle, however the two stars with the most arms (*C. papposus* and *S. stimpsoni*) also had the greatest number of teeth per oral ossicle (Fig. 29).

Phylogeny and ecology

We compared pairwise differences in skeletal traits among nine sea star species against phylogenetic distances (from Janies et al., 2011 and Mah & Foltz, 2011). Morphological

differences in armor morphology were weakly correlated with phylogenetic distance (cor.test in R; p = 0.007, C= 0.44; Fig. 30). Three species generated pairwise comparisons that were similar in both phylogeny and morphology: *E. troschelii*, *P. ochraceus*, and *Leptasterias sp.* In contrast, these three species had rather high phylogenetic distance from *Henricia* sp., but convergent morphology (Fig. 30, lower right-hand corner). Morphological distance also had a positive but weak correlation with ecological distance (p = 0.03, C=0.37; Fig. 31). Correlation of phylogenetic and ecological distance (p = 0.02, C= 0.39) was high relative to how well ecological distance correlated with morphological relationships but low relative to how well phylogenetic distance correlated with morphological relationships.

Discussion

Endoskeletons of sea stars exhibit morphological variety that extends well beyond the description of the diagnostic shapes of particular ossicles. While all sea stars share the same five basic types of ossicles, the amount of skeletal armoring across the body varies by an order of magnitude or more across species and differs in its distribution across ossicle types. Heavily armored stars invest in larger, boxy body wall ossicles, whereas a reduction in armor volume is often paired with more intricately shaped body wall ossicles and an increase in the number and complexity of spines. While individual ossicle shapes have been thoroughly described through dissection and scanning electron microscopy (e.g. Blowes et al., 2017; Fau & Villier, 2020; Gale, 2018), these arrangement patterns at the scale of whole-specimen and ossicle type have typically not been included as morphological traits in a phylogenetic or ecological context. Computed tomography gives us the opportunity to observe arrangement patterns at the scale of the whole

organism and body region as well as shape of individual ossicles, all while maintaining three dimensional positional relationships among ossicles.

Placing these skeletal trait comparisons in the context of echinoderm phylogenies raises an ongoing challenge of which traits are used to construct phylogenies. The phylogeny of Asteroidea is yet to be resolved, and the organization of higher-level taxonomic relationships is sensitive to which parameters and analytic tools are chosen in building trees (Janies et al., 2011). However, we know that some aspects of sea star morphology can depart substantially from close evolutionary relatives. For instance, multi-armed stars (6+ arms) show convergence of morphological traits across multiple families, namely shape and articulation of ossicles around the oral frame and a reduced aboral body wall (Fau & Villier, 2020). These convergences indicate functional value, likely for active predatory behavior, rather than expression of homologous characters. In other cases, morphological traits continue to align with (and are possibly constrained by) phylogenetic similarities, such as the presence of pedicellariae exclusively in Forcipulatida or pointed tube feet in Paxillosida (C. L. Mah & Blake, 2012).

Overall, these examples illustrate the importance of differentiating which traits are phylogenetically constrained and which are malleable to ecology or function. Computed tomography offers a different suite of traits that can be quantified and compared, including advancements in soft tissue imaging in echinoderms (Ziegler, 2019). Schwertmann et al., 2019 identified two new joint types between ossicles using CT scans of *Asterias rubens* and developed biomechanical models of ray bending based on ossicle shape and connections. CT has previously been used in only a handful of publications to examine skeletal traits in sea stars (Blowes et al., 2017; O'hara et al., 2019; Schwertmann et al., 2019; Ziegler, 2019). Indeed, CT scanning is still relatively new to the invertebrate community compared to the vertebrate community which has

built up an online, open-source repository for CT data (Morphosource, www.morphosource.org). One present limitation is that a micro-CT scanner is too small for the maximum body size in most sea star species in this study. In some cases, juvenile (pre-reproductive) individuals may have been scanned, which could influence the body volume to armor ratio due to the lack of gonads in these individuals (Barker & Nichols, 1983). For all samples, age was unknown: sea stars have indeterminate growth and the capacity to both grow and shrink in size (Feder, 1970; Sebens, 1987). We defined skeletal traits in this study that were size-standardized, in order to reduce any influence of absolute specimen size. At the same time, we did not age- or stage-standardize, since some specimens were from relatively small and others from relatively large individuals for that species. Overall, longest ray length ranged 12-79mm with a mean of 43mm. In a follow up study, it would be important to scan individuals of varying size within one species to understand these shape and pattern changes over ontogeny. Additionally, there are more species locally, but for the larger species we could only scan them if we happened to come across an individual small enough to fit in the scanner, which may or may not have been a juvenile. From this starting point, opportunities exist for more sea star species to be scanned and made available so that we can continue to understand these patterns across a broader range of ecologies and phylogenetic relationships.

Acknowledgements

This work would not have been completed without my collaborator, Cassandra Donatelli, who introduced me to the micro-CT scanner and the world of morphology and would both be considered a co-author when developing the manuscript for publication. I would also like to thank Karly Cohen for her insights into armoring and morphology. Finally, thank you to the UW Friday Harbor Laboratories and Karl Liem Imaging Facility for allowing me access and use of the imaging equipment.

Tables

Table 1. Morphological traits defined in this study for nine species of sea stars.

Scale	Robustness	Quantity
Whole specimen	Skeleton : whole body volume	Central disc radius : longest ray length
Ray (whole)	Skeleton : whole ray volume	No. of arms
Ray (cross-section)	Surface area : volume	No. of spine clusters / ray band
Ambulacral groove	Ambulacral groove : ray skeleton	No. of spines / adambulacral ossicle
Body wall	Carinal (ossicle + spine) : whole ray band volume	Presence/absence of pedicellariae
Spines	All spines : whole ray band volume	No. of spines / cluster
Mouth	Teeth length : central disc radius	No. of teeth / oral ossicle

Table 2. Ecological traits defined in this study for nine species of sea stars.

Categories	Binary Columns: each trait scored as 0/1 for each species
Diet	Cnidarians, sponge, gastropods, bivalves, barnacles, tunicates, echinoderms
Habitat	Rock, cobble, sand/mud
Predator	Echinoderms, (removed gulls because of high correlation with “intertidal”)
Location	Intertidal

Table 3. Qualitative comparison of endoskeletal arrangement

Scale	Pattern	Species
Body wall organization	1. One or more distinct rows of ossicles running from ray tip to central disc	*Evasterias, Leptasterias, Pisaster*
	2. More grid-like, evenly distributed	*Henricia, Mediaster, Pteraster, Solaster*
	3. Meshwork of ossicles form regular polygons	*Crossaster, Dermasterias*
Body wall ossicle shape	1. Uniform shape and size throughout body wall	*Henricia, Leptasterias, Mediaster, Pteraster, Solaster*
	2. A few larger ossicles connected to each other by a webbing of thin, elongated ossicles	*Crossaster, Evasterias, Leptasterias, Pisaster*
Spines	1. No spines on the body wall	*Dermasterias*
	2. Spines on select, larger ossicles	*Crossaster, Evasterias, Pisaster*
	3. Spines on every ossicle	*Henricia, Leptasterias, Pteraster, Solaster*

Figures

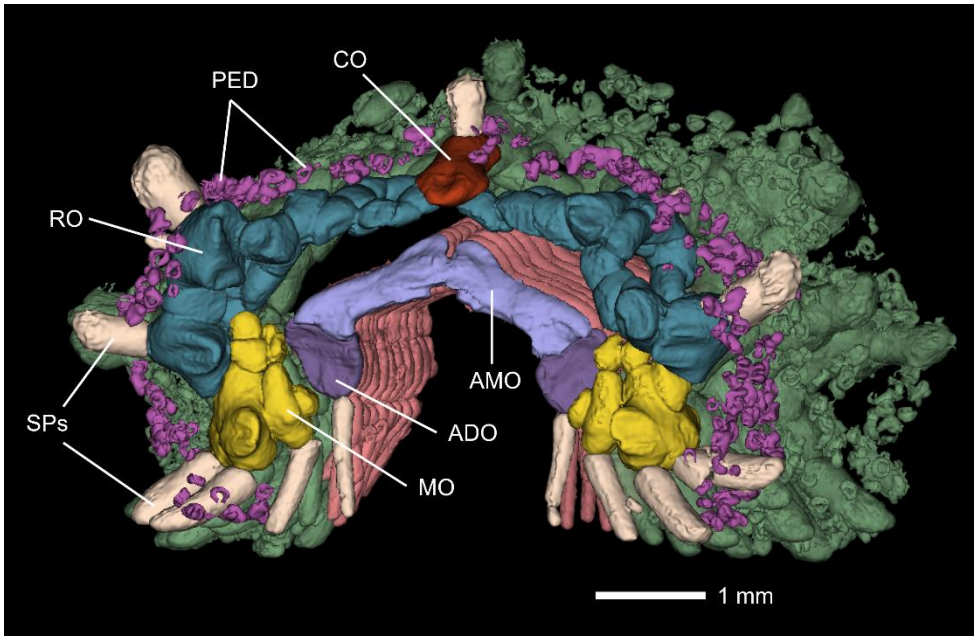

Figure 1. Sea star ray skeletons comprise five types of ossicles: ambulacral ossicles (AMO), adambulacral ossicles (ADO), marginal ossicles (MO), reticular ossicles (RO), and carinal ossicles (CO). The presence of pedicellariae (PED) and spines (SPs) is species specific.

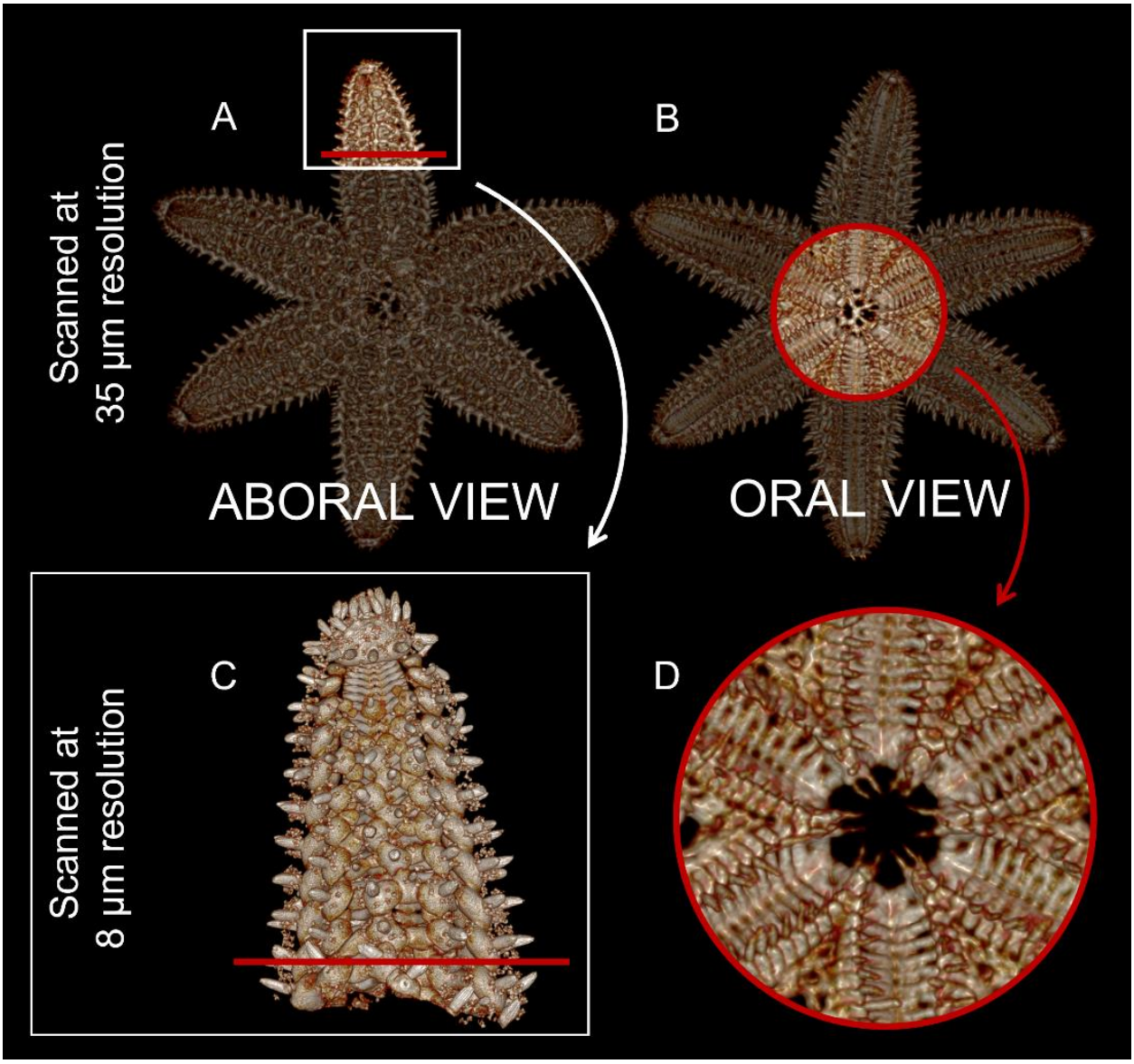

Figure 2. Reference for figures 4-21. A) Aboral view of the whole specimen. Red line indicates where the panel A and C align. B) Oral view (shares scale with panel A). C) Skeletal ray tip of specimen, aboral view. D) Close-up oral view of central disc and mouth. Aboral skeleton removed for clarity.

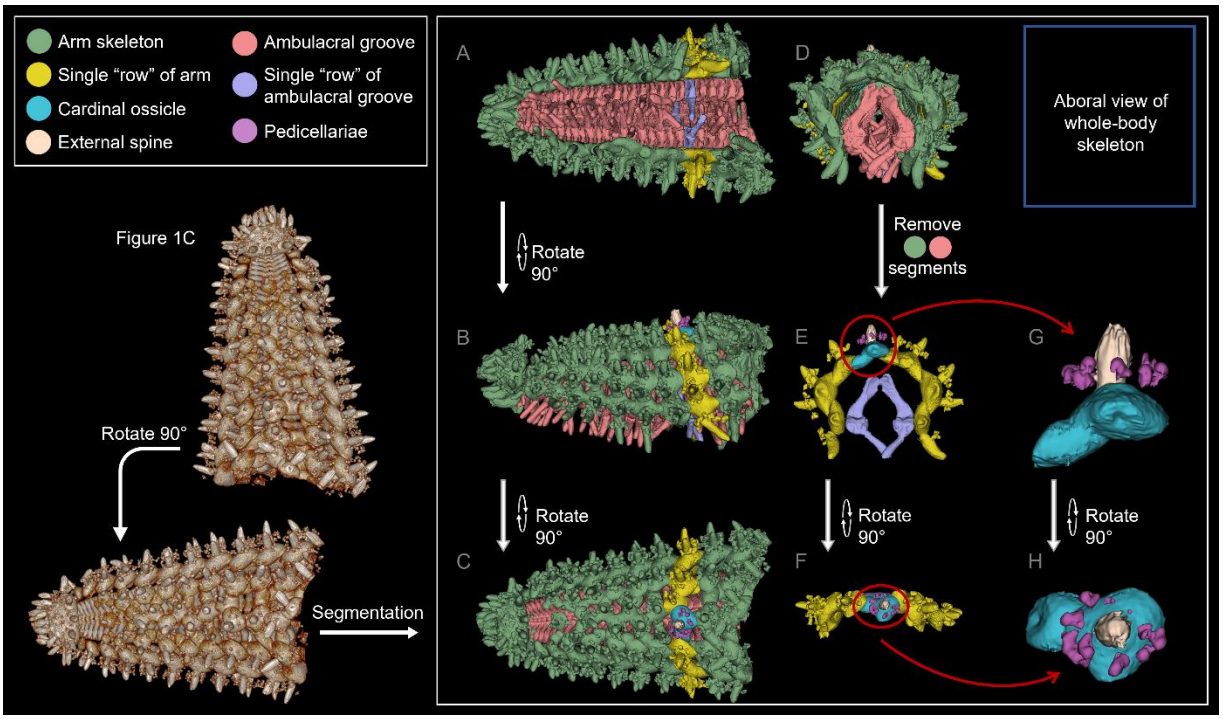

Figure 3. Reference for figures 4-21. µCT volume rendering of the endoskeleton in the ray tip of a sea star, scanned at 8µm resolution. Top-right image is the aboral view of the whole skeleton for reference. A) Oral view, B) lateral view, C) aboral view, and D) coronal view of the whole ray tip. A single, cross-sectional row of the ray body wall ("ray band") and the ambulacral groove were isolated to better visualize the organization of the ossicles. E) Coronal view and F) aboral view of the ray band. G) Coronal and H) aboral view of a single carinal ossicle with its affiliated external spines and pedicellariae (when present).

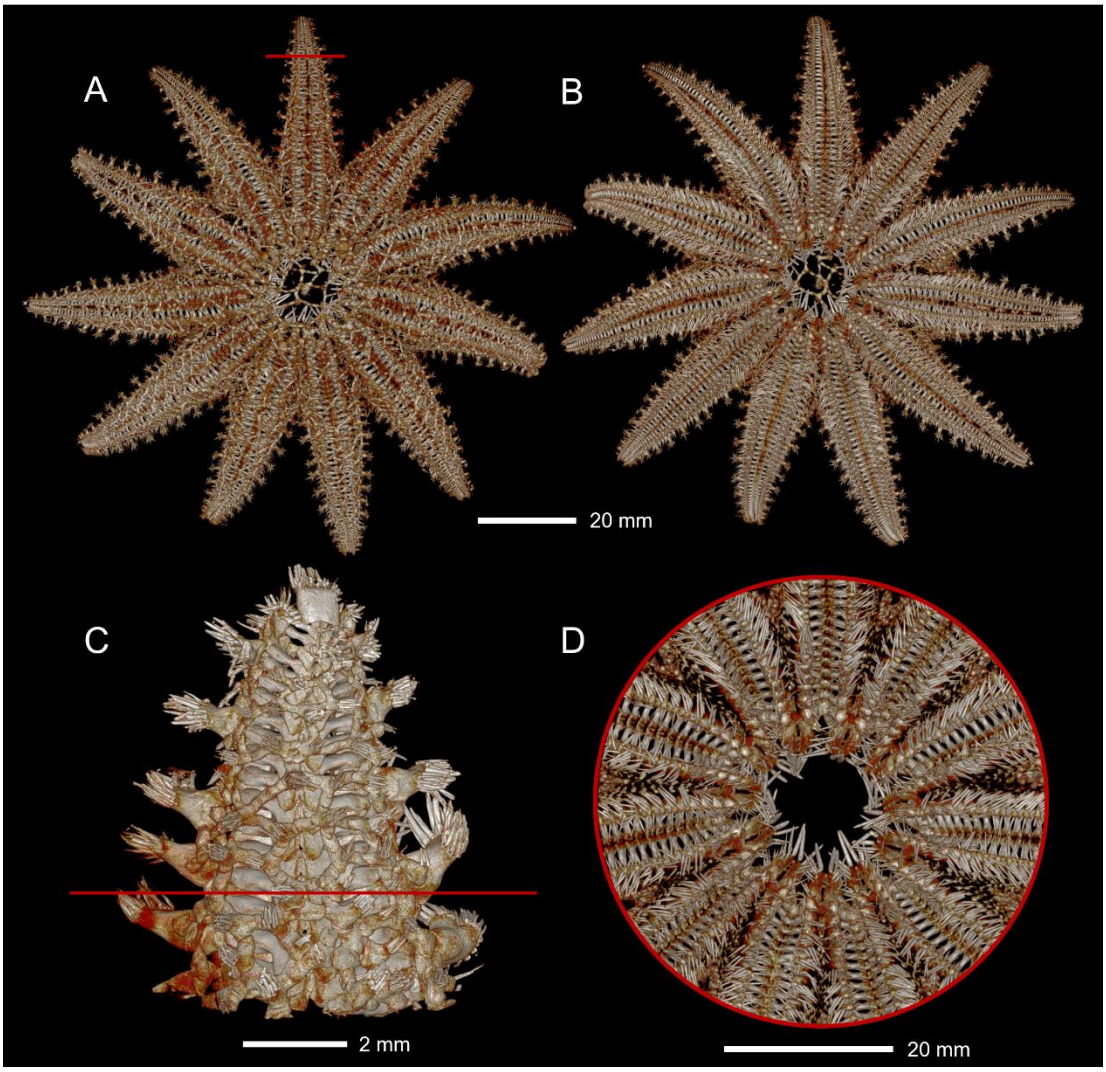

Figure 4. µCT volume rendering of the endoskeleton of *Crossaster papposus*. A) Aboral view of the whole specimen. B) Oral view. C) Skeletal ray tip of specimen, aboral view. D) Close-up oral view of central disc and mouth. Aboral skeleton removed for clarity. Scanning resolution as in Figure 1.

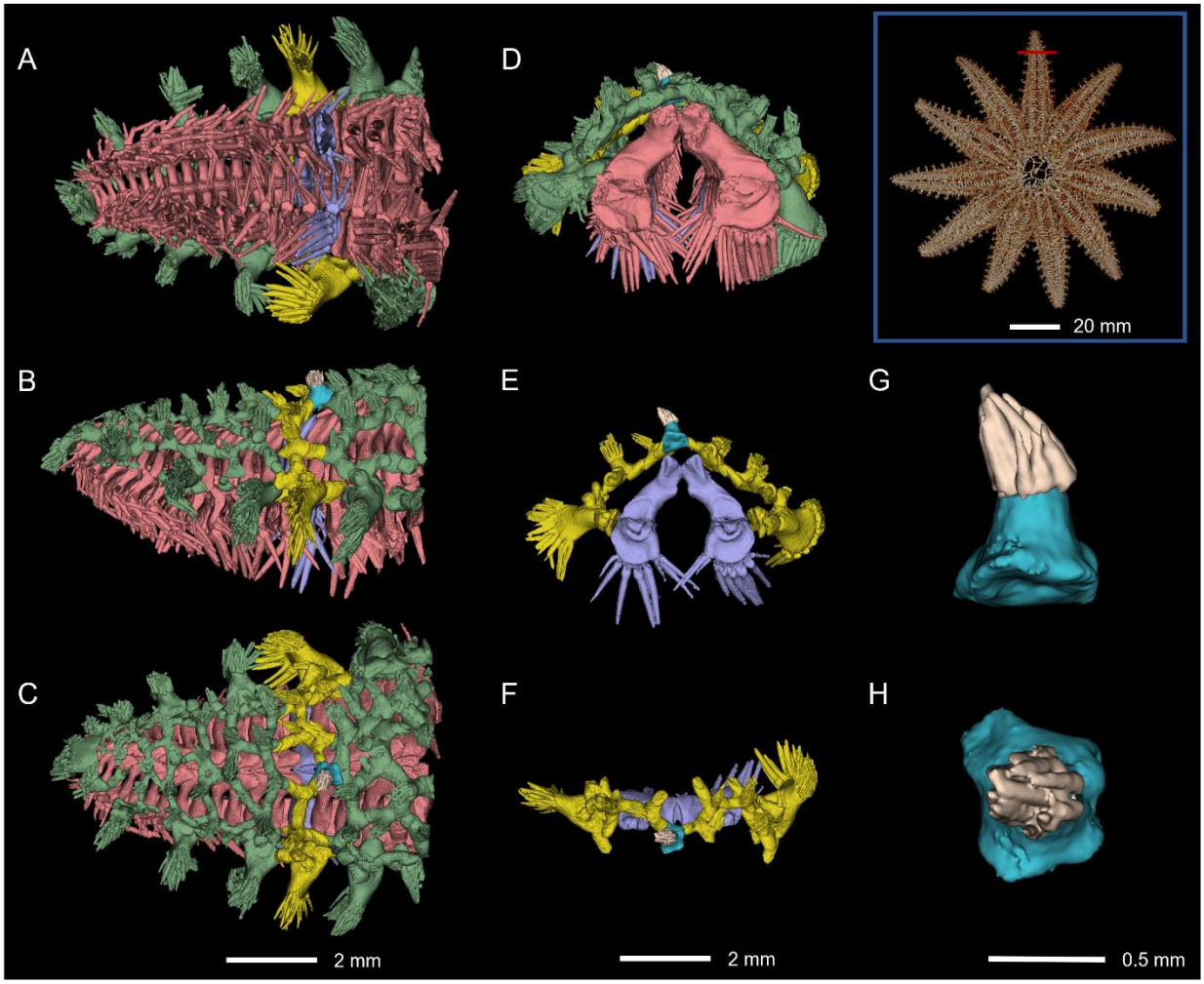

Figure 5. µCT volume rendering of the endoskeleton in the ray tip of *Crossaster papposus.* A) Oral view, B) lateral view, C) aboral view, and D) coronal view of the whole ray tip. E) Coronal view and F) aboral view of a single row of ossicles. G) Coronal view and H) aboral view of a single cardinal ossicle with its affiliated external spines and pedicellariae (when present). Segmentation color coding as in Figure 2.

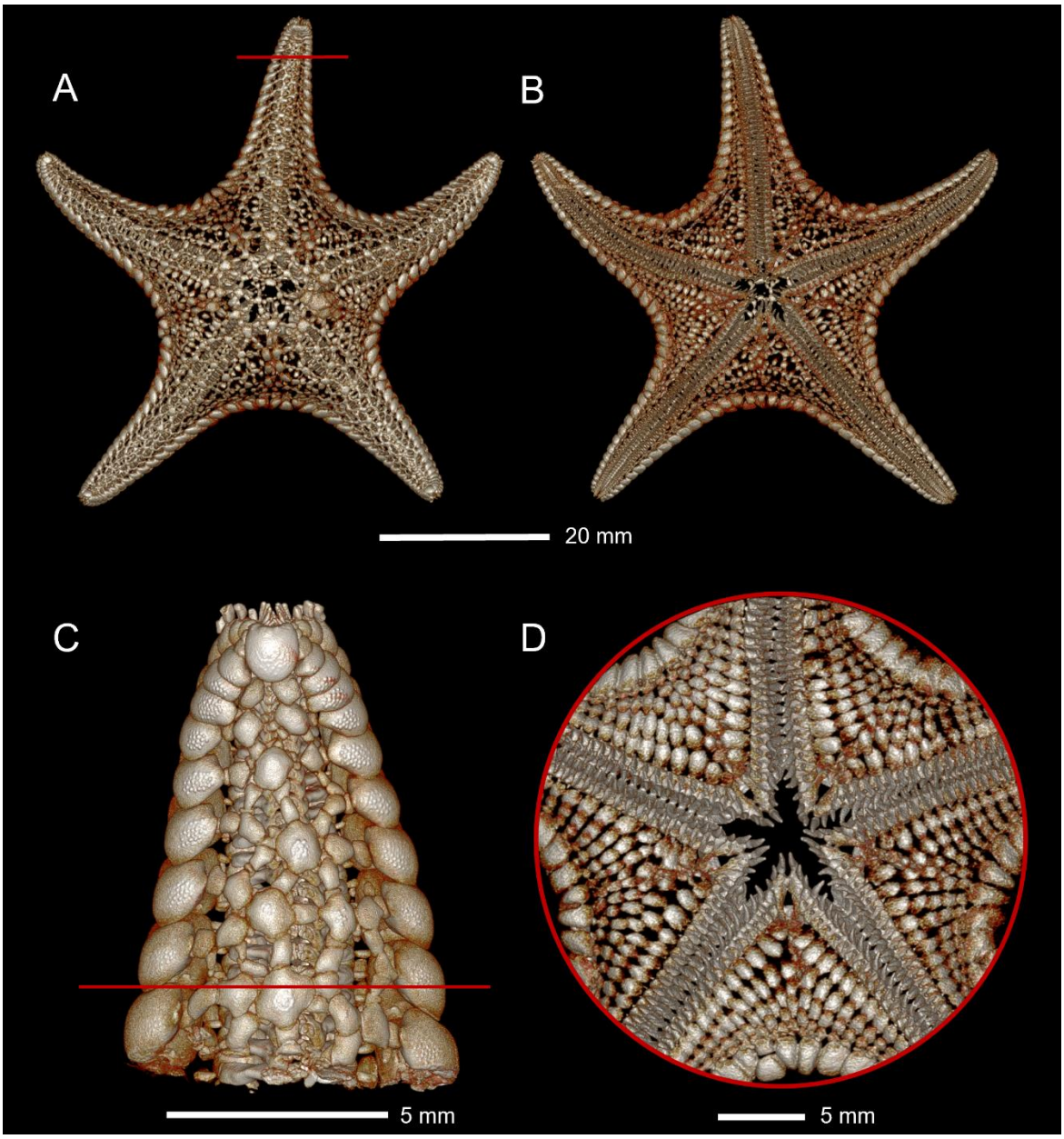

Figure 6. µCT volume rendering of the endoskeleton of *Dermasterias imbricata*. A) Aboral view of the whole specimen. B) Oral view. C) Skeletal ray tip of specimen, aboral view. D) Close-up oral view of central disc and mouth. Aboral skeleton removed for clarity. Scanning resolution as in Figure 1.

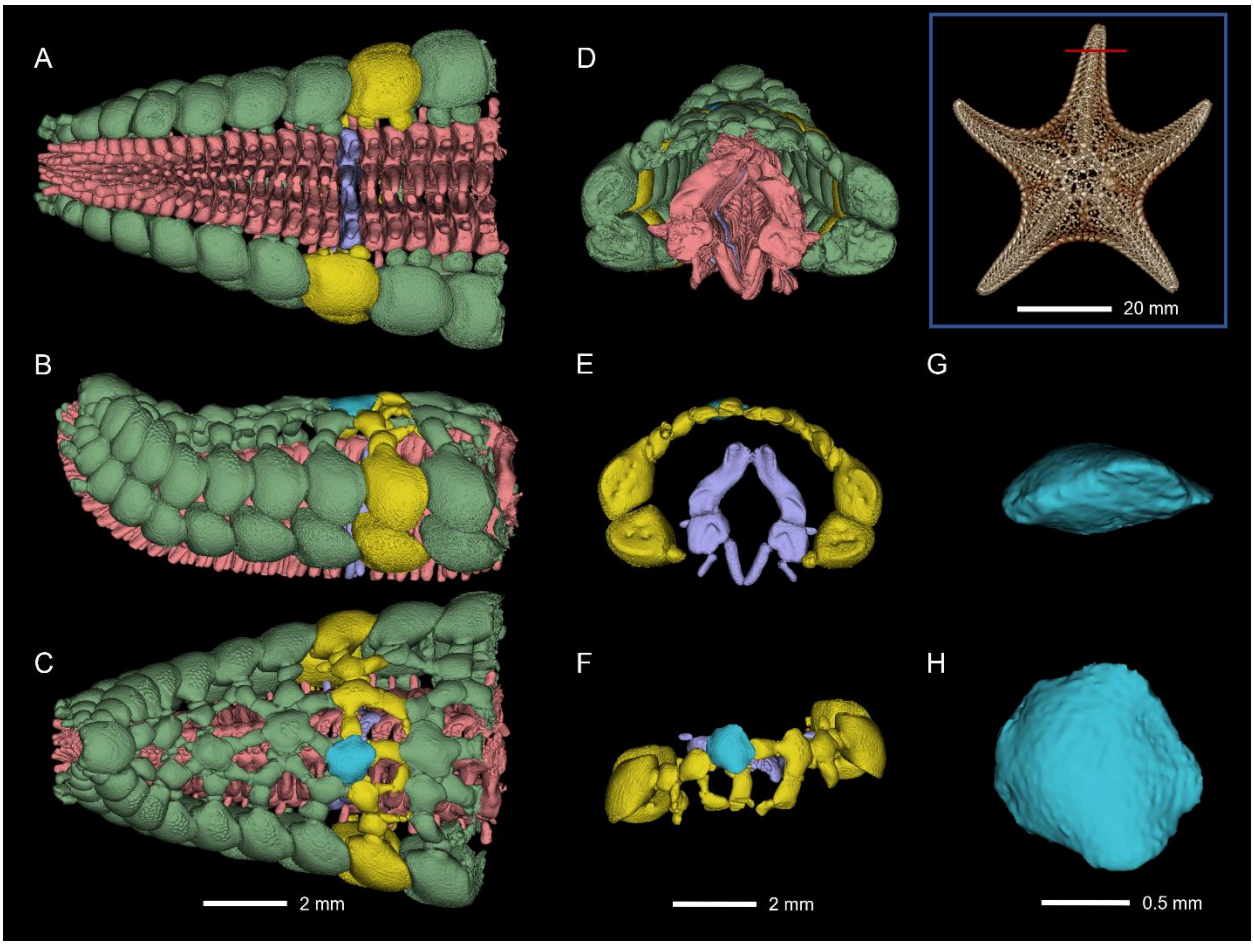

Figure 7. µCT volume rendering of the endoskeleton in the ray tip of *Dermasterias imbricata.* A) Oral view, B) lateral view, C) aboral view, and D) coronal view of the whole ray tip. E) Coronal view and F) aboral view of a single row of ossicles. G) Coronal view and H) aboral view of a single cardinal ossicle with its affiliated external spines and pedicellariae (when present). Segmentation color coding as in Figure 2.

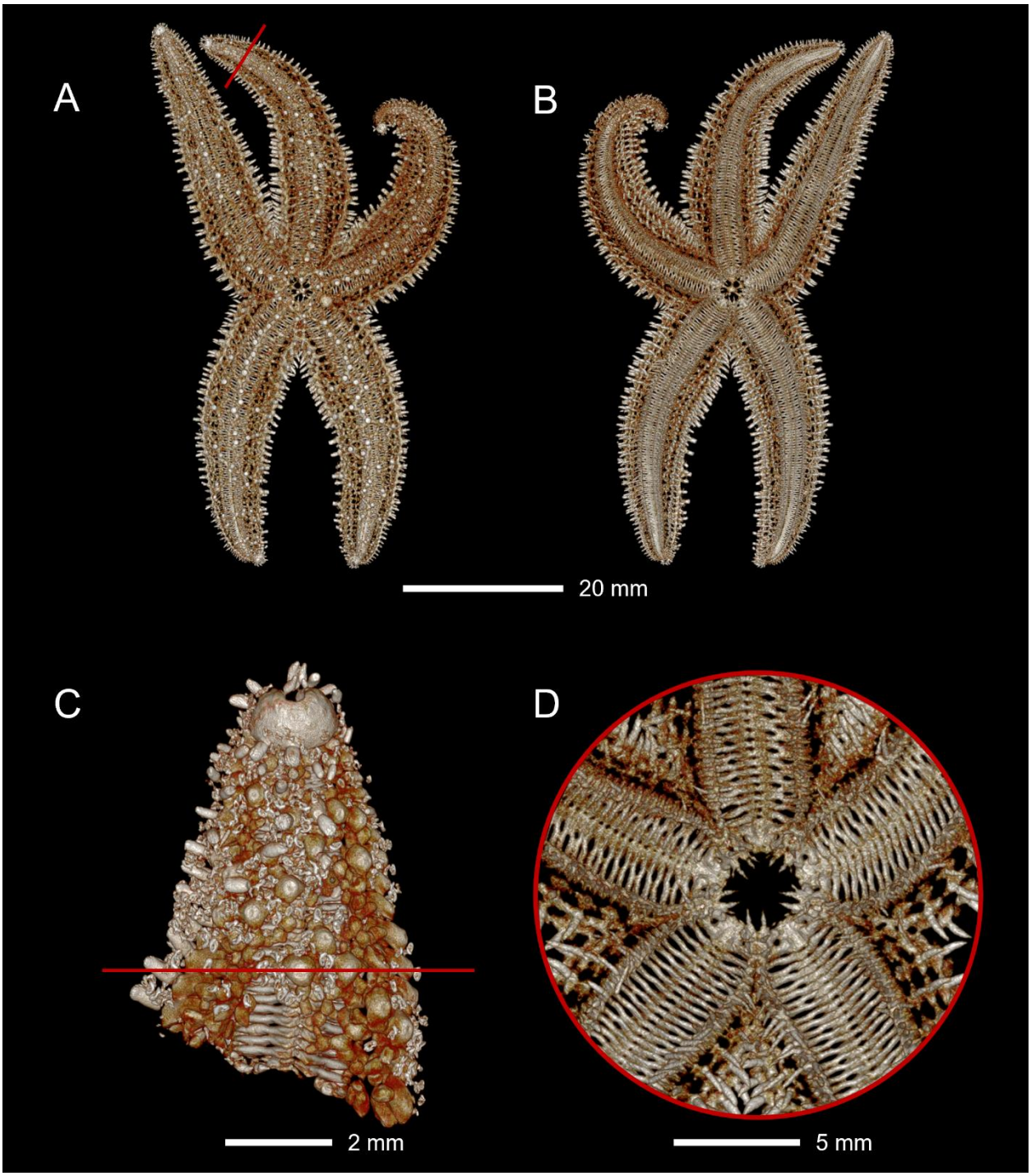

Figure 8. µCT volume rendering of the endoskeleton of *Evasterias troschelii*. A) Aboral view of the whole specimen. B) Oral view. C) Skeletal ray tip of specimen, aboral view. D) Close-up oral view of central disc and mouth. Aboral skeleton removed for clarity. Scanning resolution as in Figure 1.

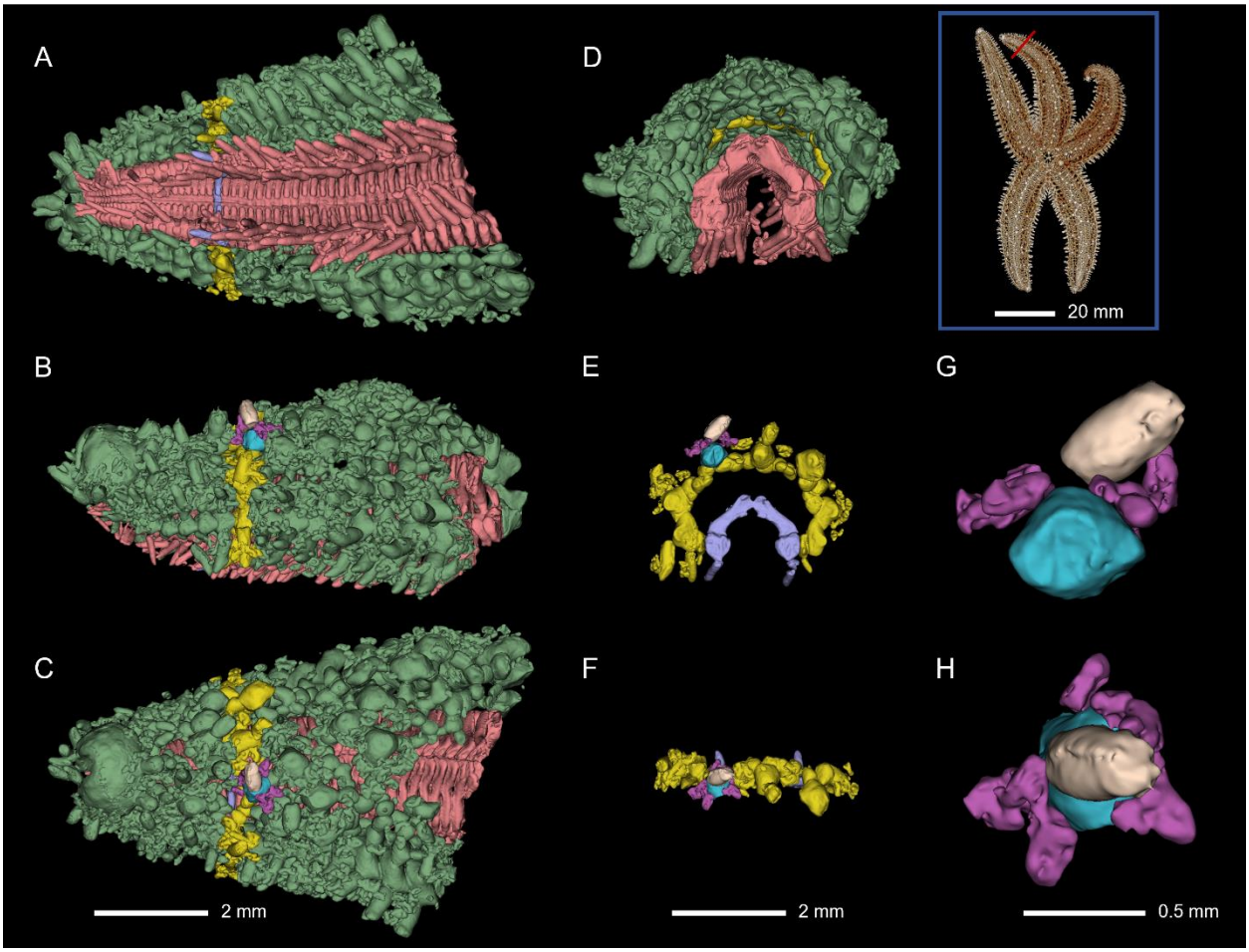

Figure 9. µCT volume rendering of the endoskeleton in the ray tip of *Evasterias troschelii.* A) Oral view, B) lateral view, C) aboral view, and D) coronal view of the whole ray tip. E) Coronal view and F) aboral view of a single row of ossicles. G) Coronal view and H) aboral view of a single cardinal ossicle with its affiliated external spines and pedicellariae (when present). Segmentation color coding as in Figure 2.

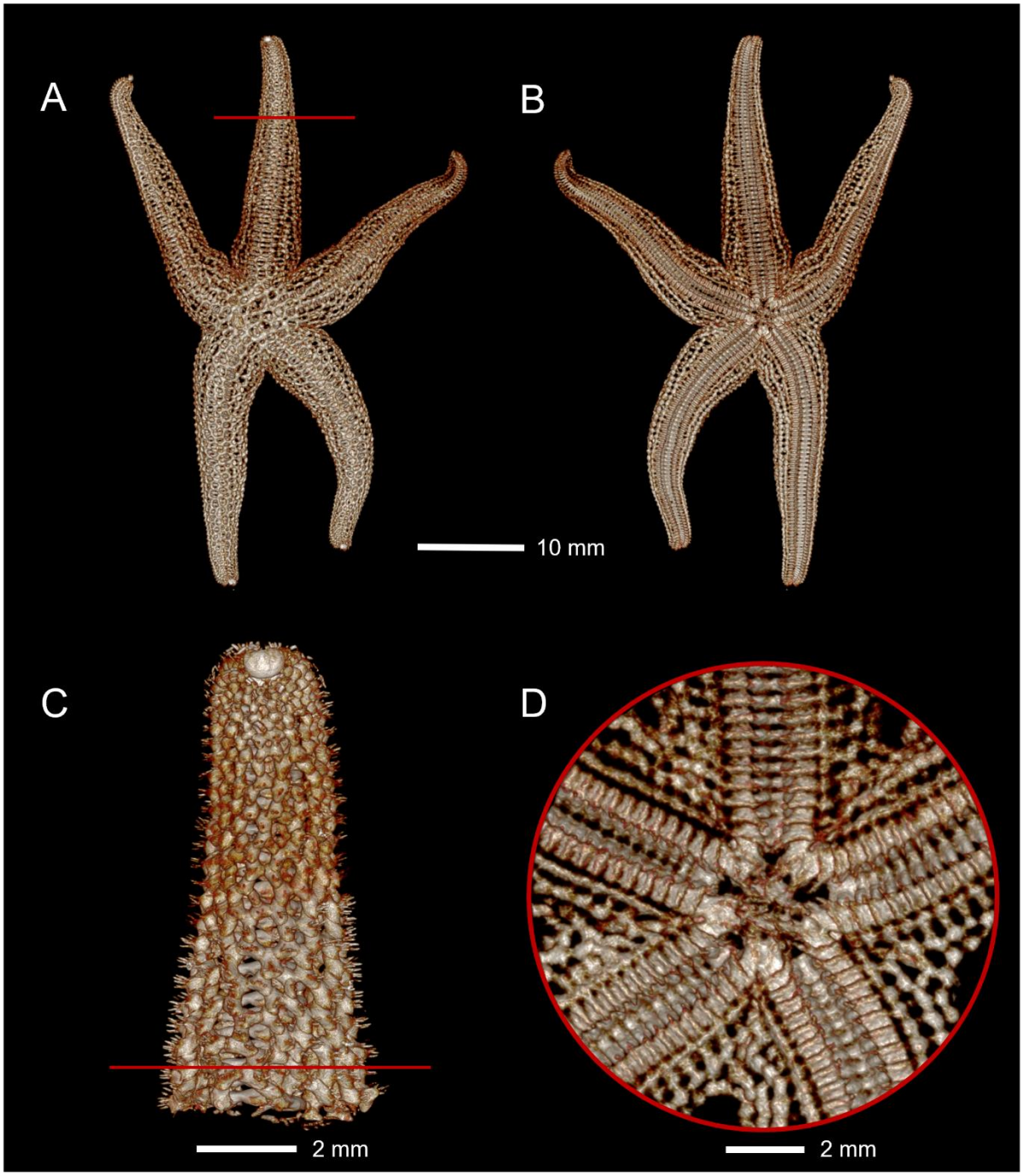

Figure 10. µCT volume rendering of the endoskeleton of *Henricia sp*. A) Aboral view of the whole specimen. B) Oral view. C) Skeletal ray tip of specimen, aboral view. D) Close-up oral view of central disc and mouth. Aboral skeleton removed for clarity. Scanning resolution as in Figure 1.

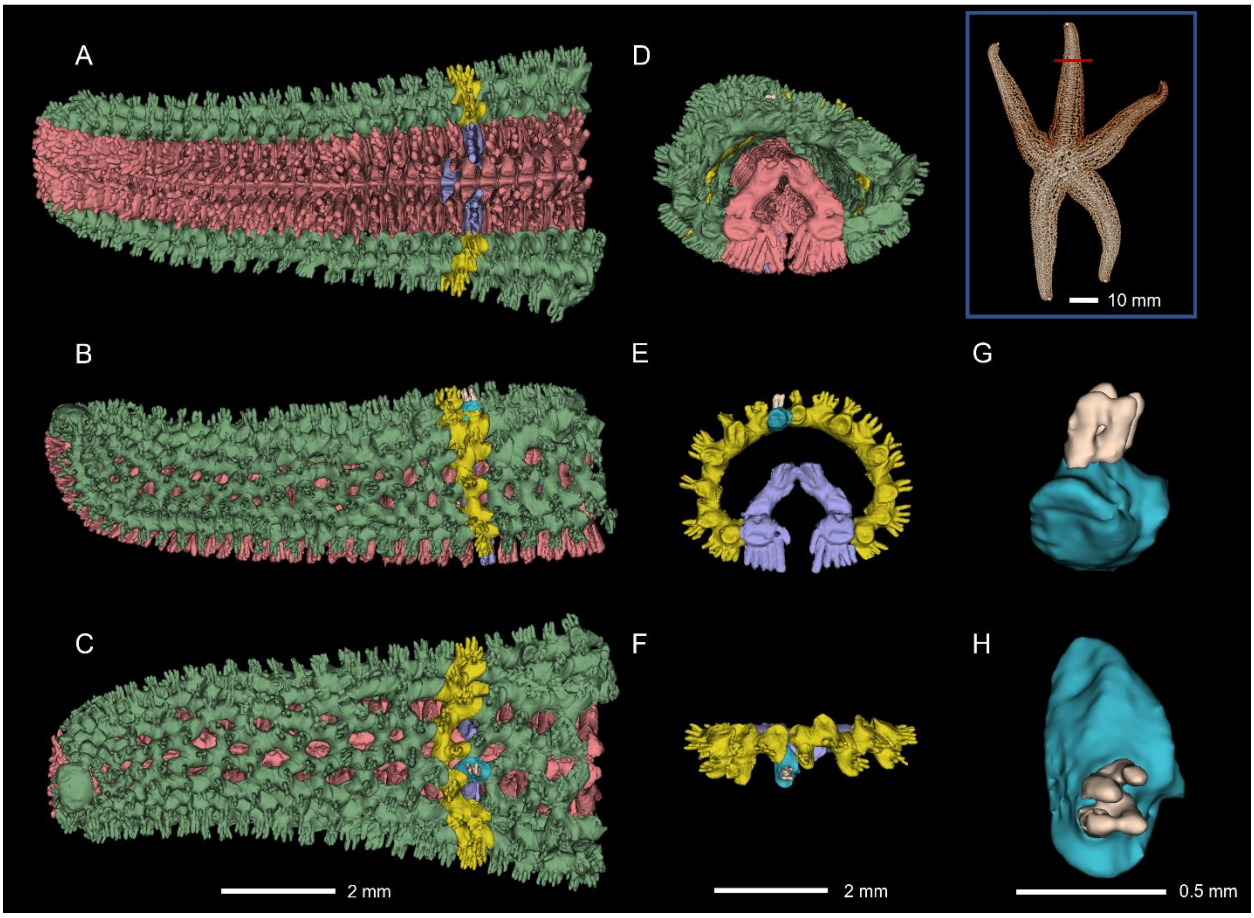

Figure 11. µCT volume rendering of the endoskeleton in the ray tip of *Henricia sp.* A) Oral view, B) lateral view, C) aboral view, and D) coronal view of the whole ray tip. E) Coronal view and F) aboral view of a single row of ossicles. G) Coronal view and H) aboral view of a single cardinal ossicle with its affiliated external spines and pedicellariae (when present). Segmentation color coding as in Figure 2.

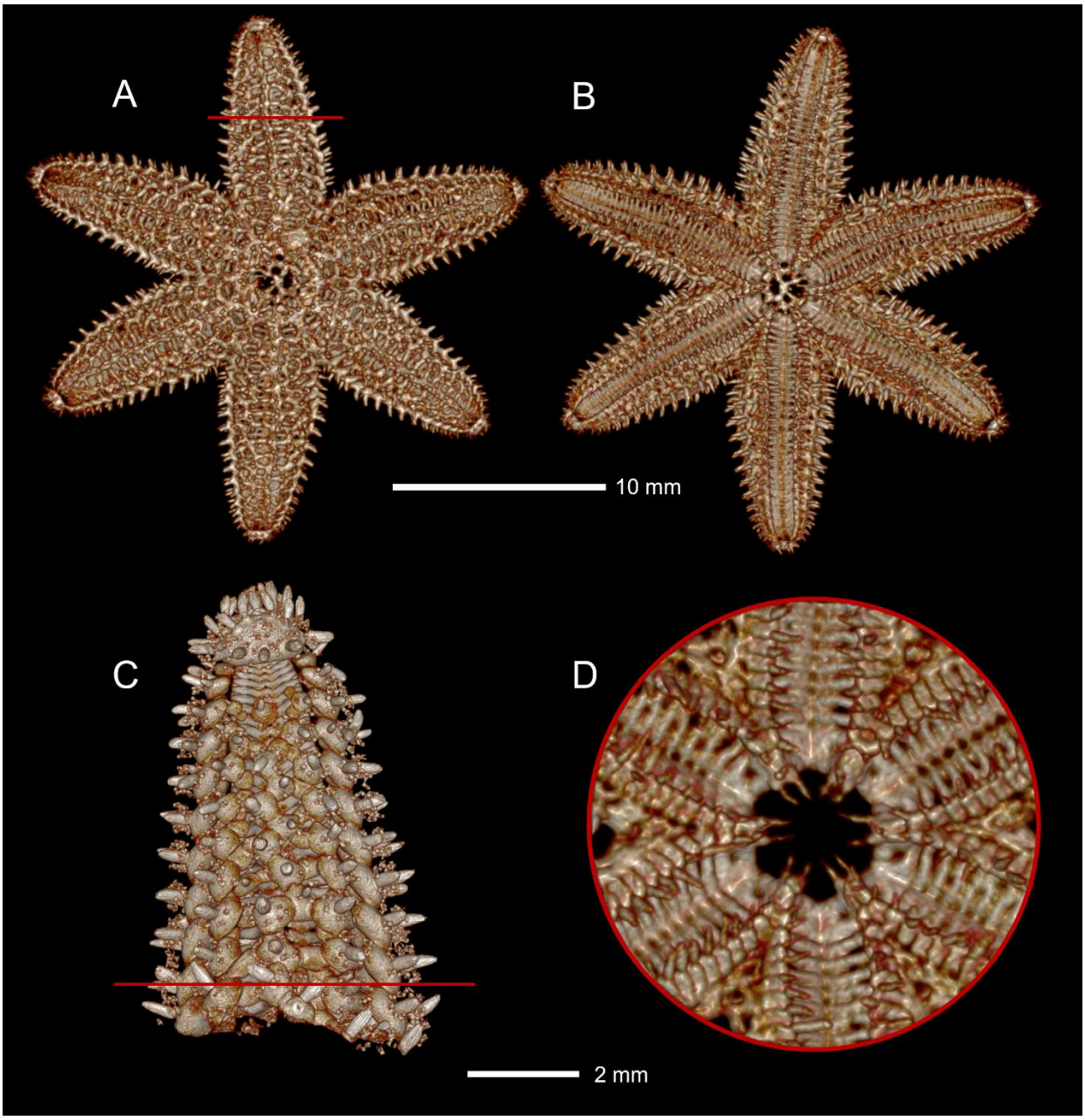

Figure 12. µCT volume rendering of the endoskeleton of *Leptasterias sp.* A) Aboral view of the whole specimen. B) Oral view. C) Skeletal ray tip of specimen, aboral view. D) Close-up oral view of central disc and mouth. Aboral skeleton removed for clarity. Scanning resolution as in Figure 1.

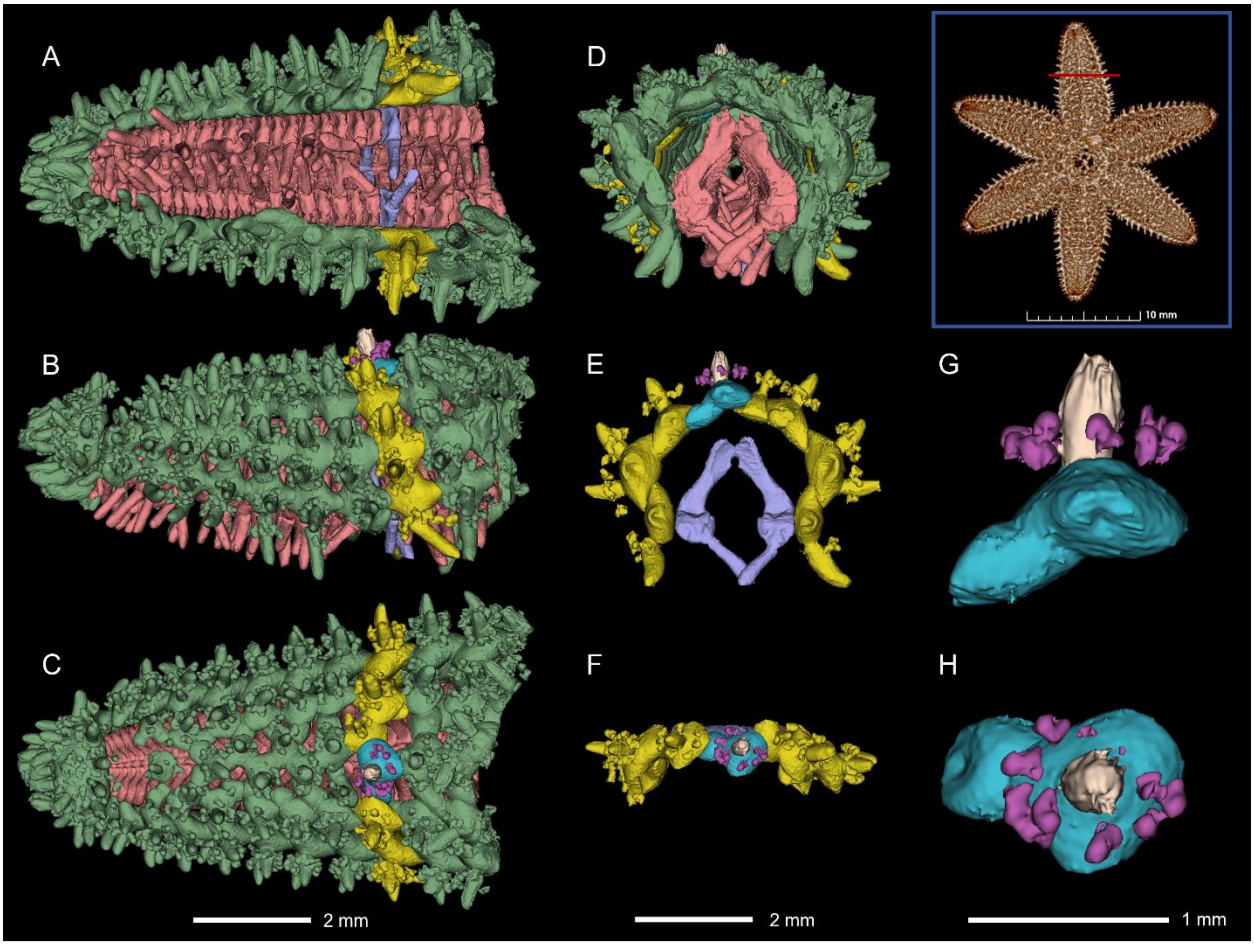

Figure 13. µCT volume rendering of the endoskeleton in the ray tip of *Leptasterias sp.* A) Oral view, B) lateral view, C) aboral view, and D) coronal view of the whole ray tip. E) Coronal view and F) aboral view of a single row of ossicles. G) Coronal view and H) aboral view of a single cardinal ossicle with its affiliated external spines and pedicellariae (when present). Segmentation color coding as in Figure 2.

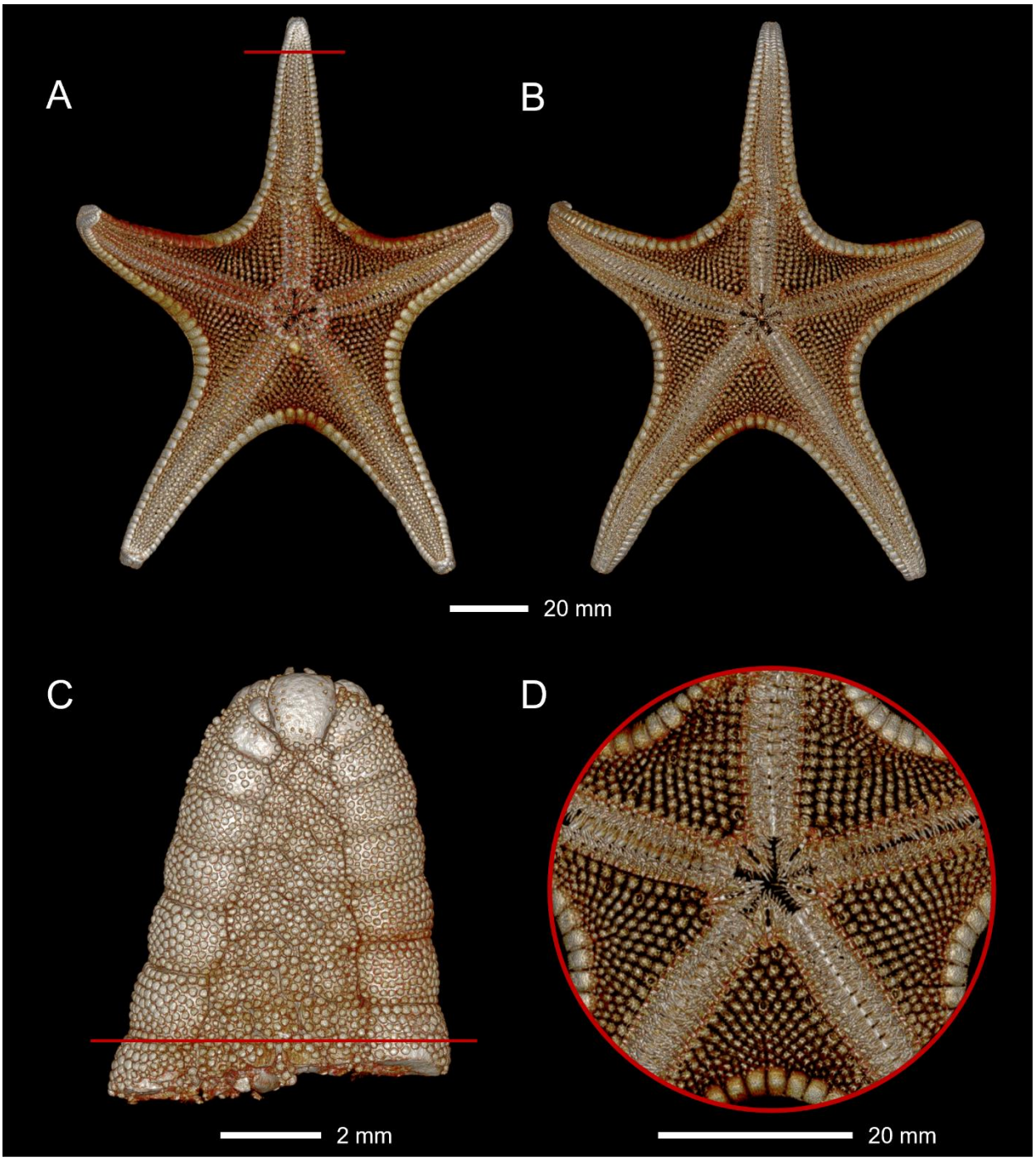

Figure 14. µCT volume rendering of the endoskeleton of *Mediaster aequalis*. A) Aboral view of the whole specimen. B) Oral view. C) Skeletal ray tip of specimen, aboral view. D) Close-up oral view of central disc and mouth. Aboral skeleton removed for clarity. Scanning resolution as in Figure 1.

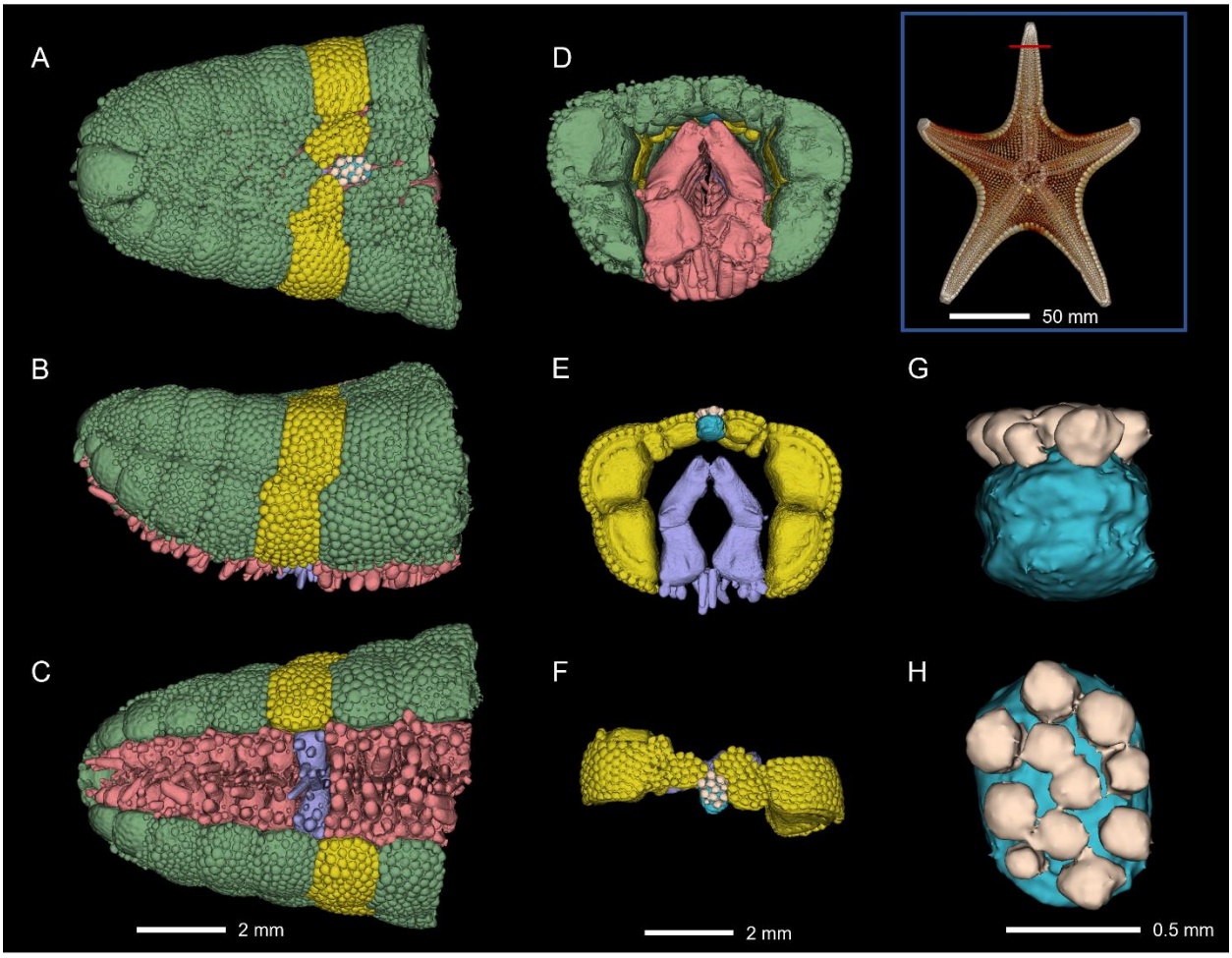

Figure 15. µCT volume rendering of the endoskeleton in the ray tip of *Mediaster aequalis.* A) Oral view, B) lateral view, C) aboral view, and D) coronal view of the whole ray tip. E) Coronal view and F) aboral view of a single row of ossicles. G) Coronal view and H) aboral view of a single cardinal ossicle with its affiliated external spines and pedicellariae (when present). Segmentation color coding as in Figure 2.

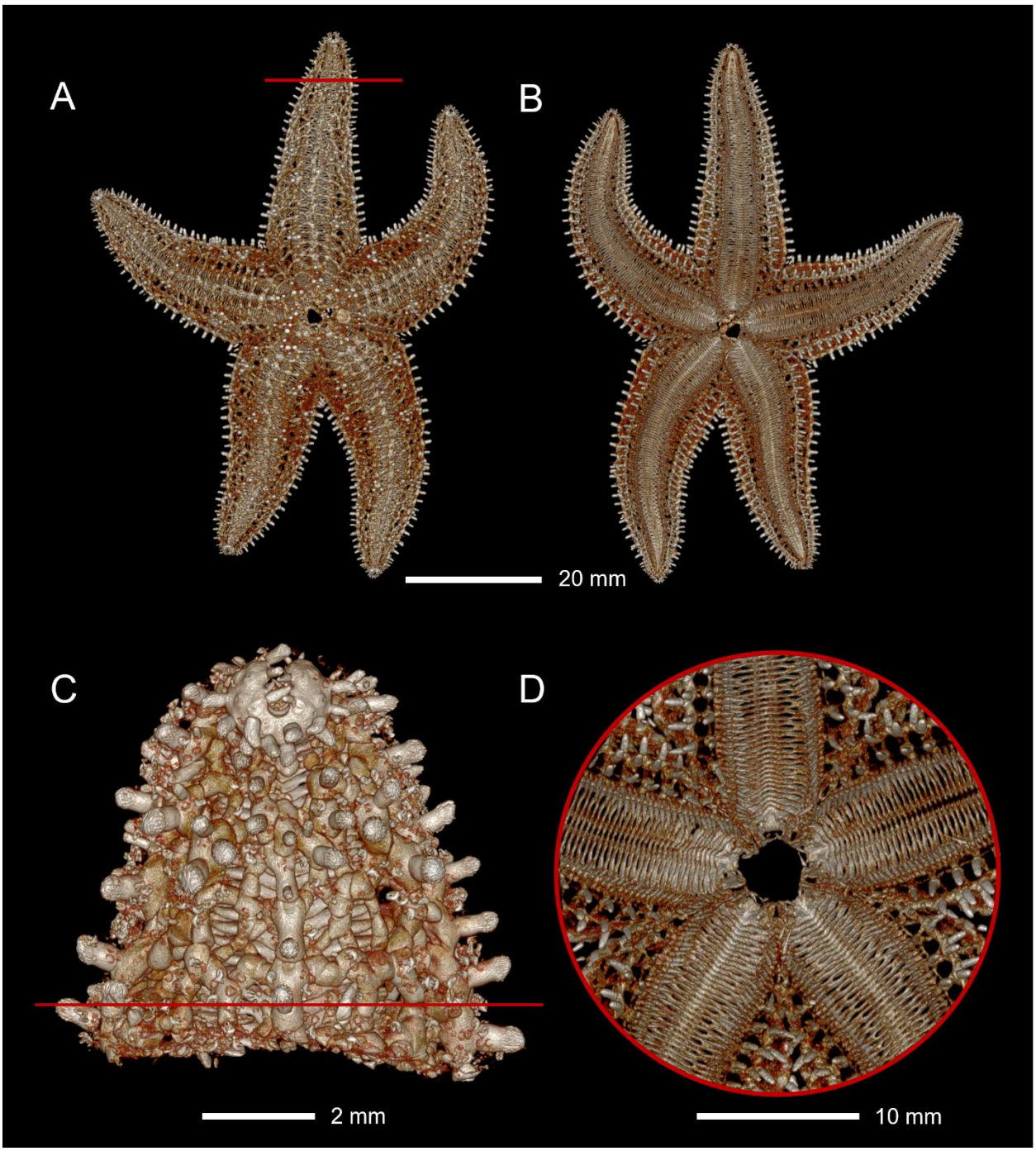

Figure 16. µCT volume rendering of the endoskeleton of *Pisaster ochraceus*. A) Aboral view of the whole specimen. B) Oral view. C) Skeletal ray tip of specimen, aboral view. D) Close-up oral view of central disc and mouth. Aboral skeleton removed for clarity. Scanning resolution as in Figure 1.

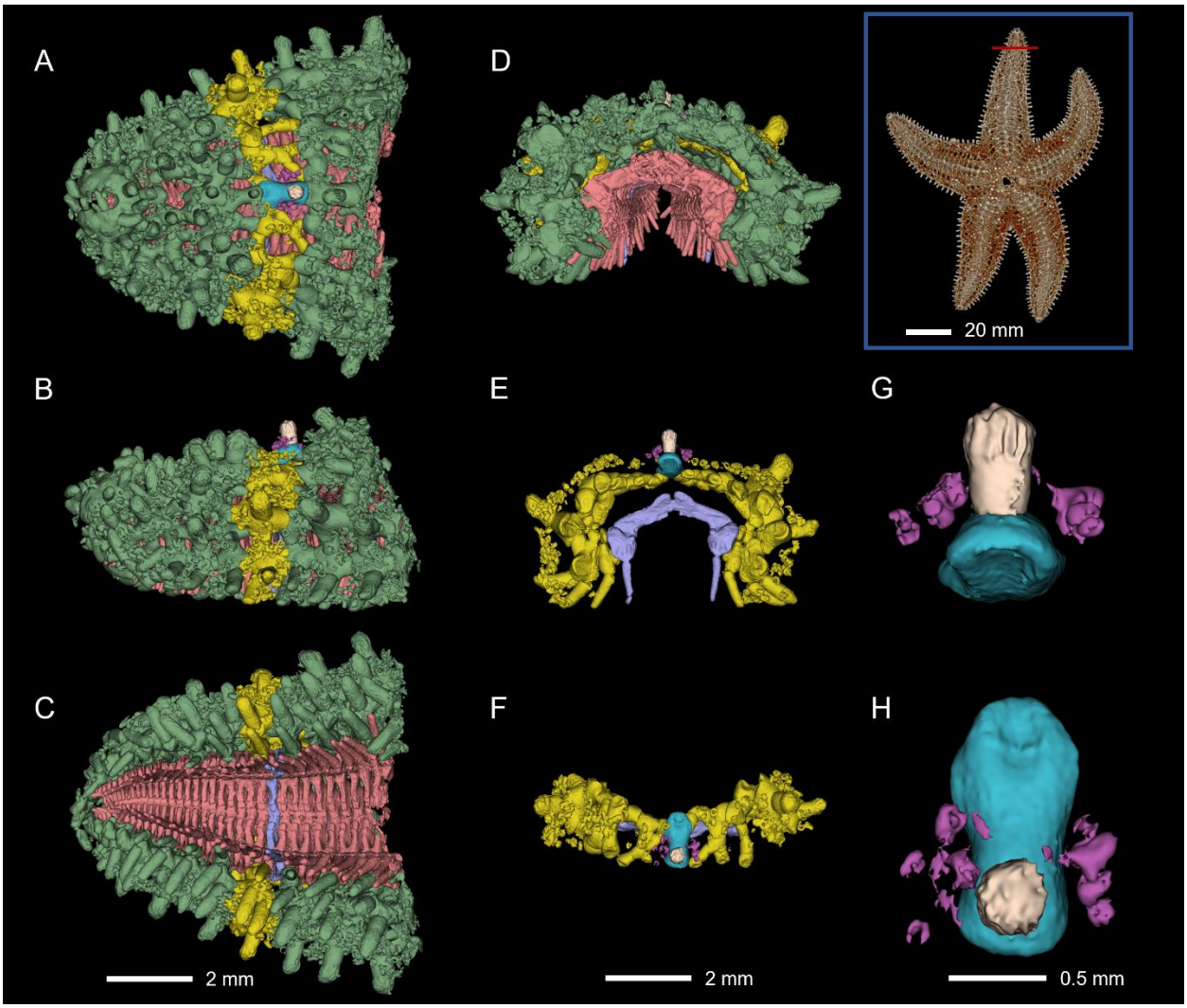

Figure 17. µCT volume rendering of the endoskeleton in the ray tip of *Pisaster ochraceus.* A) Oral view, B) lateral view, C) aboral view, and D) coronal view of the whole ray tip. E) Coronal view and F) aboral view of a single row of ossicles. G) Coronal view and H) aboral view of a single cardinal ossicle with its affiliated external spines and pedicellariae (when present). Segmentation color coding as in Figure 2.

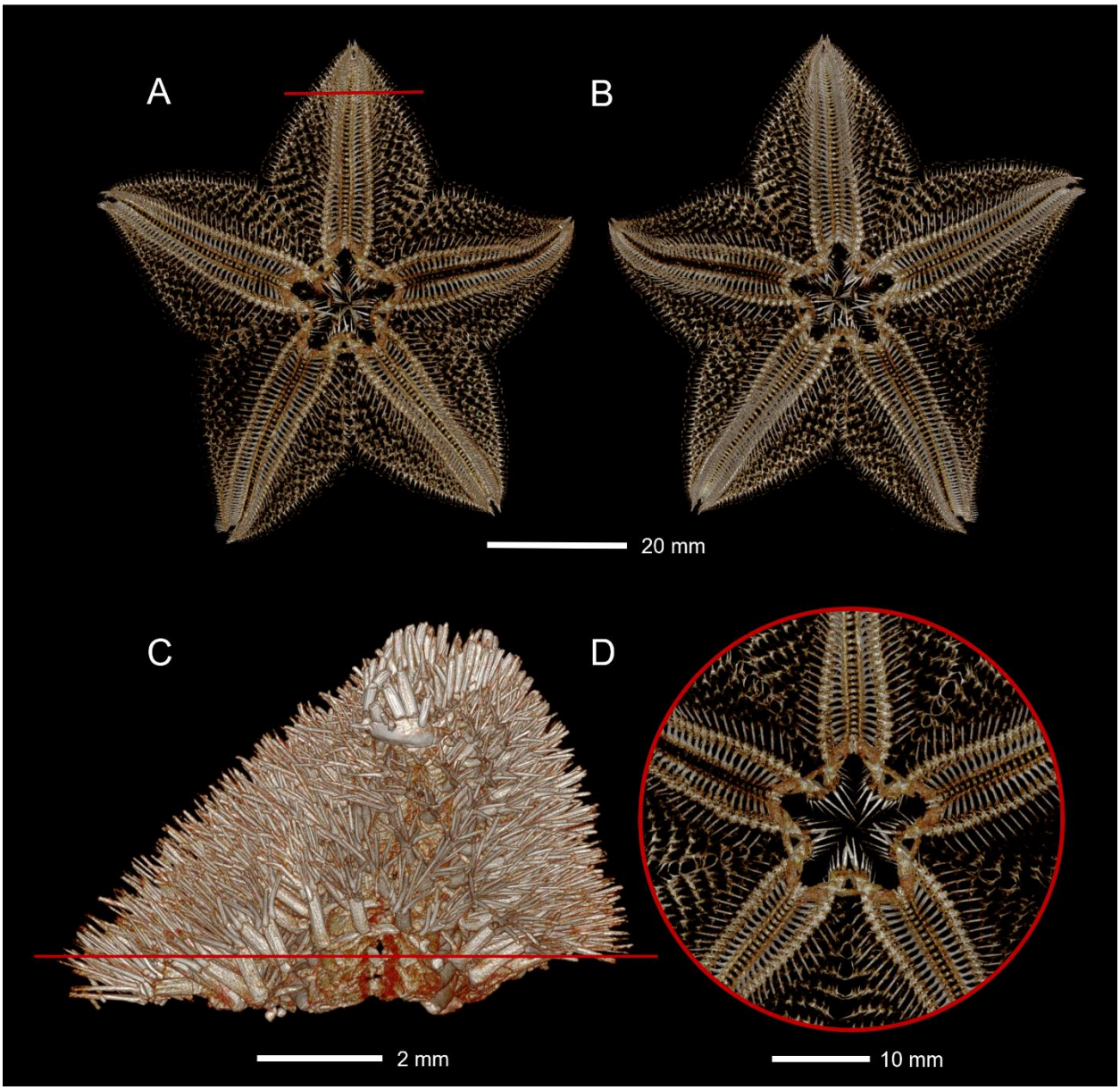

Figure 18. µCT volume rendering of the endoskeleton of *Pteraster tesselatus*. A) Aboral view of the whole specimen. B) Oral view. C) Skeletal ray tip of specimen, aboral view. D) Close-up oral view of central disc and mouth. Aboral skeleton removed for clarity. Scanning resolution as in Figure 1.

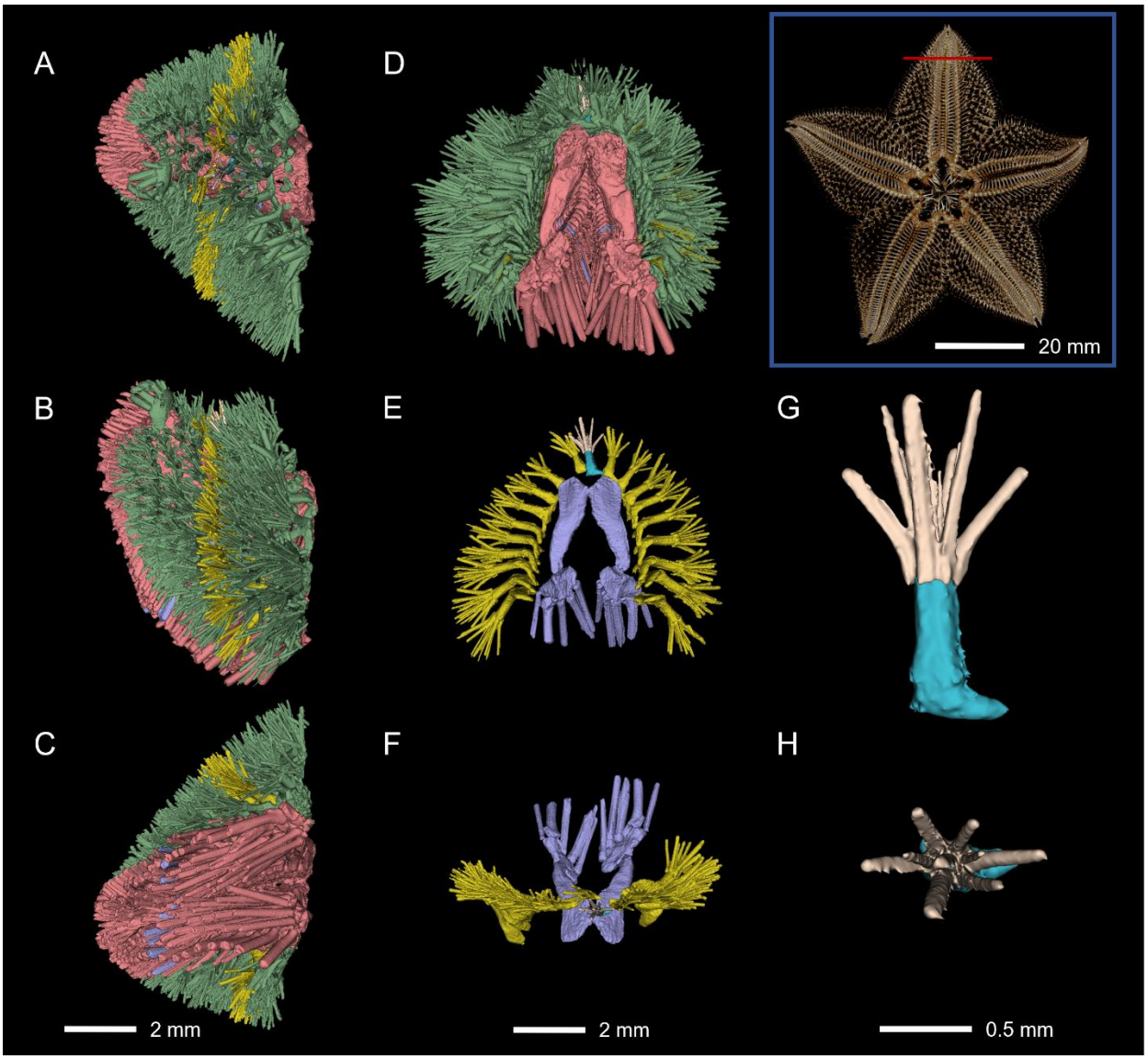

Figure 19. µCT volume rendering of the endoskeleton in the ray tip of *Pteraster tesselatus.* A) Oral view, B) lateral view, C) aboral view, and D) coronal view of the whole ray tip. E) Coronal view and F) aboral view of a single row of ossicles. G) Coronal view and H) aboral view of a single cardinal ossicle with its affiliated external spines and pedicellariae (when present). Segmentation color coding as in Figure 2.

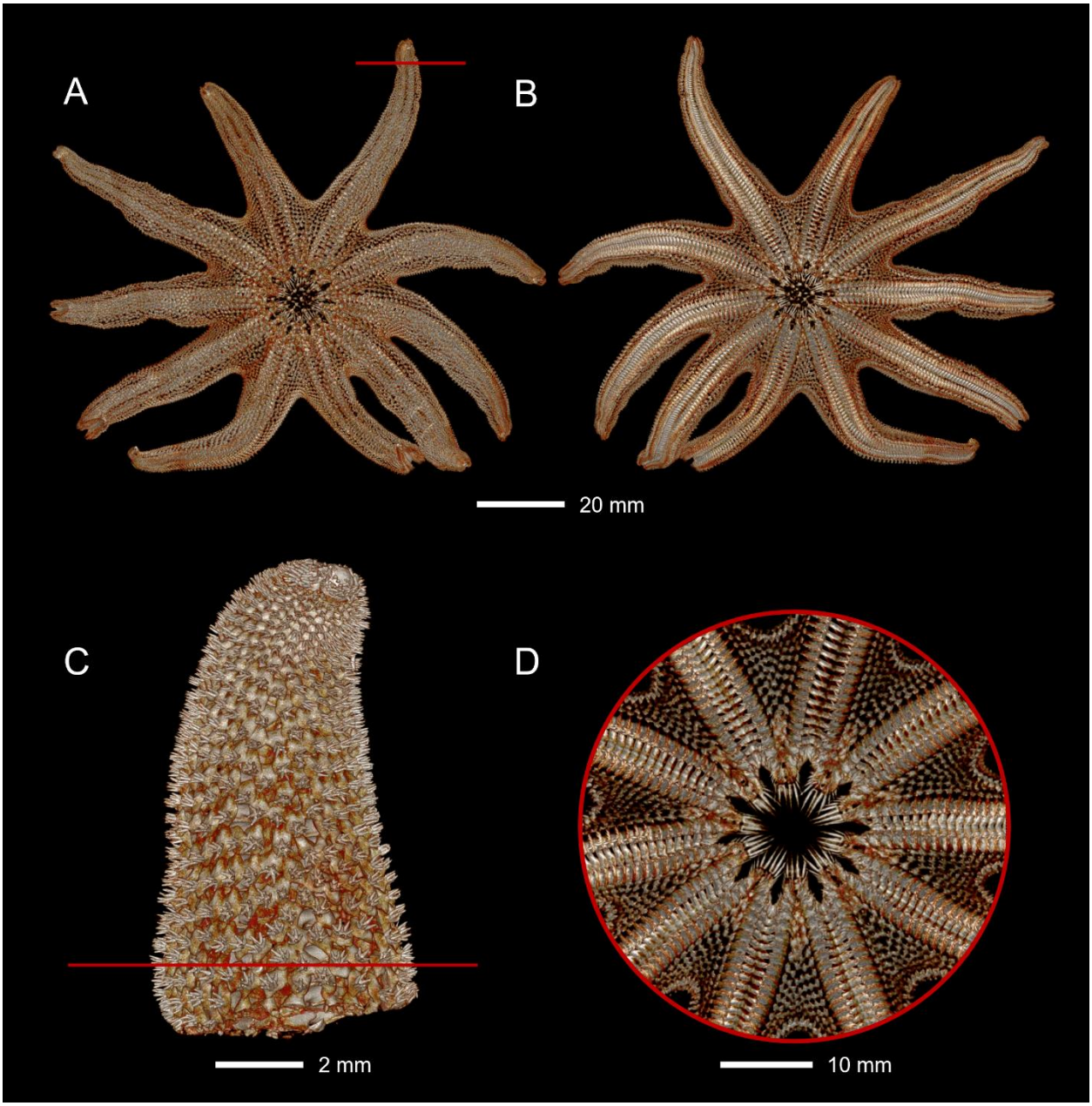

Figure 20. µCT volume rendering of the endoskeleton of *Solaster stimpsoni*. A) Aboral view of the whole specimen. B) Oral view. C) Skeletal ray tip of specimen, aboral view. D) Close-up oral view of central disc and mouth. Aboral skeleton removed for clarity. Scanning resolution as in Figure 1.

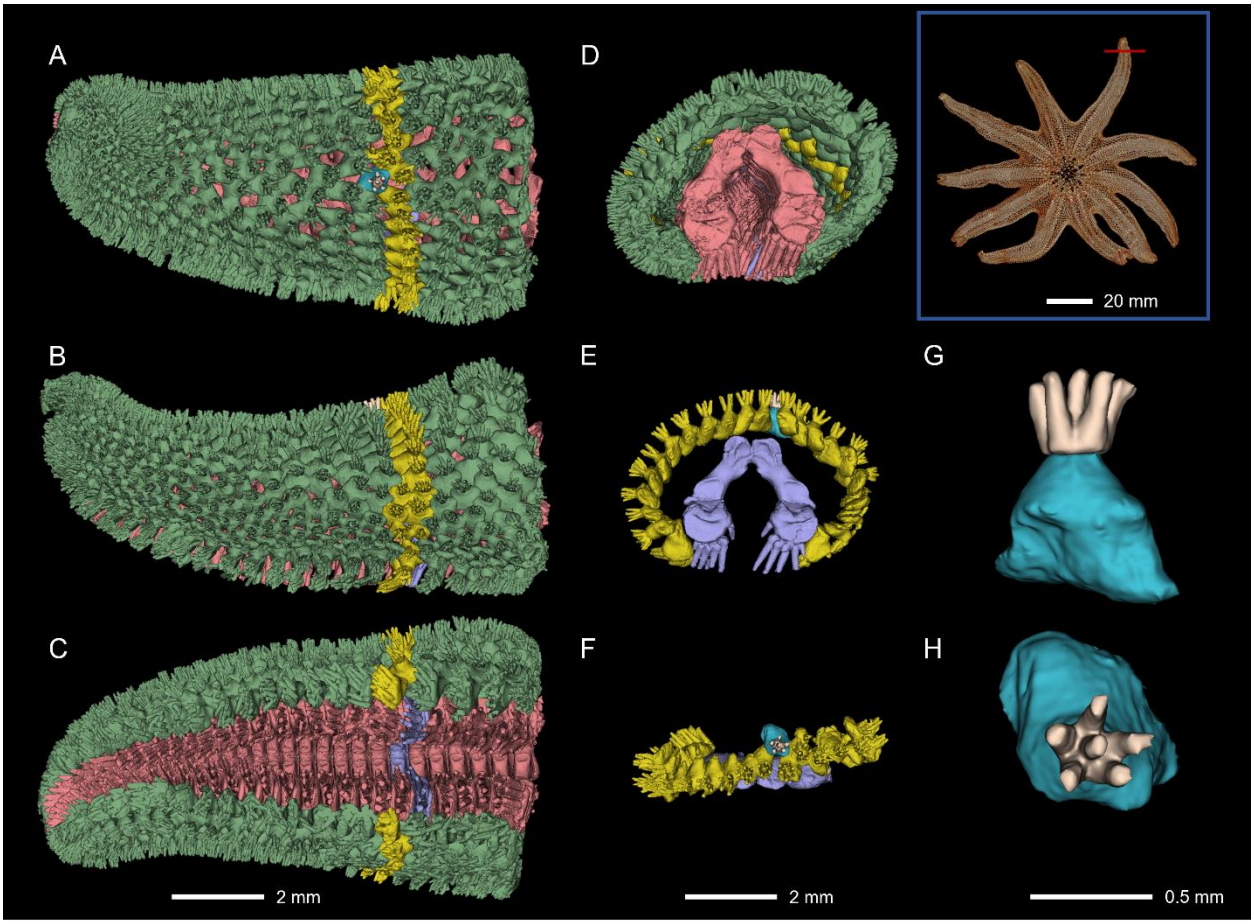

Figure 21. µCT volume rendering of the endoskeleton in the ray tip of *Solaster stimpsoni.* A) Oral view, B) lateral view, C) aboral view, and D) coronal view of the whole ray tip. E) Coronal view and F) aboral view of a single row of ossicles. G) Coronal view and H) aboral view of a single cardinal ossicle with its affiliated external spines and pedicellariae (when present). Segmentation color coding as in Figure 2.

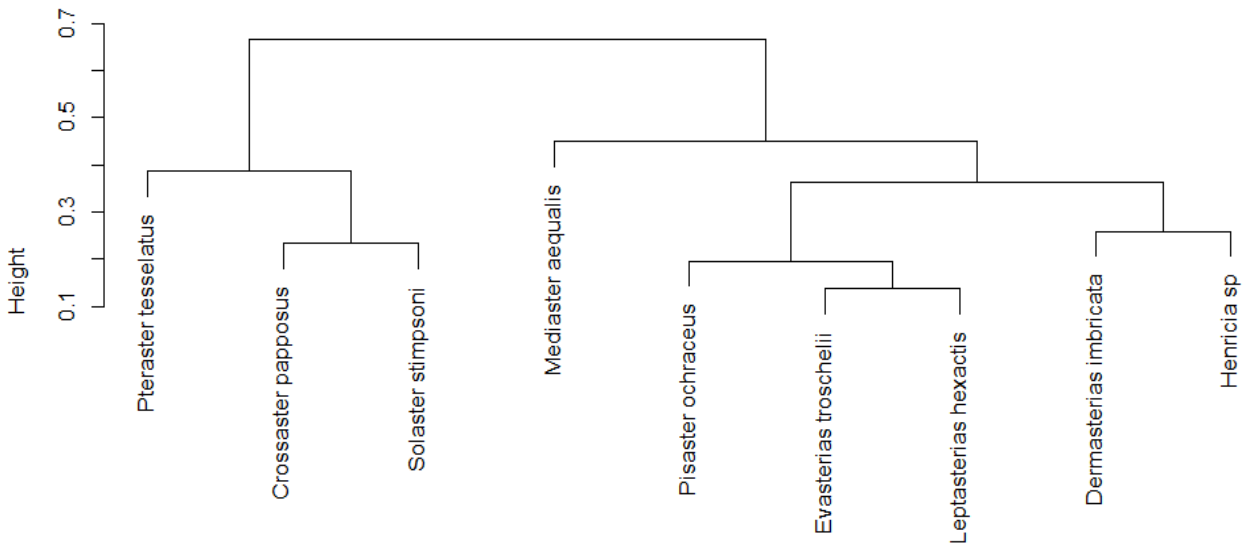

Figure 22. Dendrogram using complete linkage hierarchical clustering of 14 numeric, morphological traits of nine sea star species.

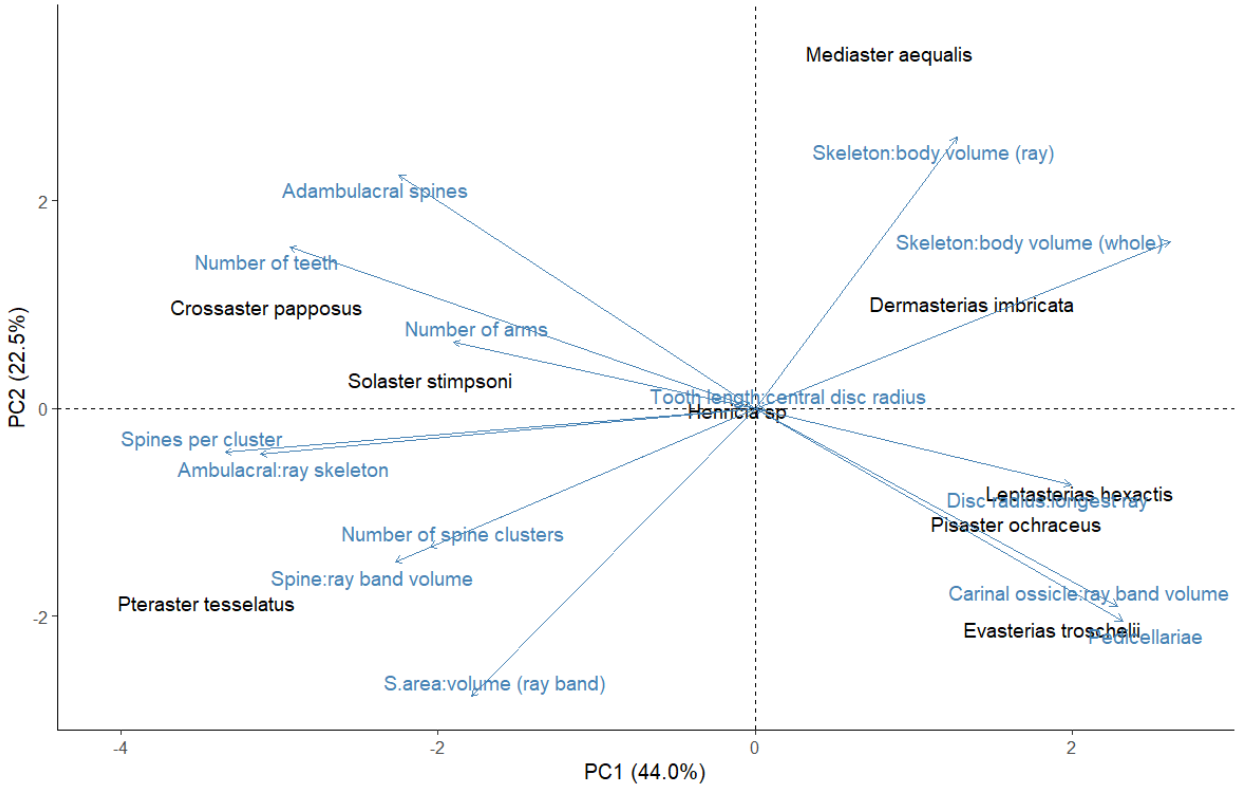

Figure 23. The principal components analysis (PCA) biplot based on 14 numeric, morphological traits of nine sea star species.

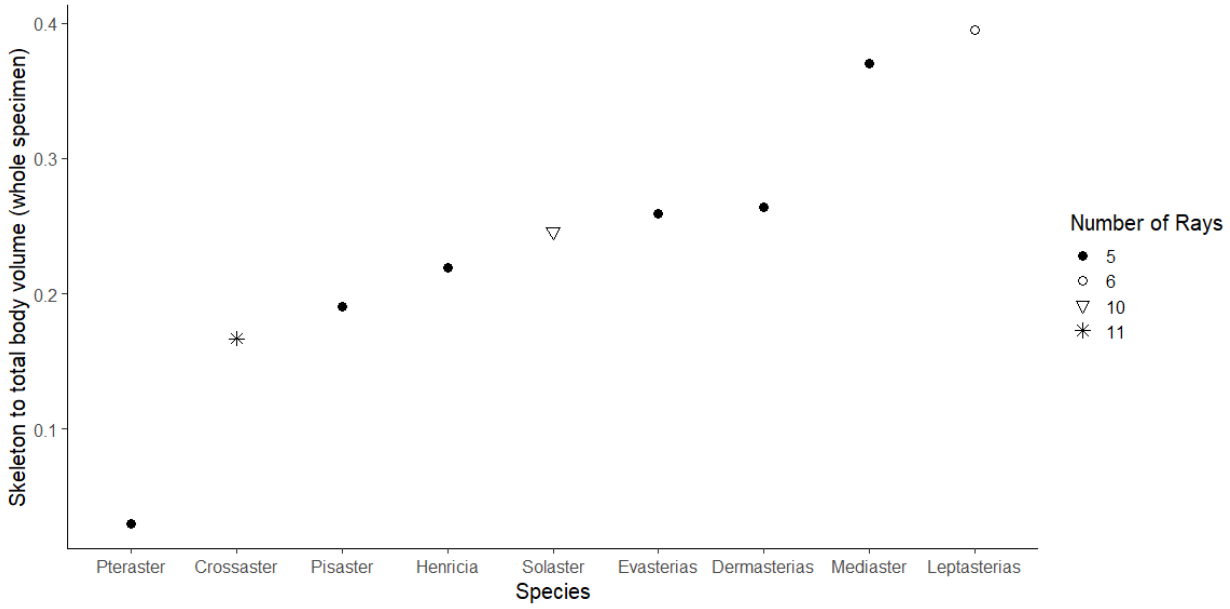

Figure 24. Armoring in nine sea star species, as represented by the fraction of the total body volume consisting of skeleton (ossicles). Species are ordered from least to most armored and coded by number of arms.

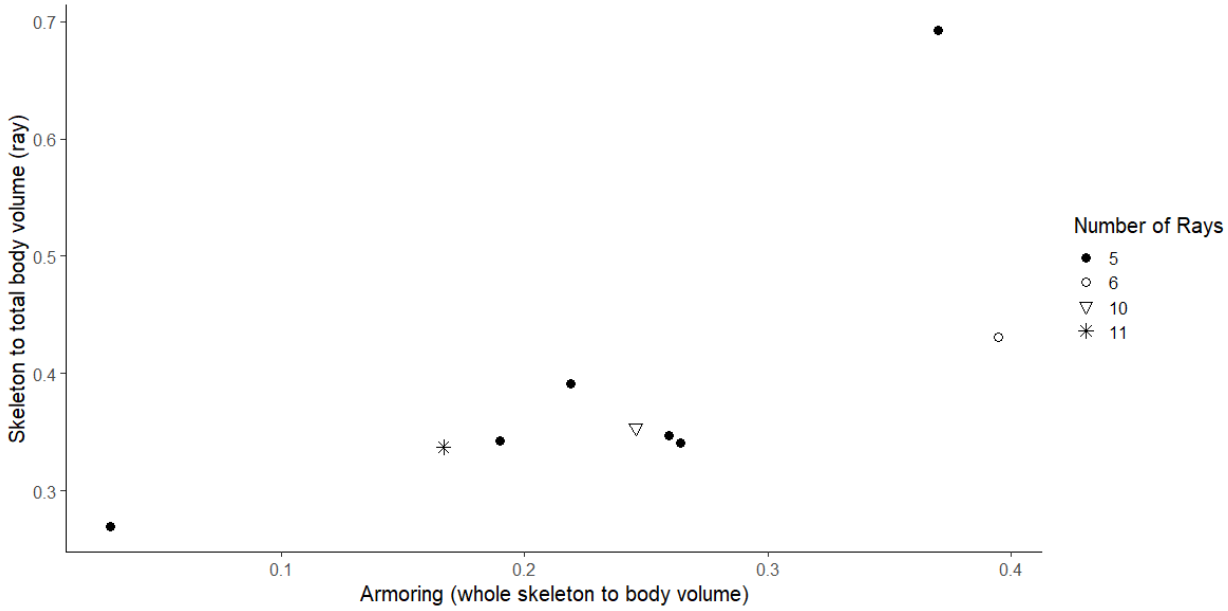

Figure 25. Armoring in nine sea star species, comparing ray tips to the whole body (which includes less than 5% of that total volume as ray tips). Armoring is represented by the fraction of volume consisting of skeleton (ossicles) for the whole body (x axis) and ray tip (y axis).

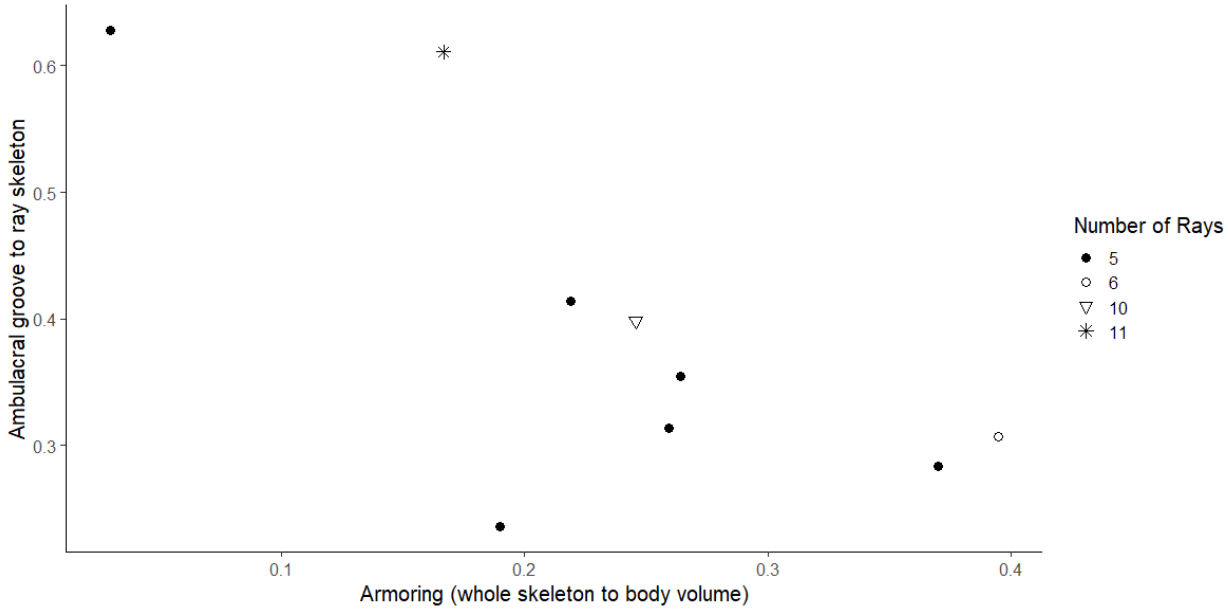

Figure 26. Allocation of skeletal investment to the ambulacral groove across nine sea star species varying in whole body armoring. The fraction of skeleton around the ambulacral groove was in relation to total ossicle volume in ray tips (y-axis). Armoring is represented by the fraction of total body volume consisting of skeleton (ossicles).

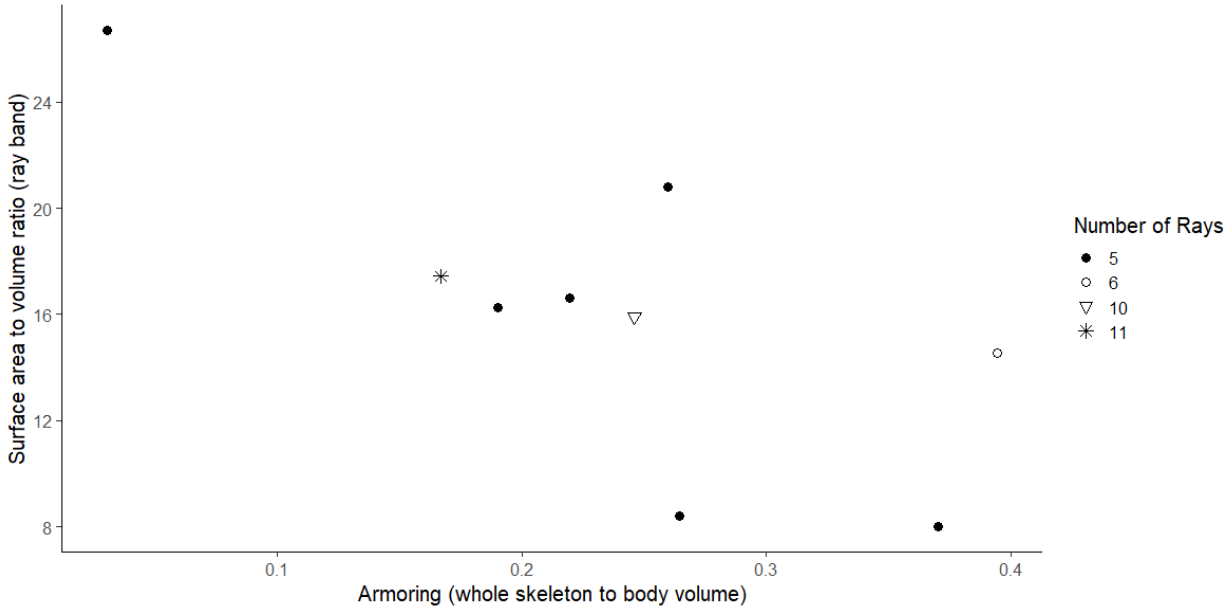

Figure 27. Ossicle shape of nine sea stars varying in whole body armoring. More convoluted ossicle shapes appear high on the y-axis with elevated surface area to volume ratios in ossicles. These surface area to volume ratios were calculated for cross-sectional unit of ossicles (ray band) in the ray tip, Armoring is represented by the fraction of total body volume consisting of skeleton (ossicles).

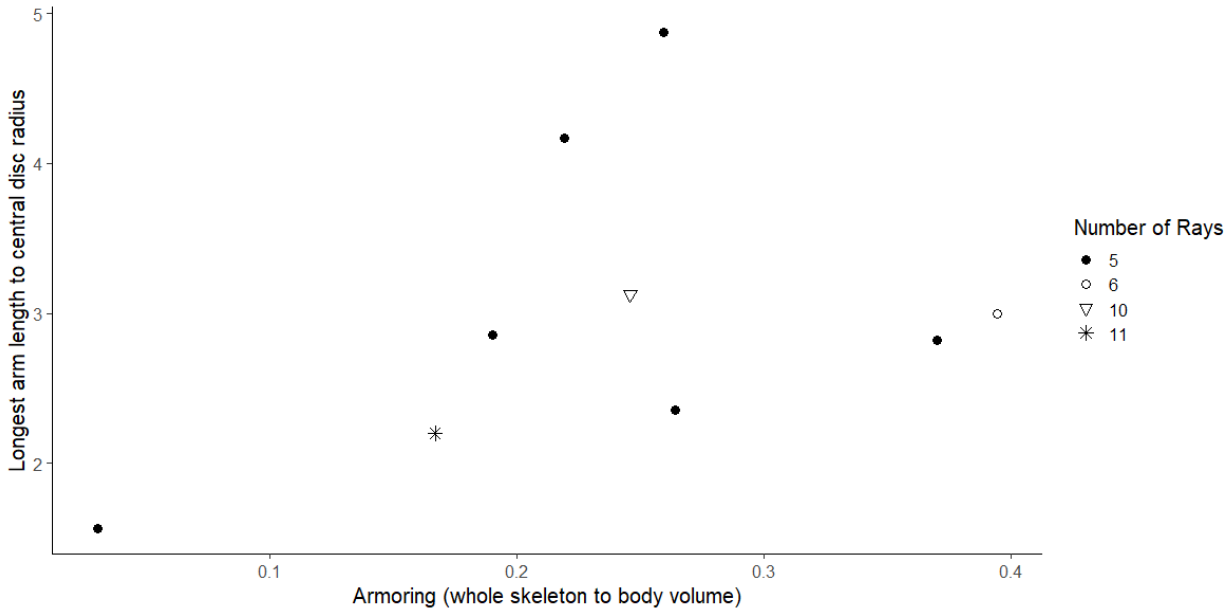

Figure 28. Whole body shape of nine sea stars varying in armoring. Shape traits depicted in this figure include number of rays and length of rays.

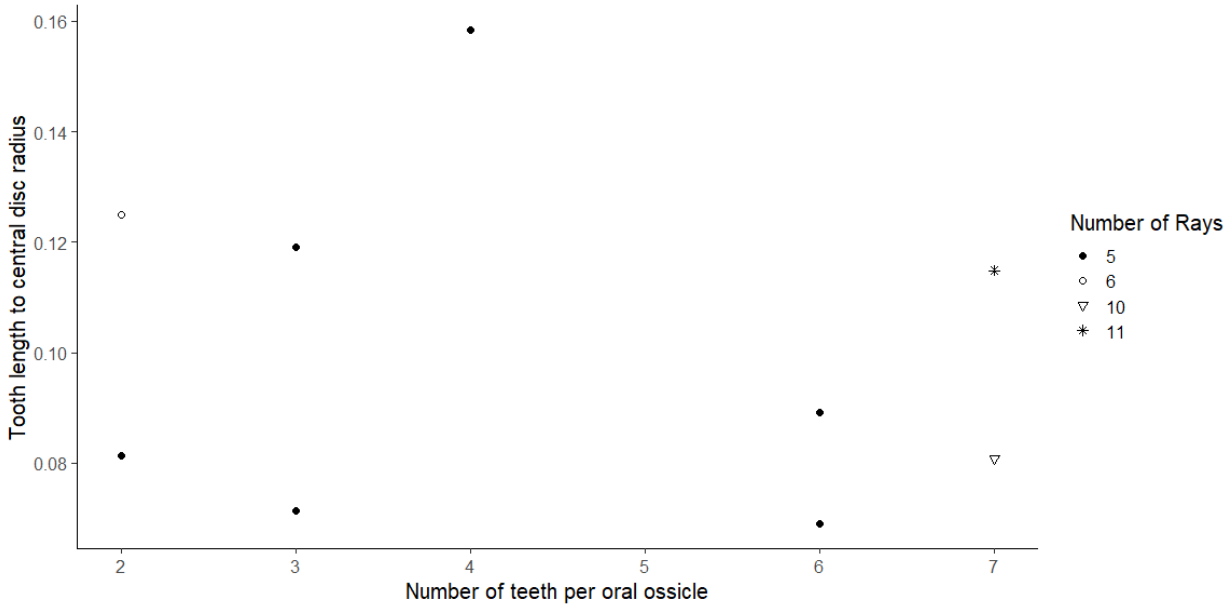

Figure 29. Characteristics of oral ossicle teeth in nine sea star species. Teeth shape traits depicted in this figure include length of teeth and number of teeth per oral ossicle (2 oral ossicles per armpit).

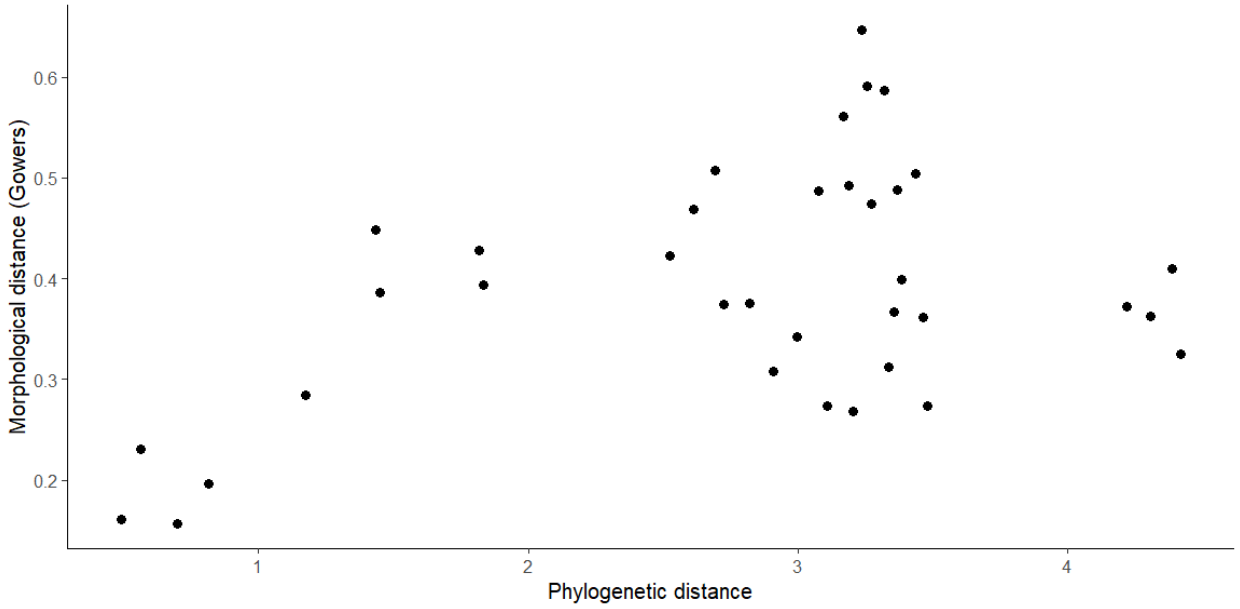

Figure 30. Morphological pairwise distance predicted by phylogenetic distance. Morphological distances calculated from 14 numerical traits on ossicle shape and pattern across nine species of sea stars.

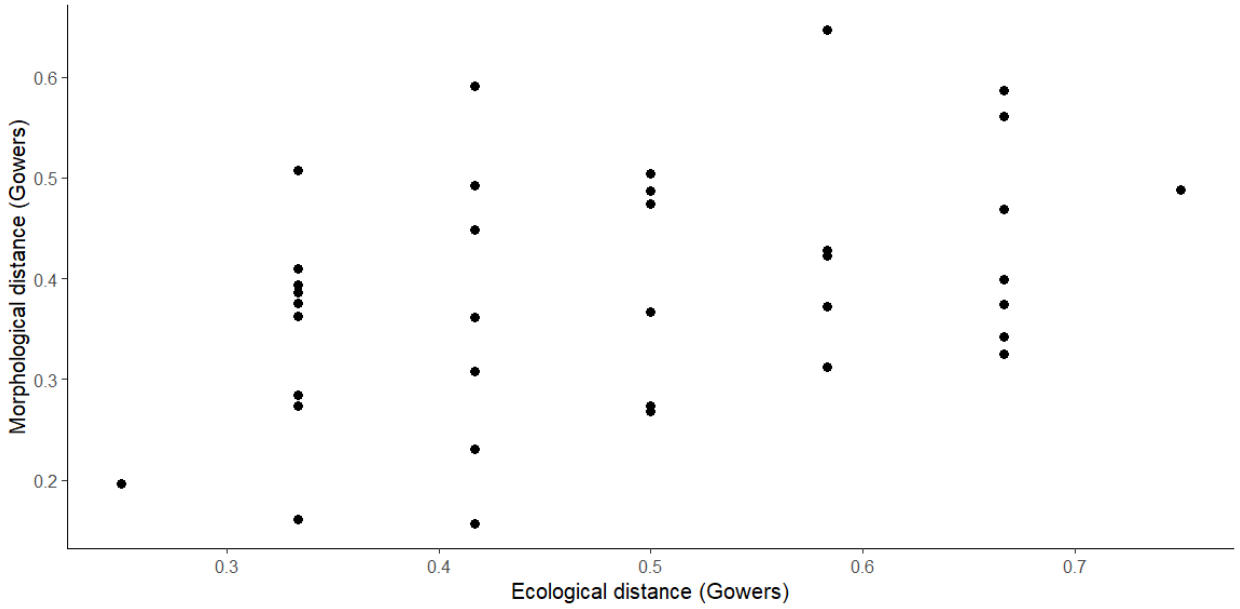

Figure 31. Morphological pairwise distance predicted by ecological distance. Morphological distances calculated from 14 numerical traits on ossicle shape and pattern across nine species of sea stars. Ecological distances calculated from 12 binary traits representing diet, habitat, and predators.

Literature Cited

Barker, M. F., & Nichols, D. (1983). Reproduction, recruitment and juvenile ecology of the starfish, *Asterias rubens* and *Marthasterias glacialis*. *Journal of the Marine Biological Association of the United Kingdom*, *63*(4), 745–765. https://doi.org/10.1017/S0025315400071198

Blowes, L. M., Egertová, M., Liu, Y., Davis, G. R., Terrill, N. J., Gupta, H. S., & Elphick, M. R. (2017). Body wall structure in the starfish *Asterias rubens*. *Journal of Anatomy*, *231*(3), 325–341. https://doi.org/10.1111/joa.12646

Edmunds, M. (1974). *Defence in animals: A survey of anti-predator defences*. Longman.

Eylers, J. P. (1976). Aspects of skeletal mechanics of the starfish Asterias forbesii. *Journal of Morphology*, *149*(3), 353–367. https://doi.org/10.1002/jmor.1051490305

Fau, M., & Villier, L. (2020). Comparative anatomy and phylogeny of the Forcipulatacea (Echinodermata: Asteroidea): insights from ossicle morphology. *Zoological Journal of the Linnean Society*, *189*(3), 921–952. https://doi.org/10.1093/zoolinnean/zlz127

Feder, H. M. (1970). Growth and predation by the ochre sea star, *Pisaster ochraceus* (Brandt), in Monterey Bay, California. *Ophelia*, *8*(1), 161–185. https://doi.org/10.1080/00785326.1970.10429557

Fedorov, A., Beichel, R., Kalpathy-Cramer, J., Finet, J., Fillion-Robin, J.-C., Pujol, S., Bauer, C., Jennings, D., Fennessy, F., Sonka, M., Buatti, J., Aylward, S., Miller, J. V., Pieper, S., & Kikinis, R. (2012). 3D Slicer as an image computing platform for the Quantitative Imaging Network. *Magnetic Resonance Imaging*, *30*(9), 1323–1341. https://doi.org/10.1016/j.mri.2012.05.001

Flowers, J., & Foltz, D. (2001). Reconciling molecular systematics and traditional taxonomy in a species-rich clade of sea stars (Leptasterias subgenus Hexasterias). *Marine Biology, 139*(3), 475–483. https://doi.org/10.1007/s002270100595

Gale, A. S. (2018). Origin and phylogeny of velatid asteroids (Echinodermata, Neoasteroidea)—New evidence from the Jurassic. *Swiss Journal of Palaeontology*, *137*(2), 279–318. https://doi.org/10.1007/s13358-018-0155-z

Hazerli, D., & Richter, S. (2020). Why "swimming crabs" are able to swim – The importance of the axial skeleton: A comparison between the "swimming crab" Liocarcinus depurator and two other brachyuran crabs (Cancer pagurus, Carcinus maenas) using μCT and 3D-reconstruction. *Arthropod Structure & Development, 59*, 100972. https://doi.org/10.1016/j.asd.2020.100972

Janies, D. A., Voight, J. R., & Daly, M. (2011). Echinoderm phylogeny including Xyloplax, a progenetic asteroid. *Systematic Biology*, *60*(4), 420–438. https://doi.org/10.1093/sysbio/syr044

Kozloff, E. N., Price, L. H., & Kozloff, E. N. (1996). *Marine invertebrates of the Pacific Northwest* (1st pbk. ed., with additions and corrections). University of Washington Press.

Kruppert, S., Chu, F., Stewart, M. C., Schmitz, L., & Summers, A. P. (2020). Ontogeny and potential function of poacher armor (Actinopterygii: Agonidae). *Journal of Morphology, 281*(9), 1018–1028. https://doi.org/10.1002/jmor.21223

Lakowitz, T., Brnmark, C., & Nystrm, P. (2008). Tuning in to multiple predators: Conflicting demands for shell morphology in a freshwater snail. *Freshwater Biology,* ???-??? https://doi.org/10.1111/j.1365-2427.2008.02045.x

Laliberte, E., Legendre, P., & Shipley, B. (2014). *FD: measuring functional diversity from multiple traits, and other tools for functional ecology* (1.0-12) [Computer software].

Laver, R. J., Morales, C. H., Heinicke, M. P., Gamble, T., Longoria, K., Bauer, A. M., & Daza, J. D. (2020). The development of cephalic armor in the tokay gecko (Squamata: Gekkonidae: *GEKKO GECKO*). *Journal of Morphology*, *281*(2), 213–228. https://doi.org/10.1002/jmor.21092

Lawrence, J. M. (2013). *Starfish: Biology and ecology of the Asteroidea*. Johns Hopkins University Press. http://site.ebrary.com/id/10661907

Mah, C., & Foltz, D. (2011). Molecular phylogeny of the Valvatacea (Asteroidea: Echinodermata): Molecular phylogeny of the Valvatacea. *Zoological Journal of the Linnean Society*, *161*(4), 769–788. https://doi.org/10.1111/j.1096-3642.2010.00659.x

Mah, C. L., & Blake, D. B. (2012). Global diversity and phylogeny of the Asteroidea (Echinodermata). *PLoS ONE*, *7*(4), e35644. https://doi.org/10.1371/journal.pone.0035644

Mauzey, K. P., Birkeland, C., & Dayton, P. K. (1968). Feeding Behavior of Asteroids and Escape Responses of their Prey in the Puget Sound Region. *Ecology*, *49*(4), 603–619. https://doi.org/10.2307/1935526

O'hara, T. D., Mah, C. L., Hipsley, C. A., Bribiesca-Contreras, G., & Barrett, N. S. (2019). The Derwent River seastar: Re-evaluation of a critically endangered marine invertebrate. *Zoological Journal of the Linnean Society*, *186*(2), 483–490. https://doi.org/10.1093/zoolinnean/zly057

Paine, R. T. (1966). Food web complexity and species diversity. *The American Naturalist*, *100*(910), 65–75.

Paine, R. T. (1969). A note on trophic complexity and community stability. *The American Naturalist*, *103*(929), 91–93.

Rodenhouse, I. (Zintheo), & Guberlet, J. E., 1887-1940. (1946). *The morphology and behavior of the cushion star Pteraster tesselatus Ives, by Irma Zintheo Rodenhouse and John E. Guberlet.* University of Washington Press.

Schwertmann, L., Focke, O., & Dirks, J. (2019). Morphology, shape variation and movement of skeletal elements in starfish (*Asterias rubens)*. *Journal of Anatomy*, *234*(5), 656–667. https://doi.org/10.1111/joa.12964

Sebens, K. P. (1987). The Ecology of Indeterminate Growth in Animals. *Annual Review of Ecology and Systematics*, *18*, 371–407. JSTOR.

Taylor, J. R. A., & Patek, S. N. (2010). Ritualized fighting and biological armor: The impact mechanics of the mantis shrimp's telson. *Journal of Experimental Biology*, *213*(20), 3496–3504. https://doi.org/10.1242/jeb.047233

Vermeij, G. J. (1989). The Origin of Skeletons. *PALAIOS*, *4*(6), 585. https://doi.org/10.2307/3514748

Vu, V. Q. (2011). *A ggplot2 based biplot* (0.55) [Computer software]. http://github.com/vqv/ggbiplot

Yang, W., Chen, I. H., Mckittrick, J., & Meyers, M. A. (2012). Flexible Dermal Armor in Nature. *JOM*, *64*(4), 475–485. https://doi.org/10.1007/s11837-012-0301-9

Zelditch, M., Swiderski, D. L., & Sheets, H. D. (2012). *Geometric morphometrics for biologists: A primer* (Second edition). Elsevier/Academic Press.

Ziegler, A. (2019). Combined visualization of echinoderm hard and soft parts using contrast-enhanced micro-computed tomography. *Zoosymposia*, *15*(1), 172–191. https://doi.org/10.11646/zoosymposia.15.1.19